MODEL BUILDING AND COLLIDER PHYSICS ABOVE THE WEAK SCALE

A Dissertation

Presented to the Faculty of the Graduate School

of Cornell University

in Partial Fulfillment of the Requirements for the Degree of

Doctor of Philosophy

by

David Curtin

August 2011

MODEL BUILDING AND COLLIDER PHYSICS ABOVE THE WEAK SCALE

David Curtin, Ph.D.

Cornell University 2011

The Standard Model of particle physics, formulated in the 1970s, has been tremendously successful in explaining almost all experimental results from high-energy colliders. Nevertheless, there are both theoretical and experimental reasons to look for a more fundamental description of nature. With the Large Hadron Collider finally being online and delivering data, we might soon be in a position to fathom the solutions to some of the most fundamental questions in our field, first and foremost the nature of electroweak symmetry breaking and the solution to the hierarchy problem.

The research presented in this thesis represents the author's contribution to the ongoing theoretical effort to develop theories beyond the Standard Model, as well as new methods of extracting information about the Lagrangian from experimental data.

We start by developing a realistic quark sector for Higgsless Randall-Sundrum models, which show that this novel way of breaking the electroweak symmetry can be brought into agreement with highly constraining data on flavor violating interactions. We then move on to models involving supersymmetry, and construct a model of metastable SUSY-breaking that avoids several problems that traditionally plague models of Direct Gauge Mediation: low gaugino masses and loss of perturbative gauge coupling unification. Finally, we propose new experimental measurements which could provide a non-trivial consistency check that SUSY solves the hierarchy problem, and show for the first time how the family of M_{T2} kinematic variables can be used in the presence of large combinatorics background.

BIOGRAPHICAL SKETCH

David Curtin was born in Hamburg, Germany, on July 15 1983 as the first child of Richard and Barbara, two opera singers originally from Australia and Poland, respectively. He was followed four years later by his brother James, and together they spent their childhood and early adolescence in Hamburg until 1997, when the family moved to Essen so Richard could pursue a contract with the Essen Staatsoper.

Less than two years later, when David was in 10^{th}grade, the family moved again, this time to Sydney, Australia. It was in Sydney that David graduated from high school and went on to study Physics and Mathematics at the University of Sydney in 2002. Completing his Bachelor of Science in 2004, David then moved to Melbourne for one year to pursue his Honors degree in theoretical physics at the University of Melbourne. There he worked on the construction of brane-world models with $SO(10)$ grand unification under the supervision of Professor Raymond Volkas.

He graduated from Melbourne at the end of 2005, and was accepted to start his Ph.D. at Cornell University in Ithaca, NY. Tragedy struck the family when Richard died unexpectedly of cancer in June 2006, but with the encouragement of Barbara and James, David moved to Ithaca in August to begin his studies at Cornell.

In the following year, David was accepted into the research group of Professor Csaba Csáki. He worked on developing theories of physics beyond the Standard Model, concentrating on extra dimensions and supersymmetry, as well as the study of collider physics to verify these theories and determine their parameters. After receiving his degree, he will move to New York City to join the high energy research group at Stony Brook University as a postdoctoral research associate.

The research of my Ph.D. is dedicated to the loving memory of my father.

Richard Curtin

27. October 1945 - 26. June 2006

Richard Curtin performing in Bonn, Germany (1996)

My father was born in 1945 in Canberra, Australia, second son of Dr. Pearce Curtin (economist) and Lorna Curtin (brn. Newman, actress and journalist). Though his true calling was the stage, he was initially trained as a lawyer in Sydney. Even while finishing his law degree he took singing lessons at the Sydney Conservatorium, and after working briefly as a solicitor from 1970 - 1973 he moved to Austria in 1974 to become an opera singer. His beautiful, rich bass voice and his singular dedication to his craft quickly earned him high acclaim, and it wasn't long before he started singing in all of Europe's major venues.

In 1981, while they were both singing in Essen, Germany, he met my mother, the soprano Barbara Idźkowska, and married her soon after. Our family life was an extraordinarily happy one. This was in large part thanks to a father who was always there for his children, and always did the right thing, not the easy thing, when it came to raising his sons, as well as a husband who showed how much he loved his wife every single day.

He is my role model; a man of towering intellect, deep wisdom and iron-clad integrity, whose wonderfully gentle sense of humor nevertheless prevented him from taking himself too seriously. Growing up as a child in Hamburg I hardly remember him being gone, because no matter how high his workload he always made time for us. He passed away unexpectedly from cancer in June 2006, just before I moved to Cornell. Even though the emptiness his early death has left behind can never be filled, I am always thankful to have had a father like him, and to feel so loved. This is to you Dad.

ACKNOWLEDGEMENTS

I thank my mother Barbara, my late father Richard and my brother James for always being there for me with love and support. It was hard for the three of us after Dad died and I had to move to the United States, but we got each other through it. You are the most important people in my life.

Thank you Csaba for believing in me and giving the chance to prove myself to you. Thanks for all the time you patiently spent teaching me, and for always being there when I needed help or advice. I couldn't have gotten a better advisor.

Thank you Maxim for working with me and teaching me collider physics. Thank you Peter for always making time to talk to me, and providing a valuable window into the experimental world. Thank you Yuval and Liam and everybody in the theory group for creating such a wonderful atmosphere for everyone to work and thrive together.

Thank you Yuhsin for being a wonderful friend and esteemed collaborator. Thank you Praveen and Sohang for the great conversation and company. Thank you Flip for always organizing things, it is much appreciated. Thank you Naresh and Mario for teaching me how to play ping pong while putting up with my overly-competitive half-serious temper-tantrums and distinct lack of talent. Thank you Bibhushan, Greg, Sumiran, Mike, Thomas, Johannes, Dan, Gang, Josh, Dean, David, Itay, Julian, Yang, Mathieu and Ben for making the last few years so much more enjoyable and interesting.

Thank you to the administrative staff, to Katerina, Kasey, Monica, Cindy, Deb and John, they kept all the wheels turning smoothly and put up with many last-minute requests and changes.

Thank you to all my friends back home in Germany and Australia, who kept in contact with me despite my sporadic correspondence and always make me feel welcome when I visit. These are the friends I have for a lifetime.

TABLE OF CONTENTS

LIST OF TABLES

LIST OF FIGURES

CHAPTER 1

INTRODUCTION

1.1 Opening Remarks

There are two main motivations for the research contained in this Ph.D. thesis. The first is to contribute to the ongoing theoretical effort aimed at developing new models to (conceivably) describe nature. These new frameworks have to be consistent with current experimental data while improving on some of the shortcomings suffered by the Standard Model (SM) of particle physics. The second motivation lies on the interface between theory and experiment, and deals with the question of how to extract information about the basic particle masses and interactions from experimental data. This is especially pertinent now that the CERN Large Hadron Collider (LHC) has started taking data, and improving our methods of analysis and model discrimination will be a major focus in our field for the foreseeable future.

We begin in this chapter with a brief introduction to the subject by first considering its history and summing up the current state of affairs, before moving on to outline the most pertinent theoretical challenges we aim to resolve in the near future. The next two chapters will be devoted to outlining two model-building developments brought forth by the author (and collaborators), one involving extra dimensions in Chapter 2 and one involving supersymmetry in Chapter 3. Chapter 4 (also in collaboration) introduces a new potential way to verify whether supersymmetry is realized in nature, and outlines how the associated experimental measurements might be performed.

1.2 Historical Perspective

The field of particle physics in its modern form can trace its origins to the development of quantum field theory (QFT) in the 1920's, which was developed in an effort to formu-

late a quantum mechanical description of electrodynamics that was compatible with special relativity. There were three main motivations for such an endeavor:

1. The desire to describe processes where the number of particles changes, e.g. a transition of an excited electron to a lower energy level via the emission of a photon;
2. proper treatment of the electromagnetic field would have to combine quantum mechanics with special relativity, since classical electromagnetism is already Lorentz invariant;
3. finally, there was a need to handle the statistics of many-body systems, which required treating particles differently based on their spin.

These (initial) challenges were addressed during the period of 1925 - 1933 by the pioneers of modern physics, including Werner Heisenberg, Max Born, Pascal Jordan, Erwin Schrödinger, Paul Dirac, Niels Bohr and Wolfgang Pauli. In quantum field theory, a field is associated with each species of particle. The field has an infinite set of internal degrees of freedom, represented as harmonic oscillators that can be canonically quantized – a process called second quantization. Particles are regarded as excitations in their respective fields, making non-conservation of particle number natural, and the fields transform under Lorentz transformation as predicted by special relativity and classical electrodynamics. The creation and annihilation operators of particles with even spin (bosons) commute, while those of odd spin (fermions) anti-commute, reproducing the correct many-body statistics. Interactions were included by perturbing around the known exact solutions of a free field theory, using the small electron-photon coupling as an expansion parameter. All this lead to the successful formulation of Quantum Electrodynamics (QED), a relativistic quantum field theory of the electromagnetic field with fermionic charges that correctly described many nontrivial processes at lowest order in perturbation theory.

The period of the 1930s and 1940s that followed was a time of crisis for quantum field theory. Calculations beyond leading order revealed infinities and seemingly nonsensical results for physically relevant quantities like the energy shift of electron states in the presence of an external electromagnetic field. These seeming inconsistencies lead some people to believe that quantum mechanics could never be reconciled with special relativity. Furthermore, more precise experimental measurements soon revealed discrepancies between the (first-order) predictions of QED and the observed energy levels of the hydrogen atom (Lamb shift & magnetic moment of the electron).

The first hint at the missing piece of the puzzle was supplied by Hans Bethe in 1947, when he computed the Lamb Shift of the hydrogen atom by absorbing the infinities in QED into the parameters of the Lagrangian, fixing the observed mass and charge of the electron to the experimental values. This intuition allowed Tomonaga, Schwinger, Dyson and Feynman to formulate QED in a fully consistent and covariant manner, whereby the infinities were absorbed into the 'bare' parameters of the Lagrangian, which in themselves, it was realized, were not physically meaningful. Feynman also developed his famous diagrammatic method of computing QFT amplitudes to any order in perturbation theory, which remains an invaluable computational and conceptual tool to this day. By the late 1950's QED was fully developed and understood, with high-order calculations producing experimental predictions of stunning precision.

QED was the first and simplest example of a fully understood and consistent quantum field theory that describes a part of nature. Its formulation lay the groundwork for the advances of the next two decades, which culminated in the formulation of the Standard Model of particle physics.

Weyl, Fock and London expressed QED as a $U(1)$ gauge theory in the 1940's. This involved extending the global $U(1)$ charge symmetry to a local symmetry with a position-depend transformation parameter. To ensure that the Lagrangian remained invariant under such an extended symmetry transformation, gauge fields had to be introduced, which correspond to the electromagnetic field with photons as their discrete quanta. This framework was generalized to non-abelian gauge groups like $SU(2)$ by Chen Ning Yang and Robert Mills in 1954, in an attempt to describe the strong interactions holding nuclei together. This was unsuccessful, because the predicted long-range forces were not seen in experiments, but with the discovery by Nambu, Goldstone and Jona-Lasinio in the early 1960's that spontaneous symmetry breaking can give mass to massless particles, Yang-Mills theory experienced a surge in interest which ultimately led to the successful formulation of the electroweak and strong sectors of the Standard Model.

The massless particles predicted by spontaneous symmetry breaking were not observed in nature, with the exception of the light (though not massless) pions which could be seen as the Nambu-Goldstone bosons of an approximate flavor symmetry of the quarks. In 1964 the generalization of spontaneous symmetry breaking to gauge symmetries was proposed by several people, most famously Anderson and Higgs. This allowed massless gauge bosons to acquire a mass by 'eating' the Nambbu-Goldstone boson of the broken gauge symmetry to acquire the additional degree of freedom necessary to self-consistently describe massive vectors.

Weak interactions, which are responsible for radioactive decay, were described via an effective 4-fermion contact interaction by Fermi in the 1930s. The structure of the coupling hinted at the possibility of a massive particle acting as the mediator of the interaction, and in 1967 Salem, Glashow and Weinberg formulated their model of electroweak interactions where electromagnetic and weak forces were unified into a single $SU(2) \times U(1)$ gauge theory.

The gauge symmetry is broken by the vacuum expectation value (VEV) of a scalar, known as the Higgs Field, to the diagonal $U(1)_{em}$ subgroup. This produces the massless photon as well as the massive $W^{\pm}, Z$ bosons, accounting for the weakness of weak interactions at low energies. By coupling the fermions to the Higgs via Yukawa interactions, the model also provides a self-consistent mechanism for generating the masses and mixings of quarks and leptons. The theory was validated in experimental measurements of neutral currents in 1973 by the Gargamelle bubble chamber experiment and the discovery of the W and Z bosons at the UA1, UA2 detectors of the CERN Super Proton Synchrotron in 1983.

A somewhat different set of challenges had to be overcome to develop an understanding of strong interactions, though of course there is much theoretical overlap with the ideas necessary for formulating the electroweak sector. A bewildering multitude of hadrons and mesons was observed in the 50's and 60's, and some way of understanding this zoology was needed. In 1963 Gell-Mann and Ne'eman proposed the *eightfold way* of organizing the hadrons into representations of $SU(3)$. Later that year, Gell-Man and Zweig recognised that this structure could emerge if the observed hadrons were made up of three light particles transforming as a vector under that flavor symmetry: the up-, down- and strange-*quarks*.

This insight shed light onto the global symmetries of the particles participating in strong interactions (though the picture was necessarily incomplete, lacking the then unknown three heavier quarks which are now part of the Standard Model). However, it became clear that an additional quantum number was needed to avoid a conflict with the Pauli exclusion principle, and in 1965 Han, Nambu and Greenberg proposed what became the theory of Quantum Chromodynamics (QCD), the idea that quarks are also charged under an $SU(3)$ gauge degree of freedom called *color*. This gauge symmetry would have to correspond to a color-force holding the quarks together in tight bound states, and the view of quarks as real, physical objects confined in hadrons was confirmed in deep inelastic scattering experiments

at SLAC in 1969.

The final ingredient was the discovery of asymptotic freedom by Gross, Wilczek and Politzer in 1973. They realized that the interactions of QCD (and indeed, many kinds of conceivable gauge theories) become weaker at smaller distance scales. This allowed perturbative calculations to make relatively precise predictions for the behavior of QCD at high-energy experiments, which were confirmed at PETRA and LEP. Asymptotic Freedom also goes some way towards explaining, or at least making plausible, the puzzling confining behavior of the strong force which seemed unique to QCD. At low energies, QCD becomes so strong that its force lines become confined to flux tubes, binding quarks into tight bound states. This idea explained the absence of any observed solitary quarks with their fractional electric charges, since separating a single quark out of a bound state would require so much energy that the snapping flux tube created a quark-anti-quark pair, creating two bound states and never leaving a single quark to stand alone.

What we know today as the Standard Model is the assemblage of all these components completed by the mid-1970s. The electroweak interactions and fermion masses are explained by GWS theory, displaying spontaneous symmetry breaking via the Higgs mechanism, and QCD with its asymptotic freedom and confining behavior accounts for the strong interactions. The Standard Model stands to this day as a theoretical triumph that stood up to (almost) all experimental enquiry (much to the chagrin of later generations of hungry theorists).

1.3 The Standard Model

This section is only meant to give the most cursory summary of the Standard Model's key features, to remind the reader of the details we need for the discussion of the research in this

thesis. More details can be found in many graduate-level particle physics and quantum field theory textbooks such as [2], and reviews such as [3].

The Standard Model is an $SU(3)_c \times SU(2)_L \times U(1)_Y$ anomaly-free gauge theory with gauge couplings g_s, g, g' respectively and the following particle content:

		$SU(3)_c$	$SU(2)_L$	$U(1)_Y$
leptons	$E_L^i = (\nu_e, e_L)$	1	$\square$	$-\frac{1}{2}$
	e_R^i	1	1	-1
quarks	$Q_L^i = (u_L, d_L)$	$\square$	$\square$	$\frac{1}{6}$
	u_R^i	$\square$	1	$\frac{2}{3}$
	d_R^i	$\square$	1	$-\frac{1}{3}$
Higgs	ϕ	1	$\square$	$\frac{1}{2}$

(1.3.1)

Here $i = 1, 2, 3$ is the generation index, and accounts for the fact that the SM particles come in three generations or *flavors*. Different flavors of the same particle have identical gauge interactions, but different Yukawa couplings to the Higgs:

$$\mathcal{L}_{yuk} = -\lambda^e_{ij} \overline{E}^i_L \cdot \phi e^j_R - \lambda^d_{ij} \overline{Q}^i_L \cdot \phi d^j_R - \lambda^u_{ij} \epsilon^{ab} \overline{Q}^i_{La} \phi^\dagger_b u^j_T + h.c. \tag{1.3.2}$$

(a, b are $SU(2)_Y$ indices). There is also a Higgs potential,

$$\mathcal{L}_{Higgs} = -V(\phi), \qquad V(\phi) = -\mu^2 |\phi|^2 + \frac{\lambda}{2} |\phi|^4, \tag{1.3.3}$$

which generates a nonzero vacuum expectation value for the Higgs. Up to unitary rotations, this is

$$\langle \phi \rangle = \frac{1}{\sqrt{2}} \begin{pmatrix} 0 \\ v \end{pmatrix} \qquad \text{with} \qquad v = \frac{\mu}{\sqrt{\lambda}}. \tag{1.3.4}$$

This breaks electroweak symmetry breaking $SU(2)_L \times U(1)_Y \to U(1)_{em}$, which is generated by $Q = T^3 + Y$, with T^3 being the diagonal $SU(2)_L$ generator.. The $W^\pm$ gauge bosons are associated with the non-diagonal generators $T^\pm = T^1 \pm i T^2$ of $SU(2)_Y$. The neutral Z^0 boson

is associated with $T^3 - Y$, while Q corresponds to the massless photon. The electroweak gauge couplings of the fermions can then be expressed in the covariant derivative

$$D_\mu = \partial_\mu - i\frac{g}{\sqrt{2}}(W_\mu^+ T^+ + W_\mu^- T^-) - i\frac{g}{\cos\theta_w} Z_\mu (T^3 - \sin^2\theta_w Q) - ieA_u Q, \tag{1.3.5}$$

where $\sin^2\theta_w = g'^2/(g^2 + g'^2)$ and is measured to be ≈ 0.23. In terms of the electromagnetic coupling constant, $g = e/\sin\theta_w$, and $m_W = m_Z \cos\theta_w \approx 80.4$ GeV.

When the Higgs condenses, the Yukawa couplings to the fermions generate mass terms. Given arbitrary Yukawa couplings as per eq. (1.3.2), one can diagonalize both the quark and lepton mass matrices with unitary rotations, which makes the $W^\pm$ interactions to the quarks non-diagonal. This is described by the Cabibbo-Kobayashi-Maskawa (CKM) matrix V_{CKM} in the current coupling to the $W^\pm$:

$$J^{\mu+} = \frac{1}{\sqrt{2}} \overline{u}_L^i \gamma^\mu V_{CKM}^{ij} d_L^j. \tag{1.3.6}$$

This leads to quark mixing via charge-changing interactions, or flavor-changing charged currents (FCCC). There are no flavor-changing neutral currents (FCNC) in the Standard Model. This is referred to as the Glashow-Iliopoulos-Maiani (GIM) mechanism.

The $SU(3)_c$ interaction becomes strong at the scale $\Lambda_{QCD} \sim$ GeV. At energies lower than Λ_{QCD}, quarks become confined in bound states. Neutrons and Protons are the only stable such states, but there is a rich spectrum of unstable mesons and baryons.

The gauge theories and particle content of the Standard Model result in a number of accidental exact symmetries, which have important experimental consequences. Baryon number as a whole is conserved, though the number of quarks of each generation are not separately conserved. Not so for the leptons: the absence of a right-handed neutrino forbids any mixing amongst the leptons, and leads to exact electron-, muon- and tau-number conservation.

The Standard Model has been tremendously successful in its agreement with experimental

data. 19 free parameters are required to completely define the model, and the number of separate experimental measurements that agree with the Standard Model predictions far exceeds that number. The table of predicted SM particles has been filled out by the discoveries of the τ lepton, W and Z bosons and the bottom and top quarks. The only particle not yet observed is the Higgs. Precision data from the LEP and Tevatron colliders verified the SM predictions for electroweak precision observables. Flavor physics experiments at high-intensity low-energy colliders like charm- and B-factories show that the physics of quark masses and mixings are in excellent agreement with SM predictions and the unitarity of the CKM matrix, and lattice calculations are starting to produce sufficiently accurate predictions for non-perturbative observables to start being competitive with experimental measurements.

Nevertheless, we know that the Standard Model cannot be the complete description of the physics governing the universe. There are two main contradicting experimental results.

- Various cosmological and astrophysical observations constrain the (current) make-up of the universe to be 72% Dark Energy, 23% Dark Matter and only about 5% ordinary atoms. The Standard Model only explains the last component. Dark Energy is something completely unknown, whereas Dark Matter could be interpreted as a massive neutral particle that only interacts with ordinary matter gravitationally. While such a particle can be incorporated into a theory in various ways, it is definitely not part of the Standard Model.
- The observation of neutrino oscillations prove that neutrinos have mass, which is not possible in the Standard Model.

In addition to concrete evidence, there are various theoretical considerations that lead one to believe that there is a more general theory describing the universe, of which the Standard

Model is merely a low-energy description valid up to about the electroweak scale. The most important issues are:

- *The Hierarchy Problem.* The mass of elementary scalars are not stable with respect to high-energy quantum corrections. In order to obtain a Higgs VEV near the electroweak scale, the parameters of the Lagrangian at the Planck Scale, the fundamental energy scale of gravity, would have to be tuned to one part in about 10^{32}. Another way of stating the problem is by asking why gravity is so weak compared to the other forces of nature. Clearly the fine-tuning is unsatisfactory, and begs a more fundamental explanation.
- *The Flavor Problem.* The Standard Model provides no explanation for the large range of quark and lepton masses observed, which spans 5 orders of magnitude (not counting neutrinos, which increase the hierarchy significantly). The Yukawa couplings are merely inputs determined from data.
- *Matter-Antimatter Asymmetry.* The Standard Model has two sources of CP-violation. One is the strong CP-angle discussed below, and the other is one phase in the CKM matrix. However, this is by far insufficient to account for the large amount of matter in the universe today, if we assume that there were equal amounts of matter and anti-matter at the time of the Big Bang. In the absence of extremely fine-tuned initial conditions, the Standard Model must be extended with additional mechanisms of CP-violation
- *The Strong-CP Problem.* On a related note, it is very puzzling that the theoretically allowed CP-violating parameter in QCD is zero, or so close to zero that we cannot tell the difference.
- *Gravity.* This is the most fundamental problem. Quantum Field Theory appears to be unable to provide us with a quantum-mechanical description of gravity that is both

well-defined at high energy scales and Lorentz-invariant. The unification of quantum mechanics with *special* relativity was achieved with quantum field theory, but to have any hope of formulating a true "theory of everything" that describes all the known forces in nature including gravity, we need to achieve unification with *general* relativity as well.

The Standard Model in many ways can be called the crowning achievement of fundamental physics in the late 20^{th}century, but its shortcomings are as obvious as its many successes. Even so, these successes greatly constrains any model for physics beyond the Standard Model that we might want to propose. Any new theory must not only fix some of the above-mentioned problems, but also agree with the huge wealth of existing experimental data that is so well explained by the Standard Model.

1.4 The LHC Era

The half-century between the 1920s and the formulation of the Standard Model was a time of rapid theoretical progress, culminating in an almost complete description of all the basic particle physics we observe today. In the four decades since then, theorists and experimentalists have been busy verifying countless predictions of the Standard Model and finding almost universal agreement. This achievement is to be celebrated, but in some sense it is also a cause for frustration. We have already outlined why we are sure that the Standard Model is only an effective low-energy description of a much more complete and theoretically satisfying theory, and there are some pieces of experimental evidence that unequivocally point towards *some* kind of physics beyond the Standard Model (BSM). But beyond that there have been precious few clues for what *exactly* that BSM physics might look like. This is about to change. After 50 years of formulating the Standard Model and 40 years of verifying it, we

are finally ready to move beyond it. This is the start of the LHC era.

The research contained in this Ph.D. thesis was produced in this context. History has shown that new insight is always produced when experimental measurements probe some new regime, and old theories that worked well on some scale are recognized as approximations that are replaced by more complete descriptions at a more fundamental scale. We are about to peel back the next layer of the onion, which is why the author chose to focus his theoretical efforts on the TeV scale and the solution of the Hierarchy Problem.

Theoretical research at the TeV scale can be roughly divided into three categories, though there is plenty of overlap. They range from the purely theoretical construction of new models, to the phenomenological investigation into observable consequences of these theories to the more practical aspects of collider physics, which is concerned with new methods of extracting information about the Lagrangian from experimental data. To take full advantage of the opportunities presented by the LHC, one must proceed on all three fronts.

The Hierarchy Problem has been known since the formulation of the Standard Model, and a number of theoretical solutions have been proposed since then. The perhaps most notable ones are

1. supersymmetry (SUSY),
2. extra dimensions,
3. strongly coupled new physics.

The next chapter will outline some ideas along the lines of extra dimensions, which can be related to the third option via the AdS/CFT Correspondence. The subsequent chapters fall within the SUSY-paradigm. Before moving on, let us briefly review some of the basics of these ideas.

Supersymmetry[1]

In 1967, Coleman and Mandula proved a 'no-go' theorem [6] which stated that the only symmetries of the scattering matrix consistent with the Poincaré symmetries was a product of the Paincare' symmetry and internal symmetry groups. This restriction only applied to symmetries with *commuting* generators. In the early 1970s, new nontrivial symmetry called *supersymmetry* relating bosons and fermions was formulated by a few people, amongst them Golfand and Likhtman [7]. The supersymmetry generators are fermionic instead of bosonic and they *anticommute*, circumventing the restrictions of the original Coleman-Mandula theorem, and 1975 Haag et. al showed that SUSY is the *only* possible extension of the Poincaré Algebra [8].

The simplest realization of supersymmetryin 4 dimensions (and by far the most useful phenomenologically) is $\mathcal{N} = 1$ SUSY with a single set of fermionic generators $Q_\alpha, Q^\dagger_{\dot{\alpha}}$ which commute with the usual Poincaré generators and obey the anticommutation relations

$$\{Q, Q\} = 0, \qquad \{Q^\dagger, Q^\dagger\} = 0, \qquad \{Q_\alpha, Q^\dagger_{\dot{\alpha}}\} = 2\sigma^\mu_{\alpha\dot{\alpha}} P_{mu}, \tag{1.4.7}$$

where $\sigma^\mu_{\alpha\dot{\alpha}} = (1, \sigma^i)$ and σ^i are the usual Pauli matrices. Fermions and Bosons fall into complete SUSY-representations, most commonly *chiral multiplets* consisting of one Weyl fermion and one complex scalar, and *vector multiplets* consisting of one massless vector and one Weyl fermion.

SUSY is incredibly attractive because it allows for a natural solution to the hierarchy problem. The existence of opposite-spin superpartners for all the known Standard Model particles cancels out the divergent contributions to the Higgs mass, stabilizing the weak scale against quantum corrections. The fact that superpartners have not already been observed implies that SUSY is a broken symmetry, and to solve the hierarchy problem it has to be restored at or just above the weak scale. This means the LHC should discover superpartners

[1]There are many great textbooks on supersymmetry, for example [4] and [5].

if SUSY resolves the hierarchy problem. Supersymmetry is also a requirement for the formulation of *String Theory*, which is currently the only known self-consistent theory of quantum gravity.

The minimal supersymmetric extension to the Standard Model (MSSM) was written down by Georgi and Dimopoulos in 1981 [9]. It contains a number of extremely desirable features:

- stabilization of the electroweak scale against quantum corrections,
- unification of the strong and electroweak forces into a single SU(5) Grand Unified Theory (GUT) [10] at a scale $M_{GUT} \sim 10^{16}$ GeV.
- a natural dark matter candidate in the form of the lightest superpartner, the Lightest Supersymmetric Particle (LSP), which has to be stable with mass around the weak scale, consistent with the 'WIMP-miracle' of dark matter.

The MSSM (and its non-minimal cousins) in itself says nothing about how SUSY is broken, instead parameterizing SUSY-breaking effects in an agnostic way via the inclusion of *soft terms*. This leads to a large number of free parameters (100), which must be determined from experiment and ideally explained by a theory of SUSY-breaking.

We know that SUSY breaking must take place in a different sector than the MSSM, with breaking effects communicated via non-renormalizable interactions (otherwise there would exist a superpartner that is lighter than its Standard Model counterpart). This leaves two fundamental questions that must be addressed: how is SUSY *broken*, and how is that breaking *mediated* to the supersymmetric Standard Model? Several options have been proposed, amongst them gravity mediation, gauge mediation, gaugino mediation and anomaly mediation. We will work with gauge mediation in Chapter 3.

Another important question is how SUSY might be discovered and verified at a hadron collider like the LHC, and how we could determine the masses and mixings of the super-partners. The research presented in Chapter 4 attempts to make some headway in this direction.

Extra Dimensions[2]

There is ample motivation to consider the existence of extra dimensions beyond the $3+1$ we see around us. Like supersymmetry, their existence is required by String Theory. They also offer a compelling way to solve the Hierarchy Problem that is fundamentally different from supersymmetry. Finally, via the AdS/CFT correspondence models with warped extra dimensions can be shown to be dual to certain Technicolor theories, providing us with a way to obtain new results in strongly coupled theories that were calculationally inaccessible previously.

One possible incarnation is the ADD model [11]. It postulates the existence of one or more 'large' additional dimensions through which gravity is free to propagate, while the SM fields are confined to 3+1 dimensional *branes*. The extra dimensions are rolled up in some way, or 'compactified', so that the world appears 4-dimensional at large scales, with gravity much weaker than the other forces. Below the compactification scale, the power law of gravity takes on its fundamental higher-dimensional form. This allows the fundamental scale of gravity to be much lower than the Planck Scale, meaning gravity becomes comparable in strength to the other forces at small scales, only appearing weak at large scales. This elegant solution of the hierarchy problem postulates a single $\sim$ mm-size extra dimension, with the required size becoming smaller the more dimensions are added. Like any theory with additional dimensions, the ADD model features a Kaluza-Klein (KK) spectrum for fields in the bulk, in this case the graviton, but the large size of the extra dimension means the KK-spectrum

[2]Many reviews exist in the literature, one example being [14]

would be almost continuous, and all the modes would only be extremely weakly coupled to SM particles via gravitational interactions. By making the fundamental scale of gravity accessible at colliders this model might put string theory within experimental reach, but this also produces problems, for example unsuppressed TeV-scale gravity mediated operators for proton decay, flavor violation and CP violation, though some of this might be ameliorated in the split-fermion scenario. Recent LHC data severely constrains this model [12].

Another scenario that has received a lot of attention in the last decade is the Randall-Sundrum (RS) Model [13]. Models with a flat extra dimensions ignore the backreaction of gravity to the presence of the branes themselves, which is a good approximation if the branes have small tensions. If instead we consider flat 4D branes with large tension along a single extra dimension compactified on an interval or the $S^2/\mathbb{Z}$ orbifold, solving the 5D Einstein gravity action yields the metric

$$ds^2 = e^{-2k|y|} dx^\mu dx^\nu \eta_{\mu\nu} - dy^2, \tag{1.4.8}$$

where $\eta_{\mu\nu}$ is the flat 4D Minkowski metric and $e^{-2k|y|}$ is called the *warp factor*. If we place a positive tension brane at $y = 0$ (gravity brane or UV brane) and a negative tension brane at $y = b$ (TeV brane or IR brane), then the 4D metric at a fixed point y along the extra dimension is $e^{-2k|y|}\eta_{\mu\nu}$. This means that the same coordinate distance on a 4D brane corresponds to a larger and larger physical distance the further we move down the extra dimension towards the negative tension brane. By the same token, a mass scale v near the positive tension brane is warped down to $e^{-2kb}v$ on the negative tension brane. It is this mechanism which allows for another solution to the hierarchy problem: the bare Higgs VEV may well be $v \sim M_*$, where M_* is the 5D Planck scale, but if the Higgs is localized on the negative tension brane its effective 4D-VEV will be $v_{eff} = e^{-2kb}v \sim$ TeV. On the other hand, the effective 4D Planck constant is almost unaffected by the warping, since the graviton zero-mode is localized in the bulk near the positive-tension brane. In this picture,

the reason for the weakness of gravity in the 4D effective theory compared to the other forces is the localization of the graviton zero mode near the positive tension brane, giving it a small exponential overlap with the negative tension brane.

If gauge fields are allowed to propagate in the bulk, their zero mode (which acquires a mass from the Higgs VEV on the IR brane) will be (almost) flat along the extra dimension. Allowing fermions to propagate in the bulk ameliorates problems with gravity-mediated TeV-scale flavor-violating operators on the IR-brane, while also providing a very elegant mechanism for generating large mass hierarchies: changing the bulk masses of the fermions by $O(1)$ factors changes their localization along the extra dimension, and exponentially affects their overlap with the TeV-brane, where the zero modes get a mass via overlap with the Higgs. Relatively small differences in bulk masses amongst the different generations of fermions can thus account for the large hierarchy of masses and mixings observed amongst quarks and leptons, while also suppressing flavor-changing neutral currents. This is called the RS-GIM mechanism, in reference to the SM GIM mechanism which forbids FCNCs at tree-level, though the RS version is not quite as effective at suppressing dangerous flavor-violation. The KK-spectrum of RS-models is very different from ADD models. The extra dimension in RS is much smaller than in ADD, making KK-modes much heavier $\sim$ TeV. All KK-modes, including the graviton, are localized near the IR brane and couple with electroweak-strength, making individual modes detectable at the LHC.

An interesting variety of the RS idea are Higgsless models. RS models suffer of a *little hierarchy problem*, since the Higgs VEV is $\sim O(100\text{GeV})$ compared to the TeV-scale of the IR-brane, leading to a $\sim 1\%$ fine tuning. One possible way to ameliorate this problem is by letting the Higgs vev be comparable to the IR-brane-scale, which leads to very different phenomenology. The Higgs decouples from the low-energy theory, WW-scattering is unitarized by exchange of KK-modes and electroweak symmetry breaking effectively takes place via the

boundary conditions for the electroweak gauge fields. Higgsless scenarios are also interesting to consider to prepare for the eventuality that we might not see a Higgs at the LHC, which is why this alternative mechanism of electroweak symmetry breaking will be the subject of the next chapter.

CHAPTER 2

A REALISTIC QUARK SECTOR FOR HIGGSLESS RS MODELS

Based on the 2009 article "A Flavor Protection for Warped Higgsless Models", written in collaboration with Csaba Csáki and published in Phys.Rev. D80 (2009) 015027.

2.1 Introduction

The standard model Higgs mechanism provides ample motivation to come up with alternatives. As we have outlined towards the end of Chapter 1, an interesting new possibility is provided by Higgsless models [15–19] with a warped extra dimension [13]. A Higgs field localized on the IR brane of an RS background is decoupled by taking its VEV to be very large, while the masses of the W and Z bosons remain finite and are set by the size of the extra dimension. Unitarity of the gauge boson scattering amplitudes can then be ensured via heavy KK gauge boson exchange. Such models would solve the little hierarchy problem of Randall-Sundrum setups and have very distinctive phenomenological consequences. However, it is not clear whether these Higgsless RS models can be made completely viable: a large correction to the S parameter makes it difficult to match electroweak precision data, the cutoff scale has to be adequately raised to ensure unitarization happens at weak coupling, and generically FCNC's are not adequately suppressed. Many of these initial difficulties have been at least partially addressed. One can tune the effective S-parameter away by making the fermion left-handed fermion wave functions close to flat [20], and choosing the right fermion representations can prevent the large top mass from introducing coupling deviations in the $Zb\bar{b}$-vertex [21, 22]. The cutoff scale can also be raised by lowering the curvature of the extra dimension [20]. However, once the fermion wave functions are required to be close to flat, the traditional anarchic RS approach to flavor [23–27] (where fermion wave function overlaps generate fermion mass hierarchies and also give a protection called RS-GIM against FCNC's [25]) can no longer be applied. A possible resolution to this problem is to introduce a genuine five-dimensional GIM mechanism, which uses bulk symmetries to suppress flavor violation [28]. The trick is to impose global flavor symmetries on the bulk, with a large subgroup left unbroken on the IR brane and flavor mixing forbidden anywhere except the

UV brane. One can then construct a model where tree-level FCNC's are genuinely vanishing, with the downside that we are no longer trying to explain the quark mass and mixing hierarchies, merely accommodating them.

The aim of this chapter is to examine the flavor bounds (similar to [29, 30] on Higgsless models and to present a viable flavor construction for these theories (see [31, 32] for other examples in an RS context). We have to circumvent the problems usually associated with Higgsless models by ensuring that

- all FCNCs are sufficiently suppressed,
- all tree-level electroweak precision constraints are satisfied,
- the cutoff scale is sufficiently high.

We show that the simplest versions of such a model cannot be realistic: imposing an exact GIM mechanism for all three generations either drives up the cutoff scale or prevents the S-parameter from being cancelled. Instead, the realistic flavor model we propose will have next-to minimal flavor violation (NMFV) [28], featuring a custodially protected quark representation for the third generation, and an exact GIM mechanism implemented for the first two generations only. This choice of representations allows us to isolate the lighter quarks from the dangerous top mass and prevent a large S-parameter without having to increase the bulk coupling and decrease the cutoff scale. Flavor-changing neutral currents are controlled by two main mechanisms:

1. The surviving flavor symmetry between the first two generations forces all the mixing to go through the third generation (hence NMFV), which is vital to reduce D and K mixing.
2. Kinetic mixing terms on the UV confine the right-handed fermions to the UV brane and reduce bulk contributions to the couplings, which are the source of off-diagonal

neutral couplings. This results in an RS-GIM-like flavor suppression mechanism for the right-handed fermions.

We also have some freedom to distribute the required charged-current mixing amongst the up- and down-sectors, which reduces neutral-current mixing in each sector. All of this is necessary to sufficiently suppress flavor violation. We find that experimental FCNC bounds systematically constrain the down-sector mixing angles, forcing them to lie within a volume of angle space that is enclosed by a well-defined surface. *Assuming* the UV kinetic mixing terms obey a Cabibbo-type mixing hierarchy, this volume occupies $\sim O(5\%)$ of available angle space.

This chapter is structured as follows: in Section 2.2 we review the 5D GIM mechanism and introduce the quark representations we will be using. In Section 2.3 we outline our NMFV quark model and show compliance with electroweak precision data (EWPD). We also examine in detail the errors introduced by the zero mode approximation, and find that one can have zero S-parameter without flatness, provided there is a lot of KK mixing on the IR brane. The flavor suppression mechanisms of the NMFV model are derived in Section 2.4 and demonstrated with the gluon KK contribution to FCNC's in Section 2.5. Numerical results for the mixing constraints are presented in Section 2.6, and we conclude with Section 2.7.

2.2 Setup

After briefly reviewing the gauge sector, we will discuss the full 5D GIM mechanism [28] and how one could apply it to various simple quark models. This will motivate the construction of our Next-to Minimal Flavor Violation Model in Section 2.3.

2.2.1 Gauge Sector

We work on an AdS_5 background and parameterize our space-time using conformal coordinates

$$ds^2 = \left(\frac{R}{z}\right)^2 (dx_\mu dx_\nu \eta^{\mu\nu} - dz^2) \tag{2.2.1}$$

where the UV and IR branes sit at $z = R, R'$ respectively. Our gauge sector takes the standard RS form [33] with $\langle H \rangle \to \infty$ on the IR brane, as outlined in [34]. This means we have an $SU(3)_c \times SU(2)_L \times SU(2)_R \times U(1)_X$ gauge group [33] in the bulk (where $X = B - L$), which is broken by boundary conditions to $SU(3)_c \times SU(2)_L \times U(1)_Y$ on the UV brane and $SU(3)_c \times SU(2)_D \times U(1)_X$ on the IR brane. The custodial $SU(2)_R$ symmetry protects the M_W/M_Z ratio from deviations at tree level, and the gauge boson mass is given by the size of the extra dimension. For future convenience, let us define

$$L \equiv \log R'/R. \tag{2.2.2}$$

Then to leading order in L,

$$M_W^2 \approx \frac{1}{R'^2 L}. \tag{2.2.3}$$

On a technical note, we include all brane-localized gauge kinetic terms (BKTs) that are allowed by symmetries, and include their corrections due to 1-loop running effects on their respective branes [35]. This means that the effective $SU(2)_L$ BKT on the UV brane can be negative at the weak scale. We will also localize some fermions on the UV brane, making the effective $U(1)_Y$ BKT always positive (but the effect is very small). Unless otherwise mentioned, we set all *effective* BKTs to zero at the weak scale except for $U(1)_Y$, for which we set the bare term to zero. We also set the effective $SU(3)$ BKTs to zero, but note that they could be made negative at the weak scale.

In addition to the BKTs, the free input parameters in the gauge sector are R and the ratio g_{5R}/g_{5L}. The SM W, Z masses then determine R' and g_{5X}/g_{5L}, while $\alpha_{\rm EM}$ and α_s at the weak scale set the overall size of the 5D couplings. All of our gauge bosons are canonically normalized, with all electroweak coupling corrections (including S and T parameters) pushed into interaction terms.

Our theory is valid up to a momentum cutoff, which in AdS_5 space is given conservatively by

$$\Lambda_{\rm cutoff} \sim \frac{16\pi^2}{g_5^2}\frac{R}{R'} \tag{2.2.4}$$

where g_5 is the largest 5-dimensional coupling. If we take $g_{5L} = g_{5R}$, then to leading order in L the 4D coupling g can be expressed as $g^2 = g_5^2/RL$ [34], which together with eq. (2.2.3) gives

$$\Lambda_{\rm cutoff} \sim \frac{16\pi^2}{g^2}\frac{M_W}{\sqrt{L}} \approx \frac{29\,\mathrm{T}eV}{\sqrt{L}}. \tag{2.2.5}$$

If we had a physical Higgs on the IR brane we could freely choose our KK scale and make the cutoff large, but in the Higgsless model we must choose a low curvature to unitarize WW-scattering before the theory becomes strongly coupled. We set $R^{-1} = 10^8\mathrm{G}eV$ which gives $L \approx 13$ and $\Lambda_{\rm cutoff} \sim 8\,\mathrm{T}eV$. We also choose $g_{5L} = g_{5R}$, since gauge matching would decrease the cutoff if we made the couplings different. The Z' mass is therefore fixed and of order $\sim 700\mathrm{G}eV$.

2.2.2 The Fermion Sector

Our notation for a 5D Dirac fermion will be

$$\Psi = \begin{pmatrix} \chi \\ \overline{\psi} \end{pmatrix} \tag{2.2.6}$$

where χ and ψ are both LH 2-component Weyl spinors, and hence $\overline{\psi}$ is a RH 2-component spinor. We write the boundary conditions for each Dirac spinor as $(\pm, \pm)$ at $z = (R, R')$, where $+$ means $\overline{\psi} = 0$ and $-$ means $\chi = 0$. The normalized left-handed zero-mode profile is given by

$$g_0(z) = R'^{-1/2} \left(\frac{z}{R}\right)^2 \left(\frac{z}{R'}\right)^{-c} f(c), \qquad \text{where} \qquad f(c) = \sqrt{\frac{1-2c}{1-\left(\frac{R'}{R}\right)^{2c-1}}} \tag{2.2.7}$$

is the RS flavor function. The right-handed profile $f_0(z)$ is defined identically, with $c \to -c$.

5D GIM Mechanism

For three generations of a given quark representation we can impose global flavor symmetries that prevent FCNCs at tree-level while generating all the required masses and mixings [25]. In broad strokes, those symmetries must satisfy the following criteria:

1. We need to have enough freedom to generate 6 different 4D quark masses and reproduce the CKM mixing matrix.
2. To ensure that flavor-violating operators are suppressed by the high scale $1/R$, we only allow flavor mixing on the UV brane, via right-handed kinetic terms for the up and down sector independently. Left-handed mixing is assumed to be forbidden by flavor symmetry, since otherwise the right- and left-handed kinetic terms cannot be diagonalized simultaneously and there would be FCNCs.
3. If we switch off the charged-current interactions we should be able to use the symmetries of the bulk and IR brane to diagonalize the UV mixing matrices. This makes the neutral currents diagonal in the 4D mass basis and forbids tree-level FCNCs.

We will now see how this mechanism can be applied to various simple quark models.

The Left-Right Symmetric Representation

The simplest potentially realistic quark representation is the left-right symmetric representation, which has been adopted in [16, 20, 34]:

$$Q_L = \begin{pmatrix} u \\ d \end{pmatrix}_L \sim (2,1)_{1/6} \qquad Q_R = \begin{pmatrix} u \\ d \end{pmatrix}_R \sim (1,2)_{1/6} \tag{2.2.8}$$

We impose the boundary conditions $(+,+)$ on u_L and $(-,-)$ on u_R to obtain left-handed and right-handed zero modes (similarly for d). On the IR brane, both Q_L and Q_R are $SU(2)_D$ doublets, so we can write a Dirac mass mixing term [36] to lift the zero modes,

$$S_{\text{IR}} = \int d^5x \left(\frac{R}{z}\right)^4 \delta(z - R')\ M_D R'\ \overline{Q}_L Q_R + h.c. \tag{2.2.9}$$

On the UV brane, the Q_R doublet breaks up into two $SU(2)_L$ singlets, allowing us to assign brane-localized kinetic terms to u_R and d_R separately and supply the proper mass splitting.

If we want to implement the full 5D GIM mechanism using this representation, we populate the bulk with three copies of Q_L, Q_R and impose flavor symmetries $G_{\text{bulk}} = SU(3)_{Q_L} \times SU(3)_{Q_R}$ and $G_{\text{IR}} = SU(3)_D$. This makes the bulk masses c_{Q_L}, c_{Q_R} and the IR Dirac mass M_D flavor blind. On the UV brane we allow only kinetic mixing of the Q_R fields, which take the form

$$\int d^5x \left(\frac{R}{z}\right)^4 \delta(z - R)\psi^\alpha \sigma^\mu D_\mu K^{\alpha\beta}\overline{\psi}^\beta \tag{2.2.10}$$

for both u_R and d_R, where K_u, K_d are two independent hermitian matrices and α, β are flavor indices. To forbid left-handed mixing, we impose the flavor symmetry $G_{\text{UV}} = SU(3)_{Q_L} \times U(1)_{u_R} \times U(1)_{d_R}$.

If we switch off the charged-current interactions, the u, d symmetries become independent and $G_{\text{IR}} \to SU(3)_u \times SU(3)_d$, similarly in the bulk. These symmetries are broken on the

UV brane, but we can use them to diagonalize the K_u, K_d mixing matrices and end up with $G_{\rm UV} \supset U(1)_u^3 \times U(1)_d^3$, which prevents tree-level FCNCs. Another way to see this is as follows: since all other mass and kinetic terms in the action are flavor singlets, we can go to the 4D mass basis by rotating the fermions in flavor space and diagonalizing $K_{u,d}$. This pushes all the physical mixing into the charged-current couplings, giving us exactly the standard model CKM structure.

The main problem with this model is the top quark. To make it heavy, we must localize it close to the IR brane and make M_D large. The flavor symmetry then forces *all* the quarks to be close to the IR, generating a large negative S-parameter. The large flavor-blind M_D has two additional dangerous effects: Firstly, the $L-R$ mixing causes left-handed quarks to live partially in the R representation (and vice versa), which induces even more coupling corrections since it has the wrong quantum numbers. Secondly, the KK mixing causes the light quarks to live partially in KK modes, resulting in dangerously high couplings to gauge KK modes.

One could try to address these problems by increasing the $SU(2)_D$ IR kinetic term, which corresponds to adding a positive bare S parameter on the IR brane, but this is not viable. The matching of gauge couplings would force the coupling in the bulk to increase, lowering our cutoff to $\sim O(1\,\mathrm{T}eV)$ and making the theory non-perturbative before the unitarization mechanism of Higgsless RS models kicks in. We clearly need some way to protect the other quarks from deviations due to the heavy top mass.

The Custodially Protected Representation

Focusing on the third generation only for a moment, the problem with the left-right symmetric representation is that the effects of the top mass are felt by the left-handed bottom

(we can localize the right-handed bottom on the UV brane). Agashe et. al [21] realized that deviations to those couplings could be avoided if

- the t_R is not in the same representation as any field which can mix with b_L, so that the top can have a separate IR Dirac mass that is not communicated to the bottom, and
- the representations that house the left-handed b are symmetric under $SU(2)_L \leftrightarrow SU(2)_R$ interchange. This ensures that the L and R couplings are the same, meaning the b_L couples to a linear combination of gauge bosons which is flat near the IR brane. Its couplings are therefore protected from deviations due to the $SU(2)_L \times SU(2)_R \to SU(2)_D$ breaking.

In the notation of [22], the simplest representation which (almost) satisfies these requirements is:

$$\Psi_L = \begin{pmatrix} X_L & t_L \\ T_L & b_L \end{pmatrix} \sim (2,2)_{2/3} \qquad \Psi_R = \begin{pmatrix} X_R \\ T_R \\ b_R \end{pmatrix} \sim (1,3)_{2/3} \qquad t_R \sim (1,1)_{2/3} \quad (2.2.11)$$

For the t, b quarks we impose the same boundary conditions as for the quarks in the left-right symmetric representation, while we make the exotic T, X quarks (with electric charge $2/3$ and $5/3$ respectively) heavy by imposing mixed boundary conditions $(-,+)$ for X_L, T_L and $(+,-)$ for X_R, T_R.

On the IR brane, the Ψ_L bidoublet breaks down into an $SU(2)_D$ triplet and a singlet, which can mix with Ψ_R and t_R.

$$\Psi_L^{\text{triplet}} = \begin{pmatrix} X_L \\ \tilde{T}_L \\ b_L \end{pmatrix} \equiv \begin{pmatrix} X_L \\ \frac{1}{\sqrt{2}}(t_L + T_L) \\ b_L \end{pmatrix}, \qquad \Psi_L^{\text{singlet}} = \tilde{t}_L \equiv \tfrac{1}{\sqrt{2}}(t_L - T_L) \quad (2.2.12)$$

Hence the allowed Dirac mass term on the IR brane is

$$S_{\rm IR} = \int d^5x \left(\frac{R}{z}\right)^4 \delta(z - R')\ R' \left[M_3 \overline{\Psi}_R \Psi_L^{\rm triplet} + M_1 \bar{t}_R \Psi_L^{\rm singlet} + \text{h.c.}\right], \tag{2.2.13}$$

so we can make M_1 large to get a heavy top without influencing any field with the quantum numbers of the bottom. Also note that the custodial protection granted by this representation is not complete: KK-mixing via the M_3 mass term causes the left-handed b to live partially in b_R, which is *not* part of a $L \leftrightarrow R$ symmetric representation.[1] This turns out to be good thing, since the fully protected coupling is a few percent too large in Higgsless models (just the effect of the S-parameter). We can reduce it by localizing the b_R closer to the UV brane, which increases M_3 (for a given 4D bottom mass) and hence increases KK-mixing. This in turn decreases the coupling, since it makes the LH bottom sensitive to the gauge boson profiles near the IR brane.

The unique features of this representation allow us to implement the full 5D GIM mechanism in a rather different fashion from the previous case. To protect the up and charm quarks from the heavy top, we make M_1 different for each quark generation and forbid all up-sector flavor mixing, including on the UV brane. The down sector symmetries, on the other hand, are chosen very similarly to the left-right symmetric representation: M_3 is flavor blind and large enough to generate the *bottom* mass, and a kinetic mixing matrix K_d on the UV brane generates quark mixing in the down sector (and hence all the physical quark mixing). This amounts to imposing the flavor symmetry $G_{\rm bulk} = SU(3)_{\Psi_L} \times SU(3)_{\Psi_R} \times SU(3)_{u_R}$, which gets broken down to $G_{\rm IR} = SU(3)_{\rm triplets} \times U(1)_{\rm singlets}$ on the IR brane, and $G_{\rm UV} = SU(3)_{\Psi_L} \times U(1)_{d_R} \times SU(3)_{u_R}$ on the UV brane (we also set all brane kinetic terms for X, T fields to zero). FCNCs are prevented in the exact same fashion as for the left-right symmetric model, except we now only have to diagonalize the down sector.

[1] To make it $L \leftrightarrow R$ symmetric we would have to extend Ψ_R to a $(1,3) \oplus (3,1)$.

Nevertheless, a Higgsless quark model using *only* the custodially protected representation is not viable. Ψ_R must be close to the UV to match $g_{d_\ell^i d_\ell^i}$ to the SM. This fixes c_{d_R} while leaving the Ψ_L bulk mass c_L unconstrained due to custodial protection. The problem is a tension between the LH up-type couplings and the RH bottom coupling. $g_{Zu_\ell^i u_\ell^i}$ can only be matched if $\Psi_L \to$ UV, since it is not protected and suffers large corrections near the IR brane. $g_{Zb_r b_r}$ has the opposite requirement. If M_3 is the minimal value to give m_b, b_R lives entirely in the bulk. It must therefore be close to the UV brane to make it insensitive to the broken symmetry on the IR brane, which is not a problem. However, if $b_L \subset \Psi_L \to$ UV, then M_3 must be very large to generate m_b, which increases KK mixing and makes $g_{Zb_r b_r}$ sensitive to the IR brane again, reducing the coupling below SM. So while matching the LH up-type couplings to the SM requires $\Psi_L \to$ UV, the RH bottom coupling requires $\Psi_L \to$ IR. It is not possible to match both simultaneously. One might try to increase M_3 and confine the RH bottom to the UV brane, allowing Ψ_L to be closer to the UV, but this also increases T-mixing with the up-type quarks, which forces Ψ_L *even closer* to the UV to get a match. One cannot achieve overlap.

So while this model can protect the left-handed bottom couplings, the 5D GIM mechanism forces *all* the up-type quarks to behave like the troublesome top, and their couplings cannot be matched to the SM simultaneously with the RH bottom.

2.3 The NMFV Quark Model

The complete 5D GIM mechanism is too restrictive for Higgsless RS model-building. We have to give up a some flavor protection in exchange for agreement with electroweak precision data, while ensuring that FCNCs are still under control. This motivates us to combine both representations in a single quark model with *next-to minimal flavor violation*, harnessing

their complementing strengths while keeping as much flavor symmetry as possible.

2.3.1 Setup

Two copies of Q_L, Q_R with bulk masses c_{Q_L}, c_{Q_R} make up the first two generations, while the third generation is contained in the custodially protected Ψ_L, Ψ_R, t_R with bulk masses c_L, c_{b_R}, c_{t_R}. This protects the other quarks from the influence of the heavy top while enabling us to match all fermion couplings to experimental data. (Note that the top couplings are poorly constrained.) The form of the respective IR Dirac mass terms are given in equations (2.2.9) and (2.2.13). We impose the flavor symmetry $G_{\text{bulk}} = SU(2)_{Q_L} \times SU(2)_{Q_R}$ in the bulk, which is broken down to $G_{\text{IR}} = SU(2)_D$ on the IR brane. This means that the first two generations have the same IR Dirac mass M_D and bulk masses. The third generation has the IR Dirac masses M_3 for the $SU(2)_D$ triplet (which includes the bottom) and M_1 for the singlet (which supplies mass to the top). To provide flavor mixing and differentiate the quark masses of the first two generations, we must introduce general hermitian 3×3 kinetic mixing matrices K_u and K_d as in eq. (2.2.10). Therefore, the flavor symmetry on the UV brane is $G_{\text{UV}} = SU(3)_{Q_L} \times U(1)_{u_R} \times U(1)_{d_R}$ (where the third Q_L is contained in Ψ_L).

We can see immediately that there will be FCNCs in this model. The flavor symmetry is explicitly broken by choosing a different quark representation for the third generation. If we switch off the charged currents, we only have $SU(2)$ symmetries available, which are not enough to diagonalize the kinetic mixing matrices on the UV brane. However, as we will see, this partial symmetry is enough to force all mixing to go 'through the third generation' and suppress 12-mixings.

2.3.2 Going to 4D Mass Basis

We can solve the bulk equations with the appropriate BC's to compute the entire KK tower of fermion wave functions. After integrating out the 5^{th} dimension, we end up with a 4D action containing the following terms (using matrix notation in flavor/KK space):

$$\begin{aligned} \text{4D mass terms} \quad & \psi_{u,d} M_{u,d} \chi_{u,d}, \\ \text{RH kinetic mixing terms} \quad & \psi_{u,d}\ \sigma^\mu (\mathbb{1} + f_{u,d} K_{u,d} f_{u,d}) \partial_\mu \overline{\psi}_{u,d} \equiv \psi_{u,d}\ \sigma^\mu \kappa_{u,d} \partial_\mu \overline{\psi}_{u,d}, \\ \text{coupling terms like} \quad & \overline{\chi}_u \overline{\sigma}^\mu Z_\mu^{(n)} g^{(n)}_{Z u_L u_L} \chi_u, \end{aligned} \tag{2.3.1}$$

where (n) is a gauge boson KK index, $f_{u,d}$ is a diagonal matrix of the right-handed fermion wave functions evaluated at $z = R$, and $K_{u,d}$ is the UV brane kinetic mixing matrix.

To go to 4D mass basis, we must first diagonalize and canonically normalize the kinetic mixing term by rotating the RH spinors with a hermitian matrix H. Once the kinetic terms are flavor singlets we can diagonalize the mass matrices with the usual biunitary transformation. We will always distinguish quantities in the physical basis with a 'mass' superscript from quantities in the original flavor basis without superscript. The quark spinors in the mass basis are related to the flavor basis in the following way:

$$\begin{aligned} \chi_u &= U_{Lu} \chi_u^{\text{mass}} & \chi_d &= U_{Ld} \chi_u^{\text{mass}} \\ \overline{\psi}_u &= H_u U_{Ru} \overline{\psi}_u^{\text{mass}} & \overline{\psi}_d &= H_d U_{Rd} \overline{\psi}_d^{\text{mass}}. \end{aligned} \tag{2.3.2}$$

Applying this transformation to the the mass terms, the left/right-handed neutral couplings (denoted generically by g_L/g_R), and the left/right-handed W couplings, we get:

$$\begin{aligned} M_u^{\text{mass}} &= U_{Ru}^\dagger H_u^\dagger M_u U_{Lu} & M_d^{\text{mass}} &= U_{Rd}^\dagger H_d^\dagger M_d U_{Ld} \\ g_{Lu}^{\text{mass}} &= U_{Lu}^\dagger g_{Lu} U_{Lu} & g_{Ru}^{\text{mass}} &= U_{Ru}^\dagger H_u^\dagger g_{Ru} H_u U_{Ru} \\ g_{Ld}^{\text{mass}} &= U_{Ld}^\dagger g_{Ld} U_{Ld} & g_{Rd}^{\text{mass}} &= U_{Rd}^\dagger H_d^\dagger g_{Rd} H_d U_{Rd} \\ g_{W u_L d_L}^{\text{mass}} &= U_{Lu}^\dagger g_{W u_L d_L} U_{Ld} & g_{W u_R d_R}^{\text{mass}} &= U_{Ru}^\dagger H_u^\dagger g_{W u_R d_R} H_d U_{Rd} \end{aligned} \tag{2.3.3}$$

There is a very useful relation which we will need later. We simply write out $|M^{\text{mass}}|^2 = M^{\text{mass}\dagger}M^{\text{mass}} = M^{\text{mass}}M^{\text{mass}\dagger}$ (since M^{mass} is diagonal). Keeping in mind that the H matrices are hermitian and $H^2 = \kappa^{-1}$, we find

$$\begin{aligned} |M_u^{\text{mass}}|^2 &= U_{Lu}^\dagger \left(M_u^\dagger \kappa_u^{-1} M_u\right) U_{Lu} = U_{Ru}^\dagger H_u^\dagger M_u M_u^\dagger H_u U_{Ru} \\ |M_d^{\text{mass}}|^2 &= U_{Ld}^\dagger \left(M_d^\dagger \kappa_d^{-1} M_d\right) U_{Ld} = U_{Rd}^\dagger H_d^\dagger M_d M_d^\dagger H_d U_{Rd}. \end{aligned} \tag{2.3.4}$$

The exotic X-quark with charge 5/3 is an interesting experimental signature of our model. Its mass is roughly half a TeV and it couples to the top via charged-current interactions (in the flavor basis) with coupling strength comparable to but generically less than $g/\sqrt{2}$. The coupling in the mass basis is

$$\begin{aligned} g_{WX_Lu_L}^{\text{mass}} &= g_{WX_Lu_L} U_{Lu} \\ g_{WX_Ru_R}^{\text{mass}} &= g_{WX_Ru_R} H_u U_{Ru}. \end{aligned} \tag{2.3.5}$$

Detection could be possible at the LHC with less than 100 pb^{-1} of integrated luminosity [37].

2.3.3 Satisfying Electroweak Precision Data and CDF Bounds

It is not hard to see why this model can satisfy electroweak precision constraints. The heavy top mass does not influence the other quarks, and the correct bottom couplings can be achieved by moving $\Psi_L \supset t_L, b_L$ and t_R close to the IR brane, while the $\Psi_R \supset b_R$ is close to the UV [22]. The top couplings will deviate from the SM value, but this is acceptable since it is poorly constrained experimentally. The first- and second-generation couplings can be made to agree with the SM by adjusting $c_{Q_L}, c_{Q_R} \sim 0.5$, and we have enough freedom to choose IR Dirac masses and UV kinetic terms to generate all the different quark masses and mixings. It is worth noting that the $Q_{L,R}$ bulk masses can take on a range of values, due to the effect of KK-mixing which we will discuss in Section 2.3.5. We explicitly demonstrated

EWPD compliance using two different numerical calculations. In the first, we assumed that there is no flavor mixing and absorbed the diagonal boundary terms into BC's. In the second there was flavor mixing, and we followed the procedure of Section 2.3.2: using the zero mode approximation in which the boundary terms act as mixing terms between zero modes and KK modes.

One of the canonical signatures of Higgsless models are light gauge KK-modes with a mass of $\approx 700\text{G}eV$. This is low enough to warrant closer inspection of current CDF bounds [38–40] to make sure our model is not already excluded. The CDF searches for heavy gauge bosons focus on resonant pair production processes of the form (light quark pair) $\rightarrow$ (heavy gauge boson) $\rightarrow$ (some fermion pair, e.g. $e\bar{e}, t\bar{b}$). Assuming that the coupling to the heavy gauge boson is the same as to the SM counterpart for both the initial and final fermion states, the CDF bounds are $m_{W'}, m_{Z'} \gtrsim 800\text{G}eV$. However, those bounds must be adjusted for our model since the coupling of gauge KK modes is very suppressed for the first two quark generations, and somewhat enhanced for the third generation.

quark generation	approx. coupling as a multiple of SM		
	Z'	W'	G'
$1,2$ (LH)	$< 1/5$	$1/100$	$< 1/4$
$1,2$ (RH)	$1/5$	$1/100$	$1/4$
3	$2-4$	1	2

(2.3.6)

Since the light left-handed quarks are not UV-localized, their couplings depend sensitively on the bulk masses and can be very small. Leptons in our model would have similar couplings to the light quarks. It is clear that the coupling suppression increases the $m_{W'}, m_{Z'}$ bounds from leptonic and tb-channel searches way beyond our KK-scale of 700 GeV. Due to low $t\bar{t}$-detection efficiencies, the $t\bar{t}$-channel also does not supply a meaningful $m_{Z'}$ bound [39].

Only the constraints on $m_{G'}$ from [40] require closer inspection. Their analysis assumed

vector-like couplings to G' which were parameterized as $g_{\text{light quarks}} = \lambda_q g_s$ and $g_{top} = \lambda_Q g_s$. The bounds on $m_{G'}$ depend on $\lambda = \lambda_g \lambda_Q$ and the width Γ of G'. If we assume that we can use those bounds for our *chiral* couplings by simply averaging and setting $\lambda_q = \frac{1}{2}(\lambda_{q_L} + \lambda_{q_R}) \approx 0.25 - 0.5$, we can extract an approximate bound of $\Gamma/m_{G'} \gtrsim 0.2$ on the width of our KK-gluon if its mass is $\approx 700\text{G}eV$. We have not calculated the width of the G' since it depends on several parameters that are not completely fixed in our model, but $\Gamma/m_{G'} \sim 0.2$ is not an atypical value for RS KK-gluons, see for example [41]. Furthermore, we can also decrease λ by another factor of ~ 4 by taking into account 1-loop RGE corrections to the $SU(3)_c$ UV brane kinetic term, as outlined in Section 2.2.1. This alleviates any concern that our model might be excluded by CDF bounds. However, the relatively light G' should certainly be detected at the LHC.

2.3.4 Counting Physical Parameters and the Meaning of Large UV Kinetic Terms

Each $N \times N$ hermitian UV kinetic mixing matrix K_u, K_d is defined by N^2 parameters, $N(N+1)$ real elements and $N(N-1)$ complex phases. For $N = 3$, this gives a total of 12 real parameters and 6 phases. We can always do an $SU(2) \times U(1)$ flavor rotation, which corresponds to eliminating unphysical parameters: it removes 1 angle and 3 phases. This leaves us with 11 real parameters and 3 phases, which includes the 6 quark masses. Hence the parameters in the flavor sector are 6 quark masses, 5 mixing angles and 3 phases, as well as 3 IR Dirac masses M_D, M_1 and M_3.

At this point a remark about the *size* of the UV kinetic terms is in order. The $K_{u,d}$ matrix elements will be very large, generically $\sim [O(10^2) - O(10^9)]R$, but this is no cause for

concern. After canonically normalizing, the magnitude of the K's will merely specify what fraction of the fermions lives on the UV brane (i.e. is elementary in the AdS/CFT picture), and how much lives in the bulk (i.e. is composite). In our model the right-handed quarks are almost entirely confined to the UV brane, only slightly dipping into the bulk to mix with the left-handed quarks on the IR brane and generate a Dirac mass.

2.3.5 The Zero Mode Calculation

The fermion zero mode approximation enormously simplifies matching and mixing calculations, and we can use it to gain a great deal of insight into the flavor protection mechanisms of our model. However, KK mixing is much more significant for Higgsless models than for standard RS with multi-TeV KK masses, so we need to investigate the range of validity of this approximation in detail if we want to trust our calculations.

Error Estimate

Consider a simple toy-model with a single generation of quarks in the left-right symmetric representation eq. (2.2.8). There is a Dirac mass term on the IR brane (2.2.9) and a UV boundary kinetic term for the right-handed fields (2.2.10). Focusing only on the *left-handed* fields for the moment, we can incorporate the IR Dirac mass term into the $z = R'$ boundary conditions of the 5D wave function profiles [36], eliminating KK-mixing on the IR brane:

$$g_{u_R} = R' M_D g_{u_L}|_{z=R'}, \tag{2.3.7}$$

similarly for the down sector. We will assume that the errors are small and $c_{Q_L}, -c_{Q_R} > 0$.

If there was no IR mixing, g_{u_L} would just be the zero mode $g^0_{c_{Q_L}}$ (i.e. g_0 from eq. (2.2.7) with $c \to c_{Q_L}$), and adding a small amount of mixing should not change the shape of that

waveform significantly. The new mode that appears due to mixing is g_{u_R}, and its shape is also independent of the size of a small mass. Hence it should be the zero mode that is normally projected out when the BC's do not include any mixing, i.e. $g^0_{c_{Q_R}}$ (which is different from the usual RH zero mode $f^0_{c_{Q_R}} = g^0_{-c_{Q_R}}$). A simple ansatz to approximately solve the exact BCs is therefore

$$g_{u_L} = a g^0_{c_{Q_L}} \quad g_{u_R} = b g^0_{c_{Q_R}}. \tag{2.3.8}$$

Using the fermion normalization condition $\int dz (R/z)^4 (|g_{u_R}|^2 + |g_{u_L}|^2) = 1$ as well as eq. (2.3.7), we can solve for the coefficients a and b. Assuming the error is small, one obtains

$$a \approx 1 - \frac{1}{2}\left(R' M_D \frac{f(c_{Q_L})}{f(c_{Q_R})}\right)^2 \qquad b \approx \left(R' M_D \frac{f(c_{Q_L})}{f(c_{Q_R})}\right) \tag{2.3.9}$$

We can now estimate the deviation of a typical coupling to gauge boson Ψ compared to the zero mode approximation:

$$\int dz \left(\frac{R}{z}\right)^4 |g_{u_L}|^2 g_5 \Psi = \left[1 - \left(R' M_D \frac{f(c_{Q_L})}{f(c_{Q_R})}\right)^2\right] \int dz \left(\frac{R}{z}\right)^4 |g^0_{u_L}|^2 g_5 \Psi \tag{2.3.10}$$

The correction due to including the g_R is at most of similar order, and in fact much smaller for electroweak couplings since $|\Psi^{R3}| < |\Psi^{L3}|$ near the IR brane and $g^0_{c_{Q_R}}$ is extremely IR localized. Hence the zero mode approximation *overestimates* left-handed couplings by roughly

$$\delta_L \sim \left(R' M_D \frac{f(c_{Q_L})}{f(c_{Q_R})}\right)^2, \tag{2.3.11}$$

which is a *relative* error independent of the gauge charge. By a similar procedure we obtain the error for the right-handed couplings. It is simplest to *not* include the UV brane term in the BCs and simply renormalize the bulk wave function. Thus we find that the zero mode approximation *overestimates* right-handed couplings by

$$\delta_R \sim \left(\frac{R' M_D}{\sqrt{1 + K f^0_{u_R}(R)^2}} \frac{f(-c_{Q_R})}{f(-c_{Q_L})}\right)^2. \tag{2.3.12}$$

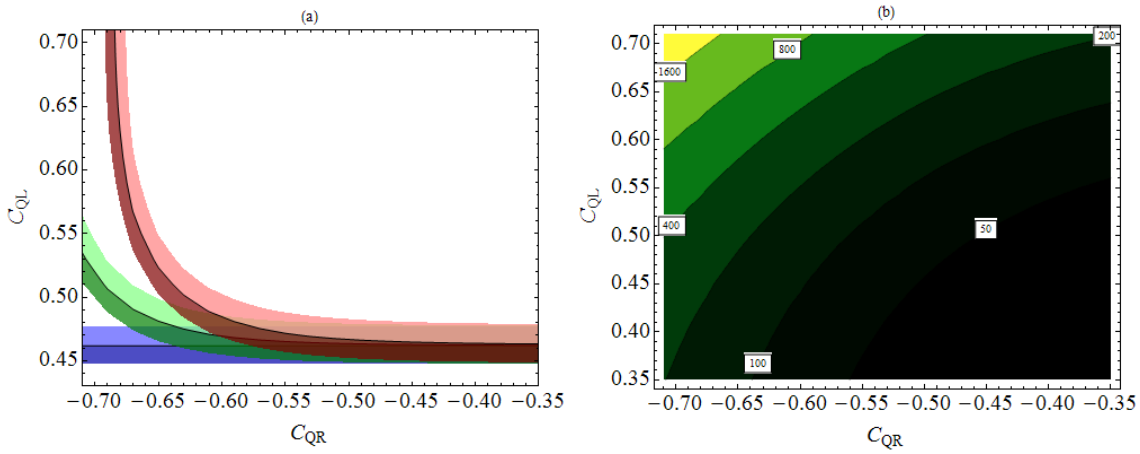

Figure 2.1: (a) shows the region of bulk masses that reproduces the SM couplings for the first quark generation with varying magnitudes of the IR brane mass. The three bands are for three values of $\rho_d = M_D/M_D^{\min}$, where $M_D^{\min}$ is the smallest possible IR brane Dirac mass which can reproduce the first generation masses. Darker (lighter) regions indicate that the coupling is up to 0.6% below (above) SM value. The blue (horizontal) band for $\rho_d = 1$ is reproduced by the zero mode approximation, and shows that Q_L must be almost flat and near the IR brane as expected. The green and red bands (successively more curved upwards) correspond to $\rho_d = 600$ and 1000, and we see significant shifts which allow the quarks to be UV localized. (b) shows $M_D^{\min}$ for the first generation in MeV. It is clear that increasing those brane terms by a factor of 1000 is not necessarily unreasonable, since it corresponds to a TeV scale M_D.

which is negligible unless the UV term is very small. Both of these error estimates have been confirmed numerically. Using eq. (2.2.3) we can express them as

$$\delta_L \sim \frac{M_D^2}{M_W^2 \log R'/R} \frac{f(c_{Q_L})^2}{f(c_{Q_R})^2} \qquad \delta_R \sim \frac{1}{1 + K f_{u_R}^0(R)^2} \frac{M_D^2}{M_W^2 \log R'/R} \frac{f(-c_{Q_R})^2}{f(-c_{Q_L})^2}. \tag{2.3.13}$$

To demonstrate how significant those errors can be, we computed the couplings in our toy model numerically for the first quark generation only, incorporating *both* UV and IR brane terms into boundary conditions. As fig. 2.1 shows, we find that one can now have *both* Q_L and Q_R localized near the UV brane without any S-parameter by turning up the value

of M_D! Thus one can get around the canonical assumption that fermions in Higgsless RS models must be almost flat and near the IR brane. If there is significant KK mixing on the IR brane, the fermions can be UV localized.

Using the Zero Mode Approximation for our Model

As we discussed in Section 2.3.3, we have used more accurate calculational methods to confirm that our model can satisfy electroweak precision constraints. The zero mode calculation without fermion KK-modes will only be used to estimate FCNC suppression. We must expect percent-level errors for all diagonal couplings and masses that do not involve the top, and $O(1)$ errors for the top mass and off-diagonal couplings in the up sector. Going from the zero mode calculation to full KK mixing preserves the general mixing hierarchy, but we would have to restore a full CKM match by adjusting the up-sector mixing angles by order unity. This level of accuracy is sufficient to estimate the tightly constrained down-sector FCNCs to within a few percent. Our estimate for D-mixing, on the other hand, will only be valid up to a factor of order unity, but this is enough to demonstrate our flavor suppression mechanism.

2.4 Flavor Matching and Protection in the NMFV Model

We will now analyze the flavor-protection mechanisms of the NMFV model in the framework of the zero-mode calculation. Our first task is to find the correct UV-localized right-handed kinetic mixing matrices K_u and K_d which reproduce the 4D CKM matrix. After obtaining a tree-level match to the Standard Model we proceed to find the off-diagonal neutral couplings which give rise to dangerous tree-level FCNCs.

2.4.1 Matching in the Zero Mode Approximation

Throughout this section we will drop the u, d subscripts whenever the derivations for the up- and down-sectors are identical. The problem of matching the zero mode calculation to the Standard Model factorizes into four steps:

1. Find bulk masses $c_{Q_R}, c_{Q_L}, c_{b_R}, c_{t_R}$ and c_L which give the correct quark couplings (noting that some deviation from SM is permissable for the top).
2. Choose a set of unitary matrices U_{Lu}, U_{Ld} that match $g^{\text{mass}}_{Wu_Ld_L} = U^\dagger_{Lu} g_{Wu_Ld_L} U_{Ld}$ to the experimental value of $\frac{g}{\sqrt{2}} V_{\text{CKM}}$. There is a lot of freedom to choose mixing matrices here, and we shall address it in Section 2.6.
3. Choose IR Dirac masses M_D, M_3 and M_1 which are at least big enough to supply the charm, bottom and top masses, and bigger if we want to confine the RH quarks to the UV brane.
4. Find the K_u, K_d kinetic matrices which are required to produce the SM masses and mixings.

The fourth step works as follows. The total kinetic term is $\kappa = \mathbb{1} + f_R K f_R$ (see eqn. 2.3.1), where $f_R = \text{Diag}(f_0^1, f_0^2, f_0^3)|_{z=R'}$ is the diagonal matrix of RH quark zero modes evaluated on the UV brane (note that $f_0^1 = f_0^2$ due to flavor symmetry). Using eq. (2.3.4) we can express κ in terms of quantities that we know:

$$|M^{\text{mass}}|^2 = U_L^\dagger (M^\dagger \kappa^{-1} M) U_L \qquad \Longrightarrow \qquad \kappa = M U_L \, |M^{\text{mass}}|^{-2} \, U_L^\dagger M^\dagger. \tag{2.4.1}$$

Hence we obtain an expression for the UV brane kinetic mixing matrix:

$$K = f_R^{-1} \left[M U_L \, |M^{\text{mass}}|^{-2} \, U_L^\dagger M^\dagger - 1 \right] f_R^{-1} \tag{2.4.2}$$

2.4.2 Flavor Protection

In the flavor basis, we can always write any left-handed neutral coupling as:

$$g_L = (g\Psi)_L \cdot \mathbb{1} + g_L^{\text{bulk}}, \tag{2.4.3}$$

where $(g\Psi)_L$ is the wave function of the gauge boson that the fermion couples to, evaluated on the UV brane and multiplied by the appropriate gauge coupling (in the AdS/CFT picture, this is the elementary part of the gauge boson). All the flavor non-universalities are contained in the diagonal matrix g_L^{bulk} which comes from bulk overlap integrals with the fermions (and corresponds to the composite gauge boson coupling). For a right-handed neutral coupling we also have the contribution from the UV kinetic term, which gives

$$g_R \;=\; (g\Psi)_R \cdot (\mathbb{1} + f_R K f_R) + g_R^{\text{bulk}} \;=\; (g\Psi)_R \cdot \kappa + g_R^{\text{bulk}}. \tag{2.4.4}$$

The form of K is known from eq. (2.4.2), and we can obtain the right-handed rotation matrix from eq. (2.3.3)

$$HU_R = \left(M^{\text{mass}} U_L^\dagger M^{-1}\right)^\dagger. \tag{2.4.5}$$

The left-handed couplings just rotate by U_L. This is all the information we need to transform the couplings into the physical basis, where the mass matrix is $M^{\text{mass}} = \text{Diag}(m_1^{\text{SM}}, m_2^{\text{SM}}, m_3^{\text{SM}})$.

Before we do that, however, it is useful to parameterize the IR Dirac masses in terms of roughly how large we want the UV kinetic terms to be, i.e. how strongly we want to confine the RH quarks to the UV brane. In the flavor basis, the mass matrix is

$$M = \text{Diag}(M_1, M_1, M_3), \tag{2.4.6}$$

where the flavor symmetry forces the first two terms to be the same and

$$\begin{aligned} M_1^{u,d} &= f(-c_{Q_R}) f(c_{Q_L}) M_D \quad \equiv \quad \rho_c m_c \\ M_3^d &= f(-c_{b_R}) f(c_L) M_3 \quad \equiv \quad \rho_b m_b \\ M_3^u &= f(-c_{t_R}) f(c_L) M_1/\sqrt{2} \quad \equiv \quad \rho_t m_t. \end{aligned} \tag{2.4.7}$$

$\rho_{c,b,t} = 1$ corresponds to choosing the minimal IR Dirac mass (and a correspondingly minimal UV kinetic term) which can generate the c, b, t 4D mass. $\rho_{c,b,t} > 1$ simply corresponds to increasing the IR Dirac mass by that factor, which also increases the UV kinetic term in order to keep the quark mass constant. This localizes the RH quark on the UV brane.

Now we can apply the basis transformations U_L and HU_R to eqns. (2.4.3) and (2.4.4). We obtain expressions for the physical 4D neutral couplings:

$$\begin{aligned} g_R^{\text{mass}} &= (g\Psi)_R \cdot \mathbb{1} + M^{\text{mass}} U_L^\dagger M^{-1} g_R^{\text{bulk}} (M^\dagger)^{-1} U_L M^{\text{mass}\dagger} \\ g_L^{\text{mass}} &= (g\Psi)_L \cdot \mathbb{1} + U_L^\dagger g_L^{\text{bulk}} U_L \end{aligned} \tag{2.4.8}$$

All the off-diagonal terms come from the flavor non-universal bulk part of the coupling, rotated by the appropriate transformation matrix.

Let us now find explicit expressions for these off-diagonal neutral coupling elements. Our flavor symmetry imposes $g_L^{\text{bulk}} \equiv \text{Diag}(g_L^{\text{bulk1}}, g_L^{\text{bulk1}}, g_L^{\text{bulk3}})$ and $g_R^{\text{bulk}} \equiv \text{Diag}(g_R^{\text{bulk1}}, g_R^{\text{bulk1}}, g_R^{\text{bulk3}})$. The most general form (ignoring phases) that U_L can take is:

$$U_L = \begin{pmatrix} c_{12}c_{13} & c_{13}s_{12} & s_{13} \\ -c_{23}s_{12} - c_{12}s_{13}s_{23} & c_{12}c_{23} - s_{12}s_{13}s_{23} & c_{13}s_{23} \\ -c_{12}c_{23}s_{13} + s_{12}s_{23} & -c_{23}s_{12}s_{13} - c_{12}s_{23} & c_{13}c_{23} \end{pmatrix} \tag{2.4.9}$$

If we assume completely anarchic UV mixing, the FCNC's will generically be too large. However, if one assumes Cabibbo-type hierarchies for both U_{Lu} and U_{Ld} mixing matrices,

$$s_{12} = O(1) \times \lambda \quad s_{23} = O(1) \times \lambda^2 \quad s_{13} = O(1) \times \lambda^3 \quad \lambda \sim 0.2, \tag{2.4.10}$$

then the flavor-changing effects will get an additional Cabibbo-suppression. This amounts to assuming that there is some systematic UV physics generating the mixing hierarchies. Substituting all this into eq. (2.4.8) and expanding to lowest order in λ, we obtain simple expressions for the off-diagonal neutral couplings. In the down sector,

$$\begin{aligned} g^{\text{mass}}_{Ld,ij} &\approx \left[g^{\text{bulk3}}_{Ld} - g^{\text{bulk1}}_{Ld}\right] U^{ji}_{Ld} && \text{where } i<j \\ g^{\text{mass}}_{Rd,ij} &\approx \left[\frac{g^{\text{bulk3}}_{Rd}}{\rho_b^2 m_b^2} - \frac{g^{\text{bulk1}}_{Rd}}{\rho_c^2 m_c^2}\right] m_d^j m_d^i U^{ji}_{Ld} && \text{and for } (i,j)=(1,2), \\ & && U^{ji}_{Ld} \to U^{32}_{Ld} U^{31}_{Ld}. \end{aligned} \tag{2.4.11}$$

For the up sector just change subscripts $d \to u$ and replace $\rho_b m_b$ by $\rho_t m_t$.

The flavor protection of our model is now apparent. Firstly, the surviving *flavor symmetry* between the first two generations forces all the mixing to go through the third generation (hence NMFV). This is vital to push D and K mixing below the stringent experimental bounds. Secondly, since we are free to increase $\rho > 1$, there is an *RS-GIM-like flavor suppression mechanism* for the right-handed fermion couplings. This is due to the kinetic mixing terms, which confine the right-handed quarks to the UV brane and suppress the bulk contributions to the couplings, which are the source of flavor violation. Finally, since the charged-current mixing matrix is made up of both the up- and down-sector mixing matrices, we have some freedom to 'divide up the mixing' between the two sectors and reduce FCNCs for each sector accordingly.

2.5 Estimating FCNCs for the NMFV Model

We are now in a position to estimate the FCNCs for our NMFV model and compare them to experimental bounds, as well as to a standard RS setup with a KK scale of $3\,\mathrm{T}eV$ and

anarchic Yukawa couplings, where the only flavor protection is due to RS-GIM (see for example [29]).

2.5.1 4-Fermi Operators

$\Delta F = 2$ FCNCs are mediated by the 4-fermi operators $C_{1,4,5}$. For the up sector (identically for the down sector), the relevant terms in the effective Lagrangian are given by

$$\begin{aligned} H^{(u)} &= C^{\alpha\beta\sigma\lambda}_{1L(\mathrm{u})}(\overline{q}^{\alpha}_{uL}\gamma_{\mu}q^{\beta}_{uL})(\overline{q}^{\sigma}_{uL}\gamma^{\mu}q^{\lambda}_{uL}) + \{L \to R\} + \\ & \quad C^{\alpha\beta\sigma\lambda}_{4(\mathrm{u})}(\overline{q}^{\alpha}_{uR}q^{\beta}_{uL})(\overline{q}^{\sigma}_{uL}q^{\lambda}_{uR}) + C^{\alpha\beta\sigma\lambda}_{5(\mathrm{u})}(\overline{q}^{c\alpha}_{uR}q^{d\beta}_{uL})(\overline{q}^{d\sigma}_{uL}q^{c\lambda}_{uR}), \end{aligned}$$

where greek letters denote flavor indices and c, d are color indices (if not shown, then color is contracted inside brackets). We will compute the FCNC operators by integrating out the massive gauge bosons, then compare them to UTfit bounds [42]. The most relevant constraints come from meson mixing processes, i.e. D mixing in the up sector and K, B_d and B_s mixing in the down sector:

$$C^{D}_{1L} = C^{1212}_{1L(\mathrm{u})} \qquad C^{K}_{1L} = C^{1212}_{1L(\mathrm{d})} \qquad C^{B_d}_{1L} = C^{1313}_{1L(\mathrm{d})} \qquad C^{B_s}_{1L} = C^{2323}_{1L(\mathrm{d})} \tag{2.5.1}$$

(similarly for C_{1R}, C_4, C_5). Integrating out the massive gauge bosons in our model, we obtain:

$$\begin{aligned} C^{\alpha\beta\alpha\beta}_{1L(\mathrm{u})} &= -\frac{1}{3}\sum_{\mathrm{KK}}\frac{1}{m_G^2}\left(g^{\alpha\beta}_{Gu_Lu_L}\right)^2 + \frac{1}{2}\sum_{\mathrm{KK}}\frac{1}{m_Z^2}\left(g^{\alpha\beta}_{Zu_Lu_L}\right)^2 \\ C^{\alpha\beta\alpha\beta}_{4(\mathrm{u})} &= -\sum_{\mathrm{KK}}\frac{1}{m_G^2}g^{\alpha\beta}_{Gu_Ru_R}g^{\alpha\beta}_{Gu_Lu_L} - 2\sum_{\mathrm{KK}}\frac{1}{m_Z^2}g^{\alpha\beta}_{Zu_Ru_R}g^{\alpha\beta}_{Zu_Lu_L} \\ C^{\alpha\beta\sigma\lambda}_{5(\mathrm{u})} &= -\frac{1}{3}\sum_{\mathrm{KK}}\frac{1}{m_G^2}g^{\alpha\beta}_{Gu_Ru_R}g^{\alpha\beta}_{Gu_Lu_L} \end{aligned} \tag{2.5.2}$$

where "KK" indicates that we sum over gauge KK modes, including the SM Z boson. For each operator, we define a suppression scale Λ by $|C| = \frac{1}{\Lambda^2}$.

2.5.2 G' contributions to FCNCs

We want to write down expressions for the suppression scales of the $C_{1,4,5}$ operators due to contributions of the first gluon KK-mode, which dominate if Z-couplings are matched to the SM and (almost) flavor universal. The mass of the first KK-gluon is given to 10% accuracy by

$$m_{G'} \approx \frac{x_1}{R'} \approx x_1 \sqrt{L} M_W \tag{2.5.3}$$

where we have used eq. (2.2.3), and $x_1 \approx 2.4$ is the first root of the bessel function $J_0(x_1) = 0$. The bulk part of its coupling to a left-handed zero mode is approximately

$$g_L^{\text{bulk}} \approx g_{S*} f(c_i)^2 \, \gamma(c_i) \equiv g_{S*} F(c), \tag{2.5.4}$$

where $\gamma(c) = \frac{\sqrt{2}}{J_1(x_1)} \int_0^1 x^{1-2c} J_1(x_1 x) dx \approx \frac{\sqrt{2}}{J_1(x_1)} \frac{0.7}{6-4c}(1 + e^{c/2})$ is an $O(1)$ numerical correction factor [29][1]. Gauge matching sets $g_{S*} = \sqrt{4\pi\alpha_S L}$, and we find that numerically, $m_{G'}/g_{S*} \approx 2M_W$.

Now put everything together by substituting eq. (2.5.4) into eq. (2.4.11), and using those couplings in eq. (2.5.2). We obtain the following expressions for the down-sector flavor suppression scales:

$$\begin{aligned}
\Lambda_{1L}^{(d)ij} &\approx \frac{2\sqrt{3} M_W}{U_{Ld}^{ij}} \left| F(c_{Q_L}) - F(c_L) \right|^{-1} \\
\Lambda_{1R}^{(d)ij} &\approx \frac{2\sqrt{3} M_W}{U_{Ld}^{ij}} \left| m_d^i m_d^j \left[\frac{F(-c_{Q_R})}{m_c^2 \rho_c^2} - \frac{F(-c_{b_R})}{m_b^2 \rho_b^2} \right] \right|^{-1} \\
\Lambda_4^{(d)ij} &\approx \frac{2 M_W}{U_{Ld}^{ij}} \left| m_d^i m_d^j \left[F(c_{Q_L}) - F(c_L) \right] \left[\frac{F(-c_{Q_R})}{m_c^2 \rho_c^2} - \frac{F(-c_{b_R})}{m_b^2 \rho_b^2} \right] \right|^{-1/2} \\
\Lambda_5^{(d)ij} &= \sqrt{3} \Lambda_4^{(d)ij}
\end{aligned} \tag{2.5.5}$$

[1]The accuracy of the approximate expression for $\gamma(c)$ in [29] is somewhat improved by replacing $x_1 \to (1 + e^{c/2})$

where we replace $U_{Ld}^{21} \to U_{Ld}^{31} U_{Ld}^{32}$. For the up sector just change subscripts $d \to u$ and replace $\rho_b m_b, c_{b_R}$ by $\rho_t m_t, c_{t_R}$.

To see that our model has sufficient flavor protection to satisfy FCNC constraints we plug in some typical numbers and compare them to the RS-GIM suppression and the UTfit experimental flavor bounds on BSM FCNC contributions [42][2]. The results are shown in Table 2.1 and demonstrate why we need all our suppression mechanisms. The RS-GIM-like mechanism for the right-handed couplings, together with the flavor symmetry, ensures that the C_4 and C_5 operators are easily below bounds, a great improvement on traditional RS-GIM alone. The suppression scales of the C_1 operators are set by $\Lambda_{1L} \ll \Lambda_{1R}$, which are only Cabibbo suppressed, with the direct 12 contribution forbidden by the $SU(2)$ flavor symmetry. This is another reason why we need the flavor symmetry – breaking it would increase 12-mixing by $\sim \lambda^4 \sim 500$, immediately violating bounds. Even with the flavor symmetry, the C_1 operators are close to bounds and the greatest source of angle constraints – indeed, we can see that most of the mixing will have to be in the up-sector.

2.5.3 Z contribution to FCNCs

We have not explicitly estimated FCNC contributions due to Z-exchange, however they are included in the numerical scans in Section 2.6. They are negligible for the down sector, since all three diagonal couplings are matched to the SM, but the top coupling deviates by $O(40\%)$ in the full calculation, generating off-diagonal terms in the up-sector. The scale of the Z' contributions to FCNCs (more important for LH than RH couplings, since $g_{Zu_\ell u_\ell} \approx 2 g_{Zu_r u_R}$)

[2]We evolve the UTfit bounds down to the KK scale using expressions in [43]. We thank Andreas Weiler for supplying the necessary code.

Parameter	$\Lambda_F^{\rm bound}(3\,{\rm T}eV)$	RS-GIM Λ_F	$\Lambda_F^{\rm bound}(0.7\,{\rm T}eV)$	NMFV Λ_F
${\rm Re}C_K^1$	$1.0\cdot 10^3$	$\sim r/(\sqrt{6}\,\lvert V_{td}V_{ts}\rvert f_{q_3}^2) = 23\cdot 10^3$	$1.1\cdot 10^3$	$44\cdot 10^3$
${\rm Re}C_K^4$	$12\cdot 10^3$	$\sim r(vY_*)/(\sqrt{2\,m_d m_s}) = 22\cdot 10^3$	$11\cdot 10^3$	$19000\cdot 10^3$
${\rm Re}C_K^5$	$10\cdot 10^3$	$\sim r(vY_*)/(\sqrt{6\,m_d m_s}) = 38\cdot 10^3$	$10\cdot 10^3$	$33000\cdot 10^3$
${\rm Im}C_K^1$	$16\cdot 10^3$	$\sim r/(\sqrt{6}\,\lvert V_{td}V_{ts}\rvert f_{q_3}^2) = 23\cdot 10^3$	$17\cdot 10^3$	$44\cdot 10^3$
${\rm Im}C_K^4$	$162\cdot 10^3$	$\sim r(vY_*)/(\sqrt{2\,m_d m_s}) = 22\cdot 10^3$	$150\cdot 10^3$	$19000\cdot 10^3$
${\rm Im}C_K^5$	$147\cdot 10^3$	$\sim r(vY_*)/(\sqrt{6\,m_d m_s}) = 38\cdot 10^3$	$150\cdot 10^3$	$33000\cdot 10^3$
$\lvert C_D^1\rvert$	$1.3\cdot 10^3$	$\sim r/(\sqrt{6}\,\lvert V_{ub}V_{cb}\rvert f_{q_3}^2) = 25\cdot 10^3$	$1.3\cdot 10^3$	$1.8\cdot 10^3$
$\lvert C_D^4\rvert$	$3.7\cdot 10^3$	$\sim r(vY_*)/(\sqrt{2\,m_u m_c}) = 12\cdot 10^3$	$3.5\cdot 10^3$	$200\cdot 10^3$
$\lvert C_D^5\rvert$	$1.4\cdot 10^3$	$\sim r(vY_*)/(\sqrt{6\,m_u m_c}) = 21\cdot 10^3$	$1.5\cdot 10^3$	$500\cdot 10^3$
$\lvert C_{B_d}^1\rvert$	$0.22\cdot 10^3$	$\sim r/(\sqrt{6}\,\lvert V_{tb}V_{td}\rvert f_{q_3}^2) = 1.2\cdot 10^3$	$0.22\cdot 10^3$	$0.35\cdot 10^3$
$\lvert C_{B_d}^4\rvert$	$1.7\cdot 10^3$	$\sim r(vY_*)/(\sqrt{2\,m_b m_d}) = 3.1\cdot 10^3$	$1.6\cdot 10^3$	$24\cdot 10^3$
$\lvert C_{B_d}^5\rvert$	$1.3\cdot 10^3$	$\sim r(vY_*)/(\sqrt{6\,m_b m_d}) = 5.4\cdot 10^3$	$1.4\cdot 10^3$	$41\cdot 10^3$
$\lvert C_{B_s}^1\rvert$	31	$\sim r/(\sqrt{6}\,\lvert V_{tb}V_{ts}\rvert f_{q_3}^2) = 270$	31	70
$\lvert C_{B_s}^4\rvert$	210	$\sim r(vY_*)/(\sqrt{2\,m_b m_s}) = 780$	190	1000
$\lvert C_{B_s}^5\rvert$	150	$\sim r(vY_*)/(\sqrt{6\,m_b m_s}) = 1400$	155	1800

Table 2.1: We compare lower bounds on the NP flavor scale Λ_F (all in TeV) for arbitrary NP flavor structure from the UTFit collaboration [42] to the effective suppression scale in RS-GIM [29] and our Higgsless NMFV model, see eq. (2.5.5). In this RS-GIM model, $|Y_*| \sim 3$, $f_{q_3} = 0.3$ and $r = m_G/g_{s*}$, with a KK scale of $\sim 3\,{\rm T}eV$. For the Higgsless model $L \approx 13$ determines a KK scale $m_G \approx 700{\rm G}eV$. Setting $\rho_c = 10$ gives $M_D = 110{\rm G}eV \sim 1/R'$, and $(c_{Q_L}, c_{Q_R}) = (0.48, -0.44)$ matches the couplings for the first two generations to the SM. A third generation EWPD match is most easily obtained for $\rho_{b,t} = 1$ and $(c_L, c_{b_R}, c_{t_R}) = (0.1, -0.73, 0)$. To satisfy the flavor bounds, we need to push more mixing into the up-sector by setting $\lambda^{-1}U^{13}_{L(d)} \sim U^{13}_{L(u)} \sim \lambda^3$ and $\lambda^{-1}U^{32}_{L(d)} \sim U^{32}_{L(u)} \sim \lambda^2$.

can be estimated using $C^1 \sim (g_L/m_{\rm KK})^2$ and compared to the gluon KK contribution:

$$O(0.4)\frac{g^{\rm SM}_{Zt_\ell t_\ell}}{m_Z} \sim \frac{1}{10^3{\rm G}eV} - \frac{1}{10^2{\rm G}eV} \qquad \text{and} \qquad \frac{g_{S*}F(c_L)}{m_G} \sim \frac{1}{10^2{\rm G}eV}. \tag{2.5.6}$$

Indeed, numerical scans in Section 2.6 show that Z contribution are negligible for all FCNC operators except C_D^1, where it does not invalidate the suppression mechanism but does supply a competitive contribution. In comparing FCNC's to experiment, one might worry that one has to take into account that the Z contributes to FCNCs at a much lower scale than the

KK modes. This is unnecessary, since the C_D^1 operator only changes by a few percent as we evolve it from our KK scale to the weak scale.

2.5.4 Contribution to FCNCs from Higher-Dimensional Operators in the 5D Action

Since 5D gauge theories are not renormalizable, our fermion action could include terms of the form

$$\int d^5x\sqrt{g}\frac{\Psi\overline{\Psi}\Psi\overline{\Psi}}{\Lambda^3}, \tag{2.5.7}$$

where $\Lambda = 16\pi/g_5^2 = \Lambda_{\text{cutoff}}R'/R$ (see eqn. 2.2.5) is the unwarped 5D cutoff. The $SU(2)$ flavor symmetry forbids contributions of this form to 12 mixing, but they do contribute for 13 and 23 mixing[3]. Since the right-handed quarks live almost entirely on the UV brane, where the cutoff is very high, we only have to worry about the left-handed quarks. The contribution to $C_{B_s}^1$ and $C_{B_d}^1$ is

$$\sim \frac{1}{\Lambda_{\text{cutoff}}^3}\int dz \left(\frac{R}{z}\right)^5 \left(\frac{R}{R'}\right) (g_{b_L}g_{d_L})^2 \sim \frac{1}{(200-500\,\text{T}eV)^2}, \tag{2.5.8}$$

depending on fermion localization. Comparing this to the experimental bounds in Table 2.1 of 31 and 22 TeV respectively, it is clear that we can ignore contributions by these operators.

2.6 Numerical Results and Mixing Constraints

We will now perform numerical scans to verify the results of the zero mode calculation and explicitly demonstrate that the Higgsless NMFV model can satisfy flavor constraints. This

[3]We thank Andreas Weiler for pointing this out.

is necessary because, once we have chosen our gauge sector, fermion bulk masses and IR brane terms, there is an overall rotation amongst the UV kinetic terms that is unconstrained by electroweak precision data and determines the FCNCs.

Our method for this scan is as follows: we will first perform some calculations without flavor mixing, which incorporate the diagonal brane terms into the boundary conditions to capture all KK mixing effects and match the SM couplings. Assuming any small flavor mixing would not change the diagonal couplings by much, we can use these calculations as a guideline in choosing our bulk and IR masses for a fully mixed calculation. We then explicitly calculate FCNCs for those input parameters by scanning over allowed down-sector mixing angles. This initial scan will be performed in the zero mode calculation for computational efficiency. Since there will likely be sizeable errors in the up-sector, we will take those points which passed FCNC bounds and recalculate them with full KK- and T-mixing, discarding those which now lie beyond bounds.

We should note that *exact* compliance with EWPD is not required for this scan, since a small adjustment to the input parameters (to correct any small deviations) would not change the FCNCs significantly. At any rate, using the zero mode calculation to match flavor rotations introduces order unity errors into the charged-current mixing angles, which would have to be corrected by readjusting the up-sector rotations. We can do without such complications, since we only strive for Cabibbo-*type* mixing in our scan, and most of the flavor constraints are in the down sector. If our scan indicates that FCNCs are under control for a general Cabibbo-type mixing, then they should also be under control for an exact CKM match.

2.6.1 Input Parameters

For our gauge sector, we choose $g_{5L} = g_{5R}$, $R^{-1} = 10^8 \mathrm{G}eV$ and set effective BKTs at the weak scale to zero or as small as possible. This gives $L \approx 13$ and the highest possible cutoff scale.

In order to match the bottom couplings, we set both M_1 and M_3 to their minimum values and move only the b_R close to the UV. From an unmixed calculation with full BCs we find the following values:

$$c_{b_R} = -0.73, \qquad c_{t_R} = 0, \qquad c_L = 0.1, \qquad M_1 = 600\mathrm{G}eV, \qquad M_3 = 140\mathrm{G}eV. \tag{2.6.1}$$

We also know that we need to ramp up M_D beyond its minimum value to satisfy constraints on the $C_{4,5}$ operators, so we choose $\rho_c = 10$. In order to pick bulk masses for the first two generations, we run another unmixed calculation with full boundary conditions and select three possible (c_{Q_L}, c_{Q_R}) values to run angle scans for:

Scan	1	2	3
c_{Q_R}	-0.37	-0.44	-0.57
c_{Q_L}	0.48	0.48	0.57
M_D (GeV)	76	101	445

2.6.2 Angle Scans

We will calculate FCNCs due to tree-level Z, Z', G', G''-exchange, for one million different down-sector mixings per scan. We can parametrize the CKM mixing matrix as

$$V(s_{12}, s_{23}, s_{13}, \delta) = \begin{pmatrix} c_{12}c_{13} & c_{13}s_{12} & s_{13}e^{-i\delta} \\ -c_{23}s_{12} - c_{12}s_{13}s_{23}e^{-i\delta} & c_{12}c_{23} - s_{12}s_{13}s_{23}e^{-i\delta} & c_{13}s_{23} \\ -c_{12}c_{23}s_{13}e^{-i\delta} + s_{12}s_{23} & -c_{23}s_{12}s_{13}e^{-i\delta} - c_{12}s_{23} & c_{13}c_{23} \end{pmatrix} \quad (2.6.2)$$

where, for example, $(s_{12}, s_{23}, s_{13}, \delta)_{\rm CKM} = (0.227, 0.0425, 4 \cdot 10^{-3}, 0.939)$ would satisfy the PDG constraints on $V_{\rm CKM}$ [3]. Naively, we would think that we can obtain the correct CKM matrix by defining our up- and down-sector LH rotations as

$$U_{Lu} = U V_{\rm CKM}^{\dagger} \qquad U_{Ld} = U, \quad (2.6.3)$$

and letting U be an arbitrary unitary rotation matrix which gives the down-sector mixing. This is sufficient for this scan, even though it only gives an order unity estimate of the up-sector mixing angles. In this analysis we shall also ignore phases, since we are after a scan of the *magnitudes* of the possible mixing matrices, and for our purposes we define $V_{\rm CKM} = V(s_{12}^{\rm CKM}, s_{23}^{\rm CKM}, s_{13}^{\rm CKM}, 0)$ (otherwise we could never cancel this matrix with a real rotation, introducing an up-mixing bias into our scan). To avoid obviously large FCNCs, we will make the assumption that the mixing angles of U have a *natural size* comparable to those of the final $V_{\rm CKM}$ mixing matrix. We parametrize U with angle-coordinates $(a, b, c) \sim O(1)$:

$$U = V(s_{12}, s_{23}, s_{13}, 0) \quad \text{where} \quad s_{12} = a s_{12}^{\rm CKM} \quad s_{23} = b s_{23}^{\rm CKM} \quad s_{13} = c s_{13}^{\rm CKM} \quad (2.6.4)$$

Note that $(a, b, c) = (0, 0, 0)$ and $(a, b, c) = (1, 1, 1)$ put all the mixing into the up- and down-sector respectively, so to avoid a bias in our scan we define the range of the angle coordinates to be $a, b, c \in (-2, 3)$. Once we determine which points in angle-space satisfy FCNCs in the zero mode calculation, we re-check those points using a full KK calculation.

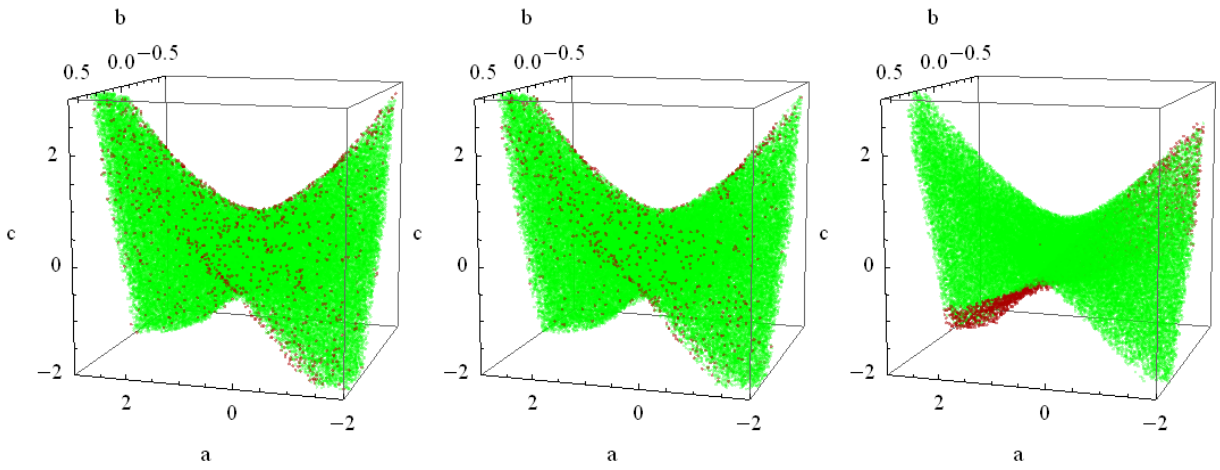

Figure 2.2: Left to right: Points in U_{Ld} angle space for scans 1, 2 and 3 that satisfy FCNC constraints in the zero mode calculation, where $s_{12} = as_{12}^{\text{CKM}}$, $s_{23} = bs_{23}^{\text{CKM}}$ and $s_{13} = cs_{13}^{\text{CKM}}$. Red (darker) points are found to violate the bounds when taking into account KK mixing.

2.6.3 Results

As we can see from the similar plots in fig. 2.2, the choice of bulk masses does not have a great effect on the nature of constraints on the down-mixing angles. This is expected since the C_1 operators, which are the greatest bottleneck, are only weakly dependent on c_{Q_R}, c_{Q_L} – the dominant contribution comes from the large $F(c_L)$, see eq. (2.5.5). In eliminating points which do not satisfy FCNC bounds with full KK mixing, we only loose a few percent of points in each scan. The zero mode calculation is therefore sufficient for estimating the angle constraints.

The FCNC bounds impose entirely systematic constraints on the down-sector mixing angles. This can be seen from fig. 2.3, where we take slices at different points on the b-axis (i.e. s_{23}) and project them onto an ac-plane. A point in angle-space satisfies FCNC bounds

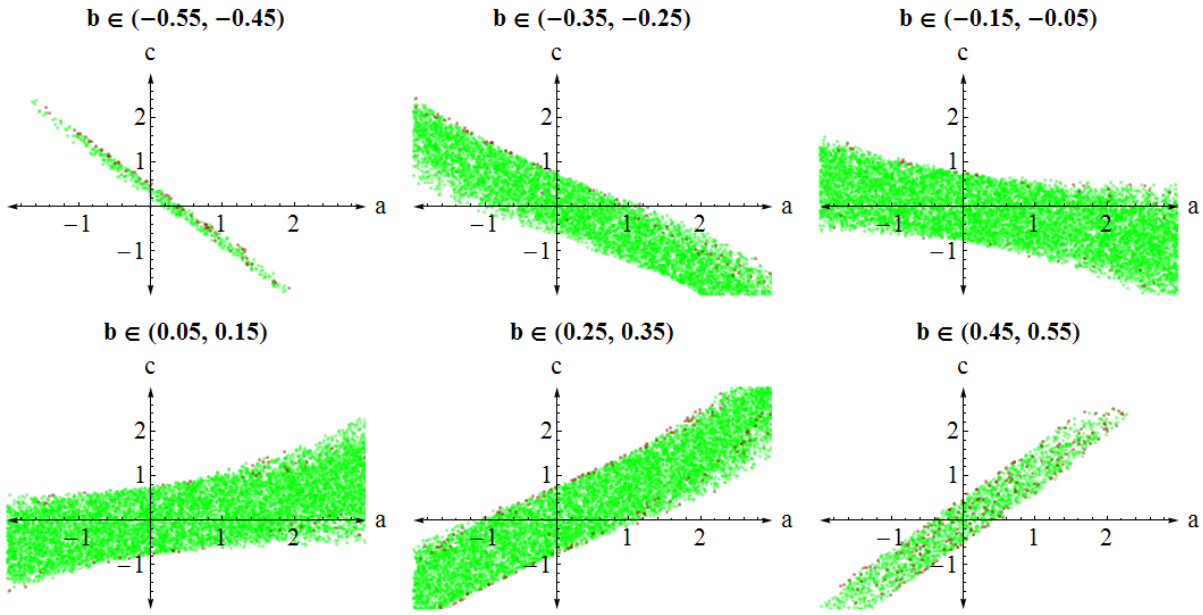

Figure 2.3: Slices of thickness 0.1 in the (a, c)-plane at different points along the b-axis, from $b = -0.5$ to $b = 0.5$, for scan 2 (scans 1 and 3 are similar). Green (light) points satisfy FCNC constraints in the zero mode calculation, and red (dark) points fail bounds when KK mixing is taken into account. The points which fail FCNC bounds in the zero mode calculation are not shown, but they fill up the entire remaining volume of angle space. There is *no overlap* between points satisfying FCNC bounds and points that do not – they occupy well defined, mutually exclusive volumes.

if and only if it lies within a well-defined sub-volume, i.e. the constraints are systematic. Assuming Cabibbo-type mixing, the good points occupy $\sim O(5\%)$ of the total angle space. This is not really 'tuning' in the usual sense, it merely means that whatever UV-scale mechanism generates the mixings should give a somewhat larger mixing in the up-sector than in the down-sector. We note that while s_{12} and s_{13} are correlated, their range is fairly unconstrained, whereas s_{23} must fall within strict limits to satisfy $C^1_{B_s}$ constraints. Roughly speaking, less than half the 23-mixing is allowed to be in the down sector.

We can conclude that our Higgsless NMFV model should have no trouble satisfying

FCNC bounds as long as certain systematic constraints on the down-sector mixing angles are met.

2.7 Conclusion

We examined various possibilities for Higgsless RS model-building, and constructed a model with next-to-minimal flavor violation satisfying tree-level electroweak precision and meson-mixing constraints, as well as CDF bounds. The theory has a sufficiently high cutoff of $\sim 8\,\mathrm{T}eV$ to unitarize WW-scattering at LHC energies, the third generation is in the custodial quark representation to protect the bottom couplings, and a combination of flavor symmetries and UV confinement of the right-handed quarks suppress FCNCs. Using numerical scans, we were able to demonstrate that our model can satisfy flavor bounds as long as the down-sector mixing angles are Cabibbo-type and satisfy systematic constraints. We also found quantitative error estimates for the zero mode approximation, which are important for RS model-building with a low KK scale.

This model has distinctive experimental signatures, allowing it to be excluded early on at the LHC. Apart from the absence of the Higgs, the usual Higgsless RS signals include [44] a relatively light G' with a mass below 1 TeV, as well as Z' and W' which are harder to detect (see Section 2.3.3). More specific to our setup is an exotic X-quark with charge 5/3 and a mass of $\sim 0.5\,\mathrm{T}eV$, which could be detected with less than 100 pb^{-1} of data [37]. This makes discovery or exclusion of this model imminent. The NMFV model also predicts non-zero correlated flavor-changing neutral currents, which lie relatively close to current experimental bounds and would be detected in the next generation of flavor experiments.

Acknowledgements

We are grateful to Andreas Weiler, Kaustubh Agashe and Yuval Grossman for many useful discussions and comments on the manuscript, and in particular we thank Andreas Weiler for his help with calculating the RGE evolution of the UTfit flavor bounds. This research has been supported in part by the NSF grant number NSF-PHY-0757868. C.C. was also supported in part by a U.S.-Israeli BSF grant.

CHAPTER 3

SINGLET-STABILIZED MINIMAL GAUGE MEDIATION

Based on the 2010 article "Singlet-Stabilized Minimal Gauge Mediation", written in collaboration with Yuhsin Tsai and published in Phys.Rev. D83 (2011) 075005.

3.1 Introduction

Supersymmetry (SUSY) is an extremely elegant proposed solution to the hierarchy problem in the Standard Model (SM). However, the question of how SUSY is broken and how this breaking is communicated to the Supersymmetric Standard Model (SSM) is far from settled. Over the years many approaches have been proposed, and one of the most promising avenues is Gauge Mediation [45, 46]. It automatically solves the SUSY flavor problem, since soft terms are generated by flavor-blind SM gauge interactions, and has the additional advantage of being calculable in many cases. The simplest GM models feature a single set of messengers that are charged under the SM gauge groups and couple to a SUSY-breaking hidden sector, generating the SSM soft masses through loop interactions (see [47] for a review). Many generalizations of this minimal theme exist in the literature (see, for example, [45,46,48–55]). For reasons of simplicity, models of Direct Gauge Mediation are particularly appealing since they do not require a separate messenger sector; the SUSY-breaking sector talks directly with the SSM [48, 49]. By defining General Gauge Mediation as any SUSY-breaking model where the soft masses vanish as the SM gauge couplings are taken to zero, it is possible to parametrize the effects of Gauge Mediation in a very model-independent fashion [54].

Gauge mediation does not answer the question of how SUSY is broken, and a large variety of SUSY-breaking models can act as its hidden sector. The most desirable scenario is a hidden sector which breaks supersymmetry dynamically.

Constructing models of dynamical SUSY breaking is extremely difficult, since the absence of any supersymmetric vacua imposes strong constraints on the theory [56]. Those requirements can be relaxed if we allow for the possibility that our universe lives in a long-lived *meta-stable* SUSY-breaking vacuum, and Intriligator, Seiberg and Shih (ISS) generated

enormous interest in 2006 when they demonstrated that such scenarios are fairly generic by showing that simple SUSY QCD with light quark masses can have metastable SUSY-breaking vacua near the origin of field space [53]. In the strict sense we speak of Dynamical SUSY Breaking as scenarios where the small SUSY-breaking scale is generated dynamically, which is not the case for ISS because the small electric quark mass has to be inserted by hand. However, it does break SUSY non-perturbatively from the point of view of the UV theory and is under full calculational control using the Seiberg Duality [57], which together with its sheer simplicity makes it an extremely attractive model-building arena for exploring SUSY-breaking and Direct Gauge Mediation, and several attempts were made to incorporate it into phenomenologically realistic models [50, 58–61].

The meta-stable ground state of the unmodified ISS model has an unbroken (approximate) R-symmetry that forbids gaugino masses. Breaking that symmetry spontaneously generates gaugino masses that are at least a factor of ~ 10 lighter than the sfermion masses. This is actually a generic feature of many Direct Gauge Mediation models, and the resulting split-SUSY-type spectrum is phenomenologically very undesirable since it exacerbates the little hierarchy problem. Explicit breaking [58, 59] can generate larger masses but creates new SUSY vacua and often creates a tension between reasonably large gaugino masses and stability of the ISS vacuum.

Recent work by Komargodski and Shih [62] sheds light on the issue. It was shown that the leading-order gaugino mass vanishes if the SUSY-breaking vacuum is stable within the renormalizable theory. This applies to unmodified ISS, where in the magnetic theory the SUSY-vacua only show up far out in field space through non-perturbative effects. The first example of a sufficiently destabilized ISS model was [58], and an existence-proof of an 'uplifted' model that is stabilized on a higher branch of the pseudomoduli space of massive SQCD was presented in [63], with later variations by [64–67].

This brings us to the motivation for this chapter. As is evident from the above discussion, there exists a large variety of ISS-based models of direct gauge mediation, uplifted or not. However, most of them share several shortcomings:

1. Landau pole in the SM gauge couplings below the GUT-scale due to (sometimes a very large amount of) excess matter in the hidden sector.
2. The addition of nongeneric or seemingly contrived couplings and deformations, which often break global symmetries. Often there is also an unexplained partial breaking of the hidden sector flavor symmetry, both to stabilize the vacuum and to embed the SM gauge group.
3. Often severe fine-tuning to stabilize the vacuum.

Putting aside the fine-tuning problem for the moment, we would like to address the first two issues. We construct a Direct Gauge Mediation model with an absolutely minimal SQCD sector which has no Landau Pole, no flavor symmetry breaking and (depending on one's judgement) no contrived deformations/couplings. The price we pay for this simplicity is the addition of the singlet sector proposed by [68]. We call this model *Singlet-Stabilized Minimal Gauge Mediation*. Our UV theory will be $SU(4)_C \times SU(5)_F$ s-confining SQCD [69] with a single quark mass scale. The IR theory has trivial gauge group and the standard model gauge group is identified with the $SU(5)_F$. There are two pseudomoduli spaces, the ISS branch with an $SU(4)$ flavor symmetry and a single uplifted branch with unbroken $SU(5)$. The vacuum is stabilized on the uplifted branch by the singlet sector. The spectrum of soft masses is precisely that of Minimal Gauge Mediation, the best possible solution from the point of view of the gaugino mass problem.

We also address an issue that may have not been explicitly discussed in the past: stabilizing an uplifted branch of massive SQCD requires *two* stabilization mechanisms: one each

for the adjoint and singlet components of the meson. This makes it extremely hard to avoid some meson deformations.

This chapter is laid out somewhat hierarchically. In Section 3.2 we outline the construction of our model and summarize all of the important results. Each summary refers to one of the later sections for details, but the essence of our work is contained in this short overview. The later chapters are organized as follows. A self-contained review of the ISS framework and related model building development is given in Section 3.3. Based on the need for two stabilization mechanisms we derive some guidelines for building uplifted ISS models in Section 3.4. We then move on to slightly more detailed discussions of the overall vacuum structure and spectrum (Section 3.5), implementation of Direct Gauge Mediation to get ISS-based model of Minimal Gauge Mediation (Section 3.6) and the mechanism of stabilizing the uplifted vacuum (Section 3.7). We conclude with Section 3.8.

3.2 Overview of the SSMGM Model

We would like to build a model of direct gauge mediation based on the ISS model [53] that avoids both light gauginos and Landau Poles. *A review of the ISS framework for metastable SUSY braking and direct gauge mediation can be found in section Section 3.3.* In this section we summarize the highlights of our model and its main physical consequences, while the details of the analysis are deferred to Sections 3.4 - 3.7.

In this chapter, we construct the smallest possible ISS model stabilized on the highest possible pseudomoduli space to ensure that all messengers contribute to the gaugino mass (i.e. we get Minimal Gauge Mediation). This model has no Landau Pole due to minimal excess matter and no flavor breaking. The uplifted vacuum is stabilized via a separate singlet

sector, so we call this setup *Singlet-Stabilized Minimal Gauge Mediation* (SSMGM).

Constructing the Magnetic Theory

We want a trivial low-energy gauge group and an $SU(N_f) = SU(5)$ flavor symmetry. This means the electric theory must be s-confining [69], and strictly speaking it is inaccurate to speak of a *magnetic* theory – at low energies we use a *confined* description, where the fundamental degrees of freedom are just the baryons and mesons of the original theory. However, s-confining SQCD displays similar metastable SUSY-breaking behavior as free magnetic SQCD, so in the interest of using familiar ISS-terminology we shall refer to the confined description as 'magnetic' and the baryons as 'magnetic squarks'.

For this choice of electric theory, pseudomoduli space of the magnetic theory only has two branches: the ISS vacuum corresponding to $k = 1$ (i.e. the magnetic squarks get a VEV) and an uplifted branch corresponding to $k = 0$ (i.e. no squarks get a VEV). If we could stabilize the uplifted branch we can identify the SM gauge group with the unbroken $SU(5)$ flavor group. The squarks would then act as a pair of Minimal Gauge Mediation messengers and generate gaugino masses at leading order in SUSY-breaking. The authors of [63] have shown that meson deformations alone cannot achieve this stabilizations for such a small flavor group. Therefore, the price we pay for the pleasing minimality in the SQCD sector is the addition of a singlet sector with its own $U(1)$ gauge group, which spontaneously breaks the $U(1)_R$ symmetry by the inverted hierarchy mechanism [70] and stabilizes the uplifted vacuum.

In the magnetic description of the ISS model, the field content is

		$SU(N_f)$	$U(1)_B$	$U(1)_R$	$U(1)_S$
SQCD sector	ϕ^i	$\square$	1	0	0
	$\bar{\phi}_j$	$\overline{\square}$	-1	0	0
	M	Adj + 1	0	2	0
singlet sector	S	1	0	0	1
	$\overline{S}$	1	0	0	-1
	Z	1	0	2	1
	$\overline{Z}$	1	0	2	-1

(3.2.1)

where $U(1)_S$ is the gauge group of the singlet sector with coupling g. The complete superpotential is

$$W = h\bar{\phi}_i M^i_j \phi^j + (-hf^2 + dS\bar{S})\mathrm{Tr}M + m'(Z\bar{S} + S\bar{Z}) - a\frac{\det M}{|\Lambda|^{N_f-3}} + m_{adj}\mathrm{Tr}(M'^2), \quad (3.2.2)$$

where a, h are unknown positive $O(1)$ numbers and f, m' are mass scales (which can be complex) much smaller than Λ. The instanton term breaks the approximate $U(1)_R$ symmetry and restores SUSY for large meson VEVs. To explain the last term, decompose the meson into singlet and adjoint components $M = M_{sing} + M_{adj}$. The M' denotes the traceless part of the meson, meaning the deformation only gives a mass to M_{adj}. This is necessary because the singlet sector couples to M_{sing} and stabilizes it away from the origin, but M_{adj} is tachyonic at the origin in the uplifted pseudomoduli space. Therefore, unfortunately, we must give it a mass by hand – this is a general feature of uplifted ISS models. *For the derivation of this model-building requirement, please refer to Section 3.4.*

The Corresponding Electric Theory & Scales of the Model

The electric description is an augmented massive s-confining SQCD with gauge group $SU(N_f - 1) = SU(4)$ and superpotential

$$W = \left(\tilde{f} + \frac{\tilde{d}}{\Lambda_{UV}} S\bar{S} \right) \mathrm{Tr} Q\bar{Q} + m'(Z\bar{S} + S\bar{Z}) + \frac{\tilde{a}}{\Lambda_{UV}} \mathrm{Tr}\big(Q\bar{Q}\big)'^2, \tag{3.2.3}$$

where $\tilde{a}$ is assumed to be some $O(1)$ number. We make no attempt at explaining the origin of the small quark mass term (see [61] for example). $\Lambda_{UV} > \Lambda$ is the scale of some UV-physics which generates the non-renormalizable $SSQ\overline{Q}$, $Q\overline{Q}Q\overline{Q}$ terms. The natural sizes of the IR parameters are therefore

$$d \sim \frac{\Lambda}{\Lambda_{UV}}, \qquad h \sim 1 \qquad m_{adj} \sim \frac{\Lambda^2}{\Lambda_{UV}} \sim d\Lambda. \tag{3.2.4}$$

To protect the Seiberg Duality transition from the physics at scale Λ_{UV}, we conservatively require $\Lambda_{UV} \gtrsim 100\Lambda$. The masses f and m' are free parameters as long as they are both smaller than $\sim \Lambda/100$.

A natural choice for Λ_{UV} would be either the GUT-scale or the Planck-scale, with Λ at least two orders of magnitude below that. In Section 3.7.2 we show that decreasing Λ much below $\sim \Lambda_{UV}/100$ makes it increasingly harder to construct uplifted metastable vacua. One can understand this quite simply as the coupling between the singlet sector and the SQCD sector becoming too weak to stabilize the magnetic meson against the effect of the instanton term, which wants to push the meson towards a supersymmetric vacuum far out in field space. This favors making Λ as large as possible and justifies choosing two plausible scenarios for us to consider:

	Λ	Λ_{UV}
Scenario 1	10^{16}	10^{18}
Scenario 2	10^{14}	10^{16}

(all masses in GeV), setting $d \sim 0.01$.

The Uplifted Vacuum

Ignoring the instanton term near the origin, F_M is given by

$$-F^*_{M^i_j} = h\bar{\phi}_i\phi^j - (hf^2 - dS\bar{S})\delta^j_i. \tag{3.2.5}$$

Since the first term has maximal rank 1 and the second term has maximal rank 5, some F-terms must be nonzero, breaking SUSY by the rank condition. We want to live in the uplifted vacuum, so we set $\langle\overline{\phi}\phi\rangle = 0$. The singlets then obtain nonzero VEV whenever $r = \sqrt{N_f hd}\ f/m' > 1$, in which case $F_Z, F_{\overline{Z}} \neq 0$ so the singlets participate in the SUSY-breaking. Some of the $\phi, \overline{\phi}$ are tachyonic for

$$\langle|M_{sing}|\rangle < \frac{m'}{\sqrt{hd}}, \tag{3.2.6}$$

but 1-loop corrections from the messengers and the singlet sector give the meson a VEV at

$$\langle|M_{sing}|\rangle \sim \sqrt{\frac{h}{d}}f, \tag{3.2.7}$$

which is large enough to stabilize the messengers and give a viable uplifted vacuum. *A complete discussion of the vacuum structure and spectrum is given in Section 3.5.*

Implementing Direct Gauge Mediation

If we identify the $SU(5)$ flavor group with the SM GUT gauge group and live in the uplifted vacuum, we obtain a model of direct gauge mediation with a single pair of $(5+\overline{5})$ messengers

$\phi, \overline{\phi}$. Since the messengers are tachyonic for small VEVs of the meson M they generate gaugino masses at lowest order in SUSY-breaking – in fact, this is just an uplifted-ISS implementation of standard Minimal Gauge Mediation. There is no Landau pole, and the singlet degrees of freedom are all heavier than the messengers (except for the pseudomodulus, goldstino and R-axion). *See Section 3.6 for details.*

Stabilizing the Uplifted Vacuum

The one-loop potential from the messengers tries to push the pseudomodulus (and hence the meson) towards the origin where the messengers are tachyonic, while the singlet sector contribution pushes it away from the origin. To cancel these competing contributions and create a local minimum it is necessary to adjust the ratio m'/f to a precision of roughly

$$\Delta \sim \left(\frac{\Lambda}{\Lambda_{UV}}\right)^2, \tag{3.2.8}$$

which is $\sim 10^{-4}$ in our two scenarios. The tuning could be significantly reduced if one were less conservative about the separation of the two scales Λ, Λ_{UV}.

In our scenarios the smallness of d compared to the other couplings raises the question of whether a one-loop analysis can be trusted. We show that two-loop corrections involving the larger couplings do not invalidate our analysis, because they neither influence the non-trivial part of the effective potential which generates the minimum, nor make it impossible to cancel the other smooth contributions to high enough precision so that this interesting part survives. Therefore, the meson can always be stabilized away from the origin.

Finally one must check that decays of the uplifted vacuum to both the ISS and the SUSY vacuum are suppressed enough to make the lifetime longer than the age of the universe. This is indeed the case for our model, since the bounce actions for decay to the ISS and SUSY vacua are enhanced by $(\Lambda_{UV}/\Lambda)^2$ and $\sqrt{\Lambda/f}$ respectively.

See Section 3.7 for a detailed discussion on stabilization of the uplifted vacuum, the effect of two-loop corrections and calculation of the vacuum lifetime.

3.3 Reviewing the ISS Framework

This section provides a brief summary of the ISS framework and related model building developments which form the basis of this chapter. After outlining the general need for metastable SUSY-breaking in gauge mediation we review the original ISS model as well as its more recent uplifted incarnations.

3.3.1 The necessity of metastable SUSY-breaking

The reasons for pursuing theories of meta-stable SUSY-breaking go beyond the significant model-building simplifications they potentially afford.

One possible argument goes as follows: A generic theory that breaks SUSY in its ground state must have an R-symmetry (see e.g. [71] for a review). Since this forbids gaugino masses the R-symmetry must be broken. If the R-symmetry is only spontaneously broken one might think that the massless R-axion causes cosmological and astrophysical problems, necessitating explicit R-breaking. By the Nelson-Seiberg theorem [72], this causes supersymmetric vacua to come in from infinity, making the SUSY-breaking vacuum metastable. However, [73] show that supergravity effects give the R-axion a mass, provided that the cosmological constant is tuned away, even if R-symmetry is merely spontaneously broken in the global SUSY theory. Therefore, avoiding a massless R-axion is *not* a reason for metastable SUSY-breaking. (It is still possible that the R-breaking effects of gravity do in fact desta-

bilize the SUSY-breaking vacuum, but it is not known whether the Nelson-Seiberg theorem applies in this case.)[1]

Within the framework of Direct Gauge Mediation there is, however, another very good reason for believing in meta-stable SUSY-breaking. As first noticed in [49], many models of Direct Gauge Mediation suffer from very small gaugino masses compared to the sfermions. This resuls in a split-SUSY-type spectrum which reintroduces fine tuning into the Higgs Sector. Komargodski and Shih [62] explored this issue in a relatively model-independent way by examining generalized O'Raifeartaigh models (renormalizable Wess-Zumino models which break supersymmetry and have canonical Kahler potentials)[2]. These theories form the low-energy effective description for the hidden sector of many direct gauge mediation scenarios.

Any generalized O'Raifeartaigh model features tree-level flat directions called pseudo-moduli emanating from the SUSY-breaking vacuum. The pseudomodulus is the superpartner of the Goldstino, and is stabilized somewhere on the pseudomoduli space by quantum corrections. One can always write the model in the form

$$W = fX + (\lambda X + m)_{ij}\psi^i\psi^j + O(\psi^3) \tag{3.3.1}$$

where the scalar part of X is the pseudomodulus. If we take the ψ's to come in $5 + \bar{5}$ pairs of $SU(5)$ then this is an example of Extra-Ordinary Gauge Mediation [55]. To leading order in the SUSY-breaking parameter F/X^2, the gaugino mass is given by

$$m_\lambda \propto f\frac{\partial}{\partial X}\log\det(\lambda X + m)_{\text{messengers}}. \tag{3.3.2}$$

One can show that if there are no tachyons for any choice of X (i.e. the pseudomoduli space is locally stable everywhere), then $\det(\lambda X + m) = \det m$. Therefore, if the pseudomoduli space

[1] We thank Zohar Komargodski and Jesse Thaler for pointing this out to us.

[2] [74] and [75] extend this discussion to semi-Direct Gauge Mediation and models with non-canonical Kahler terms, respectively.

is stable everywhere, the gaugino masses vanish at leading order. Since sfermion masses are created at leading order, we have a split-SUSY spectrum.

This shows that in models of Direct Gauge Mediation, the problem of the anomalously small gaugino mass is related to the vacuum structure of the theory. In order to have a gaugino mass at leading order in SUSY-breaking, it is necessary to live in a metastable vacuum from which lower-lying vacua (SUSY-breaking or not) are accessible within the renormalizable theory. SUSY-vacua created by non-perturbative effects far out in field space do not generate a large gaugino mass. (Notice that Minimal Gauge Mediation corresponds to $m = 0$ and a single messenger pair, so the messengers are tachyonic for $X^2 < F$ and large gaugino masses are generated.)

Since the gaugino mass formula eq. (3.3.2) is only valid to lowest order in F/X^2 one might think that sizeable gaugino masses could be generated for large SUSY-breaking. We conducted a small study within the framework of Extra-Ordinary Gauge Mediation using both analytical and numerical techniques, and like many before us [47,76], we conclude that the gaugino-to-sfermion mass ratio $m_\lambda/m_{\tilde{f}}$ can not be tuned to be larger than $\sim 1/10$ due to a curious numerical suppression of the subleading terms.

3.3.2 The ISS Model

The authors of [53] considered UV-free SQCD with an $SU(N_c)$ gauge group and N_f flavors of electric quarks with a small mass term

$$W = mQ^i\bar{Q}_i \tag{3.3.3}$$

where $m \ll \Lambda$, denoting Λ as the strong coupling scale of the theory. In the free magnetic phase $N_c < N_f < \frac{3}{2}N_c$, the low-energy theory can be studied using Seiberg Duality [57] and

is simply IR-free SQCD with an $SU(N_f - N_c)$ gauge group, a gauge singlet meson Φ and N_f flavors of magnetic quarks $q, \bar{q}$, as well as a Landau Pole at scale Λ_m.

Writing $N = N_f - N_c < \frac{1}{3}N_f$, the symmetries of the IR theory are $[SU(N)] \times SU(N_f) \times U(1)_B \times U(1)_R$ (gauged symmetries in square brackets)[3]. The fields have charges Φ: $(1, \text{Adj}+1)_{0,2}$, q: $(N, \bar{N}_f)_{1,0}$ and $\bar{q}$: $(\bar{N}, N_f)_{-1,0}$. The Kahler terms of the low-energy effective degrees of freedom are canonical and the superpotential is

$$W = hq_i^a \Phi_j^i \bar{q}_a^j - h\mu^2 \Phi_i^i \tag{3.3.4}$$

where $a, b, \ldots$ are gauge indices and $i, j, \ldots$ are flavor indices and $\mu \sim \sqrt{\Lambda m}$.

The Φ F-terms are

$$-F^*_{\Phi^i_j} = hq_i^a \bar{q}_a^j - h\mu^2 \delta_j^i. \tag{3.3.5}$$

They cannot all be zero, since the first term has rank at most N and the second term has rank $N_f \geq 3N$, so supersymmetry is broken *by the rank condition.* Expanding around the vacuum, the fields can be written as

$$\Phi = \begin{array}{c} \overset{N \quad N_F-N}{\left(\begin{array}{cc} V & Y \\ \overline{Y} & Z \end{array}\right)} \begin{array}{c} N \\ N_F-N \end{array} \end{array} \qquad q = \begin{array}{c} \overset{N \qquad\qquad N_F-N}{\left(\begin{array}{cc} \mu + \chi_1 & \rho_1 \end{array}\right)} N \end{array} \qquad \overline{q} = \begin{array}{c} \overset{N}{\left(\begin{array}{c} \mu + \overline{\chi}_1 \\ \overline{\rho}_1 \end{array}\right)} \begin{array}{c} N \\ N_F-N \end{array} \end{array} \tag{3.3.6}$$

with matrix dimensions indicated. (Writing the squark fields with a subscript 1 will be useful for comparison to the uplifted ISS case.) The gauge symmetry is completely higgsed by the squark VEVs, and the surviving global symmetry is $SU(N)_{diag} \times SU(N_f - N) \times U(1)_{B'} \times U(1)_R$. The spectrum divides into distinct sectors. (We take μ to be real for simplicity, and prime denotes traceless part.)

[3]We emphasize that this $U(1)_R$ symmetry is anomalous under magnetic gauge interactions, which leads to the non-perturbative restoration of supersymmetry discussed below.

1. V and $(\chi_1 + \bar{\chi}_1)$ get mass $\sim |h\mu|$ whereas $(\chi_1 - \bar{\chi}_1)'$ gets eaten by the magnetic gauge supermultiplet via the superHiggs mechanism. This part of the spectrum is supersymmetric at tree-level.

2. $\mathrm{Tr}(\chi_1 - \bar{\chi}_1)$: the fermion is massless at tree level and the real part of the scalar is a classically flat direction (a pseudomodulus) which gets stabilized at zero. Both these fields obtain a mass at loop-level. The imaginary part of the scalar is the Goldstone boson of a broken $U(1)$ symmetry (a mixture of $U(1)_B$ and a diagonal $SU(N_f)$ generator) and is massless to all orders. This part of the spectrum can be made massive by gauging the $U(1)$ symmetry.

3. Z is another pseudomodulus which gets stabilized at the origin and obtains a loop-suppressed mass.

4. $Y, \bar{Y}, \mathrm{Im}(\rho_1 + \bar{\rho}_1), \mathrm{Re}(\rho_1 - \bar{\rho}_1)$ get masses $\sim |h\mu|$. $\mathrm{Re}(\rho_1 + \bar{\rho}_1), \mathrm{Im}(\rho_1 - \bar{\rho}_1)$ are goldstone bosons of the broken flavor symmetry and massless

In the original ISS model as it is defined above, both pseudomoduli are stabilized at the origin by quantum corrections and get a loop-suppressed mass. This leaves the R-symmetry unbroken and forbids gaugino masses, so for use in realistic scenarios of direct gauge mediation the ISS model must be modified somehow to break R-symmetry.

In the magnetic theory supersymmetry is restored non-perturbatively: for large Φ the squarks get a large mass and can be integrated out, leaving a pure SYM theory which undergoes gaugino condensation and has SUSY-vacua at

$$\langle q \rangle = 0, \qquad \langle \bar{q} \rangle = 0, \qquad \langle \Phi \rangle_{\mathrm{SUSY}} = \Lambda_m \left(\frac{\mu}{\Lambda_m} \right)^{2N/N_f - N} \mathbb{1}. \tag{3.3.7}$$

This makes the SUSY-breaking vacuum at the orgin meta-stable, but the smallness of the ratio μ/Λ_m guarantees that the false vacuum is parametrically long-lived.

We can understand this metastability in terms of the connection between R-symmetry and SUSY-breaking. The UV theory does not have an exact R-symmetry, but it emerges as an *accidental* symmetry near the origin of the IR theory. That $U(1)_R$ is anomalous under gauge interactions and hence SUSY is restored by non-perturbative operators far out in field space. The 'smallness' of the explicit R-breaking near the origin guarantees that the SUSY-breaking vacuum is long-lived.

Since it will be of special interest to us later we should make a comment about the s-confining case of $N_f = N_c + 1$ [69]. The magnetic gauge group is trivial, but SUSY is still restored far out in field space. This is due to the slightly modified dual superpotential, which includes what looks like an instanton term:

$$W = h\mathrm{Tr}q\Phi\bar{q} - h\mathrm{Tr}\mu^2\Phi + c\frac{1}{\Lambda^{Nf-3}}\det\Phi. \tag{3.3.8}$$

Modifying the ISS model for Direct Gauge Mediation

The ISS model looks like a promising framework for models of Direct Gauge Mediation. For example, one could gauge the unbroken $SU(N_f - N)$ flavor symmetry and embed the SM gauge group, which would give gauge charges to the (anti-)fundamentals $\rho_1, \bar{\rho}_1, Y, \bar{Y}$ and make them Extra-Ordinary Gauge Mediation [55] messengers, as well as the Adjoint+Singlet Z. The main obstacle to such a construction is the unbroken R-symmetry in the original ISS model. (Many variations which break $U(1)_R$ spontaneously or explicitly have been proposed, and this discussion is not meant to be exhaustive.) Models with meson deformations [58, 59] add operators of the form $\sim \frac{1}{\Lambda_{UV}} Q\bar{Q}Q\bar{Q}$ in the UV theory which gives operators $\sim \Phi^2$ in the IR theory with suppressed coefficients. This explicitly breaks the R-symmetry and gives the singlet component of the meson a VEV, generating a gaugino mass. These deformations also make the (shifted) ISS-vacuum more unstable because new SUSY-vacua are introduced. This

is per se desirable, since a nonzero gaugino mass at leading order in SUSY-breaking requires the existence of lower-lying vacua within the renormalizable theory, however there is a strong tension between making the gaugino mass somewhat comparable to the sfermion mass and making the vacuum too unstable. Another possibility is adding a baryon deformation to the superpotential, which in the example of [60] involves adding a Λ_{UV}^2-suppressed operator in the UV theory and breaking R-symmetry spontaneously, generating a very small gaugino mass. A third possibility is the addition of a singlet-sector with its own $U(1)$ gauge symmetry to break R-symmetry spontaneously [61,68] via the Inverted Hierarchy Mechanism [70]. This again gives a small gaugino mass, and the parameters have to be fine-tuned to stabilize the vacuum.

A common problem with these embeddings is the existence of a Landau Pole, primarily due to the existence of the SM-charged adjoint meson, and some of them also feature non-generic couplings or deformations with somewhat non-trivial flavor contractions.

3.3.3 Uplifting the ISS Model

It would be desirable to obtain a large gaugino mass in a direct gauge mediation model derived from massive SQCD (mSQCD). Adding meson deformations introduces new vacua and generates a gaugino mass at leading order, but the strong tension between stability and sizeable gaugino masses motivates the search for a different kind of metastability: finding a new stable vacuum in a higher branch of the pseudomoduli space of mSQCD ('uplifting' the vacuum). This possibility was first realized by Giveon, Katz and Komargodski [63], and we will sketch out their results below.

We start with the same UV theory as the standard ISS model eq. (3.3.3). In the ISS

vacuum, the squark VEV matrix has rank$\langle q\bar{q}\rangle = N$. However, there are higher, unstable pseudomoduli spaces with rank$\langle q\bar{q}\rangle = k$, with $k = 0, 1, 2, \ldots N-1$. If we assume the squark VEV matrix has rank $k < N$ the surviving symmetry is $[SU(N-k)] \times SU(k)_D \times SU(N_f - k) \times U(1)_{B'} \times U(1)_{B''}$. (As we will see we must assume that the meson is stabilized at a nonzero value, breaking the $U(1)_R$ symmetry.) We expand around the squark VEV and split the fields into representations of the unbroken symmetries:

$$\Phi = \begin{array}{c} \begin{array}{cc} k & N_F-k \end{array} \\ \left(\begin{array}{cc} V & Y \\ \overline{Y} & Z \end{array}\right) \end{array} \begin{array}{c} k \\ N_F-k \end{array} \qquad q = \begin{array}{c} \begin{array}{cc} k & N_F-k \end{array} \\ \left(\begin{array}{cc} \mu+\chi_1 & \rho_1 \\ \chi_2 & \rho_2 \end{array}\right) \end{array} \begin{array}{c} k \\ N-k \end{array} \qquad \overline{q} = \begin{array}{c} \begin{array}{cc} k & N-k \end{array} \\ \left(\begin{array}{cc} \mu+\overline{\chi}_1 & \overline{\chi}_2 \\ \overline{\rho}_1 & \overline{\rho}_2 \end{array}\right) \end{array} \begin{array}{c} k \\ N_F-k \end{array} \tag{3.3.9}$$

The spectrum can again be described in terms of a few separate sectors:

1. $(\chi_2 \pm \bar{\chi}_2)$, $(\chi_1 - \bar{\chi}_1)$ get eaten by the massive gauge supermultiplets. Notice how $\mathrm{Tr}(\chi_1 - \bar{\chi}_1)$ is no longer massless at tree-level because the broken $U(1)$ is a mixture between a gauged diagonal generator and the $U(1)_B$.
2. V, $(\chi_1 + \bar{\chi}_1)$ get F-term mass $\sim |h\mu|$
3. The Y, ρ, Z-type fields can be analyzed separately. The $(Y, \bar{Y}, \rho_1, \bar{\rho}_1)$ fields obtain Z-dependent masses and contain $2k(N_f - k)$ flavor goldstone bosons. In a scenario of Extra-Ordinary Gauge Mediation, these fields constitute messengers that are stable for all Z and hence do not contribute to the gaugino mass. The $(\rho_2, \bar{\rho}_2)$ scalars are tachyonic for $|Z| < |\mu|$, as we would expect from living on an uplifted pseudomoduli space, but if Z can be stabilized at a large-enough value they too are stable and act as messengers which *do* contribute to the gaugino mass at leading order.

The model-building quest is now to break R-symmetry and stabilize the Z at a large enough value to ensure that all scalars are non-tachyonic. The authors of [63] show that in a

renormalizable Wess-Zumino model, no stable SUSY-breaking minimum exists for VEVs much above the highest mass scale of the theory. Hence stabilizing $Z > \mu$ is not feasible in the original model. They circumvent this problem by introducing a *mass hierarchy* into the quark masses, with the first k flavors having mass μ_1 and the remaining $N_f - k$ flavors having a much smaller mass μ_2. This means that the $\rho_2, \bar{\rho}_2$ fields are tachyonic for $Z < \mu_2 \ll \mu_1$, so stabilizing the meson VEV in the region $\mu_2 < Z < \mu_1$ is possible. They achieve this stabilization for large flavor groups and k close to N by adding finely-tuned meson deformations $\mathrm{Tr}(Z^2)$, $(\mathrm{Tr}Z)^2$. This model is a very important proof-of-principle and it does achieve sizeable gaugino masses as desired, but its drawbacks (Landau pole & non-minimal hidden sector, imposed flavor-breaking mass hierarchies and meson deformations) motivated further research into stabilizing an uplifted ISS model.

Further Developments in Stabilizing Uplifted ISS

There have since been other attempts at stabilizing the uplifted ISS model. [65] examined the equivalent case for $SO(10)$-unified Direct Gauge Mediation, [64] considered stabilization using SUGRA, and issues of cosmological vacuum selection were discussed in [66]. Stabilization of an uplifted ISS model via baryon deformations was investigated in [67], and while a stable vacuum can be achieved this way for much smaller flavor groups than the proof-of-principle case discussed above, that model also features many non-renormalizable operators with non-trivial flavor contractions and non-generic couplings, as well as an explicit breaking of the hidden sector flavor symmetry. It is in this context that we are motivated to construct an uplifted ISS model with a minimal hidden sector.

3.4 The Adjoint Instability

Before introducing our minimal uplifted ISS model in the next section we examine the general requirements for stabilizing a higher pseudomoduli space of massive SQCD (mSQCD). We emphasize a hitherto neglected point: there must actually be *two* stabilization mechanisms, one for the singlet and one for the adjoint component of the $SU(N_f - k)$ meson Z. This in turn yields to some very general requirements on model building, which suggest that single-trace meson deformations are very hard to avoid in uplifted ISS models.

3.4.1 The messenger contribution to $V_{\rm eff}(Z)$

Let us examine an uplifted pseudomoduli space in the unmodified ISS model. (We will later add some structure to stabilize it.) The $SU(N_f - k)$ meson Z is a pseudomodulus which is flat at tree-level. The leading contribution to its potential arises from one-loop corrections to the vacuum energy and can be computed using the Coleman-Weinberg formula

$$V_{\rm CW} = \frac{1}{64\pi^2}{\rm STr}M^4 \log\frac{M^2}{\Lambda_m^2} \tag{3.4.1}$$

where Λ_m is the cutoff of the magnetic theory. Since the tree-level spectrum of the magnetic gauge vector multiplet is supersymmetric it does not contribute at one-loop level, and by inspecting the superpotential it is clear that the masses of $V, (\chi_1 + \bar{\chi}_1)$ do not depend on Z at tree-level. Therefore, we only need to consider the dependence of the ρ, Y-type spectrum on Z to determine its 1-loop potential. The relevant part of the superpotential is

$$\frac{1}{h}W_Z = -\mu_2^2 Z_i^i + \rho_{2\,j} Z_i^j \bar{\rho}_2^i + \rho_{1\,j} Z_i^j \bar{\rho}_1^i + \mu_1(\rho_{1\,i}\bar{Y}^i + Y_i \bar{\rho}_1^i) \tag{3.4.2}$$

where i, j are $SU(N_f - k)$ flavor indices and we hide the trivial color contractions. We have also implemented the flavor-breaking of [63] for generality.

Since $V_{\rm CW}$ due to messengers is generated by single planar Z-loops, it can only depend on single-trace combinations of the form $\mathrm{Tr}[(ZZ^\dagger)^n]$. Furthermore, even if $\langle Z\rangle$ breaks the flavor symmetry, we can use broken $SU(N_f-k)$ generators to diagonalize $\langle Z\rangle$. Therefore it is justified to diagonalize Z and treat the diagonal components separately. It is then easy to verify that $V_{\rm CW}^{\rm mess}$ slopes towards the region where $\rho_2, \bar{\rho}_2$ become tachyonic.

It is instructive to phrase this familiar argument in a slightly different way. Decompose the meson Z into adjoint and singlet components:

$$Z_j^i = Z_{adj}^A T^{A\,i}_{\ \ j} + Z_{sing} T_S \tag{3.4.3}$$

where T^A are the usual $SU(N_F-k)$-generators with a slightly modified canonical normalization due to the Z being a complex scalar: $\mathrm{Tr}T^AT^B = \delta^{AB}$, $T_S = \frac{1}{\sqrt{N_F-k}}\mathbb{1}$. Our basic dynamical degrees of freedom are then the $(N_f-k)^2-1$ complex fields Z_{adj}^A and the flavor singlet complex field Z_{sing}.

We can do a flavor transformation and push all the VEV of the adjoint into one of the diagonal generators. Call this generator $\tilde{T}_{adj}$ and the associated meson component $\tilde{Z}_{adj}$. Then

$$\langle Z\rangle = \langle \tilde{Z}_{adj}\rangle \tilde{T}_{adj} + \langle Z_{sing}\rangle T_S \tag{3.4.4}$$

Replacing $Z \to \tilde{Z}_{adj}\tilde{T}_{adj} + Z_{sing}T_S$ in $\mathrm{Tr}[(ZZ^\dagger)^n]$ we can see that the expression is symmetric under exchange of $\tilde{Z}_{adj}$ and Z_{sing}, since the generators satisfy $\mathrm{Tr}T_S\tilde{T}_{adj} = 0$ and $\mathrm{Tr}T^2 = 1$. *The single-trace condition is therefore equivalent to saying that the adjoint and the singlet components make identical contributions to* $V_{\rm CW}$. Hence the behavior of $V_{\rm CW}^{\rm mess}$ is dictated by its dependence on the singlet component.

3.4.2 Model Building Requirements for Stabilizing Z

This reasoning shows that uplifted ISS models really need *two* stabilization mechanisms: (i) Z_{sing} must be stabilized at a nonzero VEV large enough to make the messengers non-tachyonic, and (ii) Z_{adj} must be stabilized at zero VEV. If the effective potential is a single-trace object then both requirements are automatically satisfied. However, if only the singlet is stabilized (separately from the adjoint) then the vacuum will be unstable along the Z_{adj} direction and the fields roll towards the lower-lying ISS vacuum. We call this phenomenon the *Adjoint Instability*, and it has direct model building implications. Stabilizing the adjoint in an uplifted vacuum can be done in two ways.

1. Add an additional flavor adjoint. This would allow us to give Z_{adj} a mass (either at tree-level or, more indirectly, at 1-loop).
2. Alternatively, to obtain an effective Z_{adj}^2 term we can do one of the following:
   (a) Break R-symmetry explicitly by adding meson deformations like $(\mathrm{Tr}Z)^2, \mathrm{Tr}(Z^2)$.
   (b) Break R-symmetry spontaneously, e.g. by introducing a field A with R-charge -2 which somehow gets a VEV and gives a mass to the adjoint via the coupling $W \supset AMM$.

Adding a flavor adjoint would greatly exacerbate the Landau Pole Problem, and Option 2 (b) is not very attractive because the corresponding operators in the UV would be even more non-renormalizable than meson deformations. (Not to mention the additional machinery required to give A its VEV.) 2 (a) seems like the best solution.

This was also the path taken by the authors of [63]. They stabilize the vacuum by effectively adding a *single*-trace deformation $\mathrm{Tr}(Z^2)$. This deformation treats the singlet and the adjoint equally, and therefore stabilizing the singlet also stabilizes the adjoint. To

lift the mass of Z_{adj} and avoid a Landau Pole below Λ_m without destabilizing the nonzero singlet VEV they must then add another single-trace deformation $\mathrm{Tr}(Z_{adj}^2)$. [67] must also include a single-trace meson deformation to stabilize the meson.

This leads us to conclude that meson deformations $\sim \frac{1}{\Lambda_{UV}} Q\bar{Q}Q\bar{Q}$ are extremely hard to avoid in mSQCD models with meta-stable SUSY-breaking vacua on uplifted pseudomoduli spaces.

3.5 Vacuum Structure & Spectrum

Near the origin of field space there are two branches of the pseudomoduli space for this model. One is the ISS vacuum, where $k = \mathrm{rank}\langle\bar{\phi}\phi\rangle = 1$ and the flavor symmetry is broken down to $SU(N_f - 1)$. The other is the uplifted vacuum where $k = \mathrm{rank}\langle\bar{\phi}\phi\rangle = 0$, i.e. no squark VEV. To solve the gaugino mass problem we must stabilize the uplifted vacuum. Before we can analyze that stabilization, we must understand the structure of the vacuum manifold at tree-level.

3.5.1 The Uplifted Vacuum $(k = 0)$

We want to live in this uplifted vacuum without squark VEVs to solve the gaugino mass problem. With the meson decomposed into singlet and adjoint components, the superpotential

is

$$\begin{aligned} W &= h\,\bar{\phi}\cdot M_{adj}\cdot\phi + m_{adj}\mathrm{Tr}(M_{adj}^2) \\ &\quad + \left[\frac{h\bar{\phi}\phi}{\sqrt{N_f}} + \sqrt{N_f}\left(-hf^2 + dS\bar{S}\right)\right] M_{sing} + m'(Z\bar{S} + S\bar{Z}) \\ &\quad - \frac{a}{N_f^{N_f/2}}\frac{M_{sing}^{N_f}}{|\Lambda|^{N_f-3}} + \ldots \end{aligned} \tag{3.5.1}$$

where we have omitted Λ-suppressed interactions of M_{adj}. For simplicity, let f, m' and Λ as well as a, h be real and positive throughout this analysis. For now we simply assume that the singlet sector stabilizes M_{sing} at large enough VEV to make the messengers non-tachyonic, and we postpone the detailed discussion of stabilizing the uplifted vacuum to Section 3.7.

Tree-level VEVs near origin of field space

Close to the origin of field space we can ignore the instanton term in determining the VEVs of the fields. For $\langle M_{ad}\rangle = 0$ and $\langle\bar{\phi}\phi\rangle = 0$ we then only need to analyze the second line of eq. (3.5.1) and the tree-level potential for the singlet scalar VEVs becomes

$$\begin{aligned} V_{tree} &\to \frac{1}{2}g^2\left(|S|^2 + |Z|^2 - |\bar{S}|^2 - |\bar{Z}|^2\right) \\ &\quad + \left|d\sqrt{N_f}M_{sing}S + m'Z\right|^2 + \left|d\sqrt{N_f}M_{sing}\bar{S} + m'\bar{Z}\right|^2 \\ &\quad + N_f\left|dS\bar{S} - hf^2\right|^2 + \left|m'S\right|^2 + \left|m'\bar{S}\right|^2 \end{aligned} \tag{3.5.2}$$

The first line is the D-term potential for the singlet $U(1)_S$ gauge group, and can be set to zero by imposing $|S| = |\bar{S}|, |Z| = |\bar{Z}|$. The $F_{S,\bar{S}}$-terms in the second line vanish for

$$\langle Z\rangle = -d\sqrt{N_f}\frac{\langle M_{sing}S\rangle}{m'}, \qquad \langle\bar{Z}\rangle = -d\sqrt{N_f}\frac{\langle M_{sing}\bar{S}\rangle}{m'}. \tag{3.5.3}$$

This leaves the last line as the potential for $S, \bar{S}$, which implies

$$\langle S\bar{S}\rangle = \frac{hf^2}{d} - \frac{m'^2}{d^2N_f} \quad \text{whenever} \quad r > 1 \quad \text{where} \quad r = \sqrt{N_f h d}\frac{f}{m'}. \tag{3.5.4}$$

(Often it is convenient to parametrize f in terms of r, as we will see below.) We will assume that this condition is satisfied so that the singlets get a VEV and break the $U(1)_S$ gauge symmetry, which in turn can lead to spontaneous R-symmetry breaking via the inverted hierarchy mechanism. The only nonzero F-terms are

$$\langle F_{M_{sing}} \rangle = -\frac{m'^2}{d\sqrt{N_f}}, \qquad \langle F_{Z,\bar{Z}} \rangle = \frac{m'^2}{d\sqrt{N_f}} \sqrt{\frac{hf^2 dN_f}{m'^2} - 1}, \tag{3.5.5}$$

and the total vacuum energy is

$$\langle V_0^{k=0} \rangle = 2hf^2 \frac{m'^2}{d} - \frac{m'^4}{d^2 N_f} \tag{3.5.6}$$

To be precise we decompose all the complex scalar singlets into amplitudes and phases:

$$S = \sigma_S e^{i\frac{\pi_S}{\langle \sigma_S \rangle}}, \qquad Z = \sigma_Z e^{i\frac{\pi_Z}{\langle \sigma_Z \rangle}}, \qquad M_{sing} = \sigma_{M_{sing}} e^{i\frac{\pi_{M_{sing}}}{\langle \sigma_{M_{sing}} \rangle}}, \qquad \text{etc.} \tag{3.5.7}$$

This reveals that of the 5 phases, three are fixed at tree-level whereas the other two are the $U(1)_S$ Nambu-Goldstone boson and the R-axion

$$\pi_R = \frac{1}{F_{tot}} \left(|F_{M_{sing}}| \pi_{M_{sing}} + |F_Z| \pi_Z + |F_{\bar{Z}}| \pi_{\bar{Z}} \right) \quad \propto \quad \langle \sigma_{M_{sing}} \rangle \pi_{M_{sing}} + \langle \sigma_Z \rangle \pi_Z + \langle \sigma_{\bar{Z}} \rangle \pi_{\bar{Z}} \tag{3.5.8}$$

respectively. Of the 5 amplitudes, one combination

$$\sigma_{\rm PM} = \frac{1}{F_{tot}} \left(|F_{M_{sing}}| \sigma_{M_{sing}} + |F_Z| \sigma_Z + |F_{\bar{Z}}| \sigma_{\bar{Z}} \right) \tag{3.5.9}$$

is undetermined at tree-level. This is the pseudomodulus, part of the scalar superpartner of the Goldstino, and since its value affects the masses of the other particles this flat direction is lifted at 1-loop, see eq. (3.4.1).

Tree-level spectrum

The M_{adj} has mass m_{adj}. The messenger fermion and scalar masses are

$$m_\phi = \frac{h}{\sqrt{N_f}} M_{sing} \qquad m_{\tilde{\phi}}^2 = m_\phi^2 \pm \frac{h}{dN_f} m'^2. \tag{3.5.10}$$

Quantum corrections need to stabilize M_{sing} in a region where the messengers are not tachyonic, hence we require

$$\langle |M_{sing}| \rangle > \frac{m'}{\sqrt{hd}}. \tag{3.5.11}$$

We define the singlet sector to mean the superfields $S, \bar{S}, Z, \bar{Z}, M_{sing}$ and the vector superfield of the $U(1)_S$. The singlet spectrum is complicated and we discuss it in detail when analyzing the stabilization of the uplifted vacuum in Section 3.7. The vector multiplet eats a chiral multiplet via the superHiggs mechanism and two (one) chiral multiplets get an F-term (D-term) mass. One multiplet is massless at tree-level: it contains the Goldstino, the pseudomodulus and the R-axion.

Effect of instanton term

Turning on the instanton term creates SUSY-vacua far out in field space. The additional terms in $F_{M_{sing}}$ are easily accounted for by replacing $hf^2 \to h\tilde{f}^2$ in eq. (3.5.2), where

$$h\tilde{f}^2 = hf^2 - \frac{a}{N_f^{(N_f-1)/2}} \frac{M_{sing}^{N_f-1}}{\Lambda^{N_f-3}}. \tag{3.5.12}$$

(Some of the previously undetermined phases now also get a non-zero VEV, but this does not affect the one-loop stabilization of the pseudomodulus.) As M_{sing} increases $h\tilde{f}^2 \to 0$ and hence $S, \bar{S}, Z, \bar{Z} \to 0$. Hence

$$\langle M_{sing} \rangle_{\text{SUSY}} \sim f \left(\frac{\Lambda}{f}\right)^{(N_f-3)/(N_f-1)} \overset{=}{_{N_f \to 5}} \sqrt{f\Lambda}. \tag{3.5.13}$$

The small value of f/Λ is crucial for guaranteeing longevity of the uplifted vacuum. The effect of these R-breaking terms as well as the stabilization of the uplifted vacuum via quantum corrections is illustrated in fig. 3.1.

Near the origin of field space we care about the changed behavior of the R-axion and the pseudomodulus. The explicit breaking of the R-symmetry gives a small mass to the R-axion.

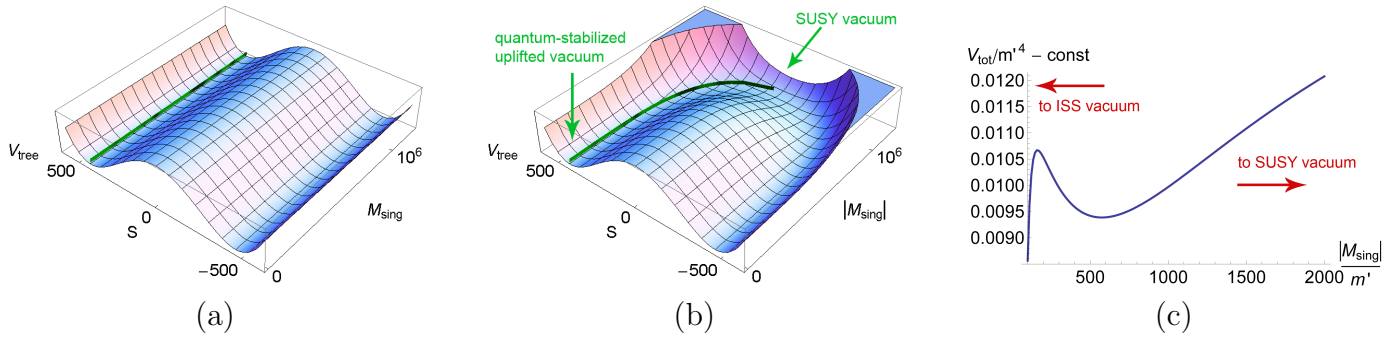

Figure 3.1: (a) The tree-level potential without the instanton term as a function of $|M_{sing}|$ and S, where we have enforced tree-level VEVs $|\bar{S}| = |S|$ and $Z = \bar{Z} = -d\sqrt{N_f} M_{sing} S/m'$. The valley marked with a green band is perfectly flat in the $|M_{sing}|$ direction and shows that the potential has a SUSY-breaking minimum for $S^2 = \frac{hf^2}{d} - \frac{m'^2}{d^2 N_f}$. Note that the messengers are tachyonic for $|M_{sing}| < m'/\sqrt{dh}$. (b) The same potential with the instanton term added. The minimum along the S-direction is approximately unchanged close to the origin but is significantly shifted as we move outwards along the $|M_{sing}|$ direction. As we walk along the the valley in the $|M_{sing}|$ direction (which now tilts slightly away from the origin) we eventually reach the SUSY-minimum at $|M_{sing}| \sim \sqrt{\Lambda f}$ and $S, Z = 0$. (c) We compute quantum corrections to the potential along the pseudomodulus direction, i.e. the green band in (b), by setting all fields to their VEVs in terms of $|M_{sing}|$. The vacuum is stabilized at $|M_{sing}| \sim \sqrt{h/d}\ f \longrightarrow Z, \bar{Z} \sim \sqrt{h/d}\ f^2/m'$. The parameters used for these plots in units of m' were $N_f = 5$, $\Lambda = 3.8 \times 10^9$, $f = 63$ and $(g, d, h) = (0.02513, 0.02, 1)$.

Note that even though the large adjoint mass represents a very large explicit R-breaking, since the adjoint does not get a VEV it is not part of the axion. The pseudomodulus is no longer a flat direction at tree-level, but is slightly tilted away from the origin.

Tree-level zero modes

The fermionic component of the tree-level zero mode multiplet is the Goldstino, which is eaten by the Gravitino once SUSY is gauged and gets the familiar mass

$$m_{\tilde{G}} \;=\; \frac{F_{tot}}{\sqrt{3}M_{pl}^*} \;\approx\; 0.4\,\frac{r}{d}\,\frac{m'^2}{M_{pl}^*} + O(r^{-1}) \qquad \text{for } N_f = 5\ , \tag{3.5.14}$$

where $M_{pl}^* = (8\pi G_N)^{-1/2} = 2.4 \times 10^{18}\mathrm{G}eV$ is the reduced Planck Mass. (Since $r = \sqrt{hdN_f}f/m' > 1$ and $d \ll 1$, it is often instructive to expand for large r or large f/m'.) The scalar components are the pseudomodulus and the R-axion (eqns 3.5.8, 3.5.9). To compute the 1-loop potential for the pseudoflat direction we set all their phases to their tree-level VEV or zero and express $\langle Z\rangle, \langle\bar{Z}\rangle$ in terms of M_{sing}, which gives $V_{\rm CW}(M_{sing})$. We emphasize that $|M_{sing}|$ is not the pure pseudomodulus, but its value parametrizes where we are along the pseudo-flat direction in field space.[1] This gives $V_{eff}(M_{sing}) = V_{tree}(M_{sing}) + V_{\rm CW}(M_{sing})$. As per the discussion above, the first term is nonzero if we include the instanton term. Minimizing V_{eff} gives $\langle M_{sing}\rangle$ and hence $\langle Z\rangle, \langle\bar{Z}\rangle, \langle S\rangle, \langle\bar{S}\rangle$. To compute the derivative V_{eff} along the flat direction we differentiate with respect to M_{sing} and multiply by a scaling factor $F_{M_{sing}}/F_{tot}$ to account for the fact that moving by δ along the M_{sing} axis moves us by $\delta\sqrt{(F_Z/F_{M_{sing}})^2 + (F_{\bar{Z}}/F_{M_{sing}})^2 + 1}$ along the pseudo-flat direction. Hence we obtain the pseudomodulus mass as

$$m_{PM}^2 = \left(\frac{F_{M_{sing}}}{F_{tot}}\right)^2 \frac{d^2V_{eff}}{d(M_{sing})^2}. \tag{3.5.15}$$

A similar argument holds for the R-axion mass if we restore the undetermined phases in the tree-level potential. To ensure that we move along the correct direction in field space we impose $\pi_{Z,\bar{Z}} = \frac{F_Z}{F_{M_{sing}}}\pi_{M_{sing}}$, differentiate with respect to $\pi_{M_{sing}}$ and apply the same scaling factor.

[1] To avoid clutter, we omit the absolute value signs around M_{sing} from now on – they are understood when we talk about M_{sing} as parameterizing the pseudomodulus direction.

These masses can be readily estimated. As we will see in Section 3.7, M_{sing} is stabilized at $\sim \sqrt{d/h}f$. Therefore it is is convenient to parametrize

$$\langle M_{sing}\rangle = b\sqrt{\frac{h}{d}}\, f, \qquad \text{where} \qquad b \sim O(1). \tag{3.5.16}$$

To obtain the R-axion mass we differentiate the tree-level potential with all VEVs subbed in. To lowest order in $1/r$ and $1/\Lambda$ we find that

$$\frac{F_{M_{sing}}}{F_{tot}} \approx -\frac{1}{\sqrt{2dhN_f}}\frac{m'}{f} \quad \longrightarrow \quad m_R \approx 0.2\; b\; \sqrt{\frac{a}{d^3}}\;\frac{m'^2}{\Lambda} \qquad \text{for } N_f = 5. \tag{3.5.17}$$

To estimate the mass of the pseudomodulus we pre-empt another result from Section 3.7. The rough *scale* of the second derivative of the 1-loop potential is

$$\left|\frac{d^2V_{\rm CW}}{d(M_{sing})^2}\right| \sim \frac{1}{16\pi^2}\frac{m'^4}{\langle M_{sing}\rangle^2} \tag{3.5.18}$$

(where $Z, \bar{Z} \to Z(M_{sing}) = -d\sqrt{N_f}M_{sing}\langle S\rangle/m'$). To lowest order in $1/r$ this yields

$$m_{PM} \sim \frac{1}{\sqrt{32N_f}\,\pi}\frac{m'}{bh}\left(\frac{m'}{f}\right)^2 \;\approx\; 0.1\,\frac{d}{b}\,\frac{m'}{r^2} \qquad \text{for } N_f = 5. \tag{3.5.19}$$

Notice the m'/f suppression, simply due to the fact that if $f \gg m'$ then $F_{M_{sing}} \ll \langle M_{sing}\rangle^2$ (similarly for Z, $\bar{Z}$) and SUSY-breaking is weak. (Effectively this can also be seen as a suppression for small d, since decreasing d increases the minimum size of f to ensure eq. (3.5.4) is satisfied.)

3.5.2 The ISS Vacuum ($k = 1$)

Since this is very similar to a standard $(N, N_f) = (1, 5)$ ISS vacuum we will use the notation of Section 3.3.2 (except for renaming the $SU(N_f - N)$ meson $Z \to \tilde{M}$ to avoid confusion with the singlets $\bar{Z}, Z$) and split up the meson according to eq. (3.4.3). The squark VEV $\langle\bar{\chi}_1\chi_1\rangle = f^2 - \frac{d}{h}S\bar{S}$ sets $F_V = 0$, with all other SQCD-sector VEVs zero (except $\tilde{M}_{sing}$). This

gives the same singlet potential as eq. (3.5.2) with $N_f \to N_f - 1$. Therefore the VEVs at tree-level close to the origin are $\langle|S|\rangle = \langle|\bar{S}|\rangle$, $\langle|Z|\rangle = \langle|\bar{Z}|\rangle$, $\langle Z\rangle = -\sqrt{N_f - 1}\frac{\langle\tilde{M}_{sing}S\rangle}{m'}$, and

$$\langle S\bar{S}\rangle = \frac{hf^2}{d} - \frac{m'^2}{d^2(N_f-1)} \quad \text{whenever} \quad hf^2 > \frac{m'^2}{(N_f-1)d}. \tag{3.5.20}$$

If this condition is not satisfied the singlets do not get a VEV and we have a standard ISS vacuum. If we assume the condition holds (slightly stronger than eq. (3.5.4)), then $\langle\bar{\chi}_1\chi_1\rangle = m'^2/(dhN_f - 1)$, meaning the scale of the squark VEV is given by m' instead of f. The total vacuum energy is

$$\langle V_0^{k=1}\rangle = 2hf^2\frac{m'^2}{d} - \frac{m'^4}{d^2(N_f-1)} \tag{3.5.21}$$

The SQCD spectrum is the same as ISS with mass scale $\sim m'$, and the singlet spectrum looks very similar to the uplifted case. We will not dwell on analyzing this vacuum, we only needed to know the potential difference

$$\Delta V_0 \equiv \langle V_0^{k=0}\rangle - \langle V_0^{k=1}\rangle = \frac{m'^4}{d^2}\frac{1}{N_f(N_f-1)} \tag{3.5.22}$$

to calculate the uplifted vacuum lifetime in Section 3.7.4.

3.6 Direct Gauge Mediation

If we weakly gauge the $SU(5)$ flavor group and identify it with the SM GUT gauge group, this model realizes Minimal Gauge Mediation with a single $5 \oplus \bar{5}$ messenger pair:

$$W_{eff} = X\bar{\phi}_i\phi^i, \tag{3.6.1}$$

where the SUSY-breaking spurions $X = X + \theta^2 F$ is given by

$$X = \frac{h}{\sqrt{N_f}}M_{sing} \quad \to \quad F = \frac{h}{\sqrt{N_f}}F_{M_{sing}} = -\frac{h}{dN_f}m'^2. \tag{3.6.2}$$

Gaugino and sfermion masses are generated via the well-known 1- and 2-loop diagrams and are parametrically the same size, solving the Gaugino Mass Problem. Using equations (3.2.4), (3.5.16) and (3.5.4) we can see that SUSY-breaking is weak:

$$\left|\frac{X^2}{F}\right| = \left(\frac{f}{m'}\right)^2 h^2 b^2 > \frac{hb^2}{dN_f} \gg 1, \tag{3.6.3}$$

and therefore the soft masses are given by the usual simple expression

$$m_{soft} \sim \frac{\alpha}{4\pi}\left|\frac{F}{X}\right|. \tag{3.6.4}$$

Requiring TeV-scale soft masses sets $|F/X| \sim 100\,\mathrm{T}eV$. This determines the scale of m' (and hence f):

$$m' \sim \left|\frac{F}{X}\right| br, \tag{3.6.5}$$

which sets the messenger mass at

$$X \sim b^2 r^2 \frac{h}{dN_f}\left|\frac{F}{X}\right| \sim r^2\ \frac{0.01}{d} \times (10^7 \mathrm{G}eV) \tag{3.6.6}$$

in the scenarios we are considering. The pseudomodulus, and Goldstino mass scales are

$$m_{PM} \sim \frac{1}{r}\ \left(\frac{d}{0.01}\right) \times (10\mathrm{G}eV) \tag{3.6.7}$$

$$m_{\tilde{G}} \sim b^2\ r^3\ \left(\frac{0.01}{d}\right) \times (\,\mathrm{k}eV). \tag{3.6.8}$$

The field theory contribution to the R-axion mass is

$$m_R \sim b^3\ r^2\ \left(\frac{0.01}{d}\right)^{3/2}\ \frac{\Lambda_{GUT}}{\Lambda} \times (100\,\mathrm{k}eV). \tag{3.6.9}$$

Depending on the size of r and b as well as the choice of scenario, this can be smaller or larger than the BPR contribution [73].

Again using results from the next section for convenience, the mass of the singlet vector multiplet is similar to the messenger mass whereas the other singlets (with the exception of

the tree-level zero modes) obtain a smaller mass $\sim r^2|F/X|$. Stabilizing the uplifted vacuum in scenarios 1 and 2 requires $r \lesssim 10^2$ and $r \lesssim 10^1$ respectively, but saturating the former bound gives a very heavy gravitino and reintroduces the SUSY flavor problem. Therefore $1 < r \lesssim 10^1$ is the relevant parameter range for our model.

Since the adjoint meson gets a mass that is only a few orders of magnitude below the duality transition scale Λ, which itself is either at or close to the GUT-scale, there is no Landau Pole in our model. (Scenario 2 is also an example of *deflected unification* [77].) However, we emphasize that due to the minimality of this hidden sector such a heavy adjoint is not required to solve the Landau Pole Problem – if the adjoint mass was generated by some other mechanism it could be as low as $\sim 10 - 100\,\mathrm{T}eV$.

3.7 Stabilizing the Uplifted Vacuum

We now examine how the singlet sector originally proposed in [68] stabilizes the uplifted vacuum. The stabilization is possible due to the singlet sector's $U(1)_S$ gauge group [70], which can supply a negative coefficient to the logarithmic dependence of V_{CW} and push the minimum away from the origin beyond the region where the messengers are tachyonic. We perform this analysis to 1-loop order even though $d \ll h$ and 2-loop effects from h might be competitive. This will be justified in Section 3.7.3. For simplicity we set $a = 1$ throughout.

The effective potential is given by

$$V_{eff} = V_{tree} + V_{\mathrm{CW}}, \tag{3.7.1}$$

where all tree-level VEVs and masses are expressed as functions of M_{sing}, which parametrizes

the pseudomodulus VEV. V_{tree} is easily obtained by combining equations (3.5.6) and (3.5.12).

$$V_{tree} = \frac{2hf^2m'^2}{d} - \frac{m'^4}{d^2N_f} - \frac{2m'^2}{d}\frac{a}{N_f^{(N_f-1)/2}}\frac{M_{sing}^{N_f-1}}{\Lambda^{N_f-3}}. \tag{3.7.2}$$

This slopes away from the origin due to the effect of the instanton term. $V_{\rm CW}$ is computed by obtaining the mass spectrum *without the effects of the instanton term*[1] and using eq. (3.4.1).

3.7.1 Organizing the Spectrum & Contributions to $V_{\rm CW}$

All nonzero tree-level masses depend on the value of the pseudomodulus, parametrized by the value of M_{sing} by imposing $Z = \bar{Z} = -d\sqrt{N_f}SM_{sing}/m'$. It is helpful to express all masses in units of m' and define the following set of parameters:

$$x = d\sqrt{N_f}\frac{|M_{sing}|}{m'}\ , \qquad r = \sqrt{hdN_f}\frac{f}{m'}\ , \qquad q = \frac{4}{N_f}\frac{g^2}{d^2}(r^2-1)\ , \qquad p = \frac{h}{dN_f}. \tag{3.7.3}$$

In this parametrization, h just rescales the other variables. $r > 1$ is required for singlet VEVs. This parametrization has the advantage that the masses in every split supermultiplet depend only on x and one of the r, q, p parameters. This allows us to study the different $V_{\rm CW}$ contributions independently as functions of just two variables each.

- The messenger masses can be written as $m_F^2 = p^2x^2$ and $m_S^2 = p^2x^2 \pm p$, and are tachyonic for $x < 1/\sqrt{p}$ (recall that we use m' as our unit of mass in this parameterization). In the leading-log approximation for large x their contribution to the 1-loop potential is $V_{\rm CW}^{mess} \approx \frac{1}{64\pi^2}8N_fp^2\log x$. (We will ignore additive constants to the potential.)
- Two singlet chiral supermultiplets have F-term masses that depend only on r and x. For large x their masses go as $\sim x$ and $\sim 1/x$, so we denote them R_{heavy} and R_{light}

[1] If the instanton term is so large that its backreaction significantly affects the 1-loop potential, its tree-contribution will be so large as to erase any minima created by $V_{\rm CW}$ anyway.

respectively. The contribution $V_{\rm CW}^{Rheavy}$ stands out because it is the only one that always has a local minimum, located at $x \approx 1.3r - 1$ to a very good approximation.

For most values of the parameters the other contributions to the 1-loop potential wash out this minimum and the uplifted pseudomoduli space is not stabilized. However, if the other components cancel to high enough precision then the minimum survives and is located at $\langle x \rangle \sim r > 1$ (see eq. (3.5.4)). This justifies the parametrization

$$\langle M_{sing} \rangle = b\sqrt{\frac{h}{d}} f \quad \text{where} \quad b = O(1). \tag{3.7.4}$$

For large x the light multiplet does not contribute to $V_{\rm CW}$, whereas $V_{\rm CW}^{Rheavy} \approx \frac{1}{64\pi^2} 4 \log x$. Near the local minimum of the total 1-loop potential, their masses to lowest order in $1/r$ are $m^2_{\substack{Rheavy \\ Rlight}} \approx \frac{1}{2}\left(4 + b^2 \pm b\sqrt{8+b^2}\right) r^2$.

- One chiral and one vector multiplet get masses from the $U(1)_S$ D-term, both $\sim x$ for large x. Call them $Q_{\rm vector}$ and $Q_{\rm chiral}$. In the leading-log approximation the contributions to the 1-loop potential are $V_{\rm CW}^{Qvector} \approx \frac{1}{64\pi^2}(-8q)\log x$ and $V_{\rm CW}^{Qchiral} \approx \frac{1}{64\pi^2} 4 \log x$. Near the local minimum of $V_{\rm CW}$, their masses to lowest order in $1/r$ are $m^2_{Qvector} \approx 4b^2 g^2 r^4/(d^2 N_f)$ and $m^2_{Qchiral} \approx b^2 r^2$.

Adding all the contributions together, we see that the total 1-loop potential in the leading log approximation valid for 'large' field values of M_{sing} corresponding to $x \gtrsim O(1) \gg 1/\sqrt{p}$ is

$$V_{\rm CW} \approx \frac{1}{8\pi^2}(1-t)\log x, \tag{3.7.5}$$

where it will be convenient to define

$$t = q - N_f p^2. \tag{3.7.6}$$

3.7.2 Conditions for local minimum

The leading-log approximation is excellent for $V_{\rm CW}^{mess}$ and $V_{\rm CW}^{Q}$, even as close to the origin as $x \sim \langle x \rangle$. Hence we can understand the tuning required for stabilizing the uplifted vacuum as follows. Imagine starting out with a choice of parameters for which there is a local minimum of $V_{\rm CW}$. If we then increase t, the coefficient of the logarithm in the potential decreases until the minimum is wiped out and the potential just slopes towards the SUSY-minimum. Conversely, if we decrease t the coefficient of the logarithm increases and the minimum gets pushed towards the origin, eventually disappearing into the region where the messengers are tachyonic. Therefore having a local minimum requires $t \in (t_{min}, t_{max})$, where $t_{min,max}$ are $O(1)$ functions of the other parameters. Expressing the singlet-sector gauge coupling in terms of t,

$$g(t)^2 = \frac{h^2 + d^2 N_f t}{4(r^2-1)}, \tag{3.7.7}$$

translates this condition into a required tuning for g. However, it is more instructive to recast the stabilization requirement as a constraint on the mass ratio

$$\left(\frac{m'}{f}\right)^2 = 4g^2 N_f \frac{d}{h}\left(1 - \frac{d^2}{h^2} N_f t\right) + O(g^4) + O(d^5). \tag{3.7.8}$$

We can see immediately that even if t is allowed to take on an $O(1)$-range of values to guarantee a local minimum, m'/f must actually be adjusted to a precision of

$$\Delta \sim \frac{d^2}{h^2} \sim \left(\frac{\Lambda}{\Lambda_{UV}}\right)^2. \tag{3.7.9}$$

This is $\sim 10^{-4}$ in the two scenarios we are considering but could be significantly larger if one were less conservative about the separation of scales for Λ, Λ_{UV}. Tuning of this order of severity is typical in uplifted models that are stabilized by 1-loop corrections, and we make no attempt to explain it here. It would be very interesting to investigate whether such a

mass ratio might be generated by some kind of UV-completion, but it lies beyond the scope of this chapter.

What is the actual allowed range of t? If we switch off the instanton term then there can be no minima of $V_{\rm CW}$ if the coefficient of the logarithm is negative for large x. Hence $t_{max}^{approx} = 1$. To find the smallest allowed value of t we numerically investigate the behavior of $V_{\rm CW}$ and we find that $t_{min}^{approx} \geq 1/2$, with the inequality becoming saturated for $r \gtrsim 10$. Switching on the instanton term has the effect of reducing t_{max} from the approximate value of 1, since the V_{tree} contribution has negative slope and increasing t beyond t_{min} causes the overall potential to have negative slope before we reach $t = 1$. This effect is more pronounced for larger r, since increasing f/Λ increases the effect of the instanton term.

To understand this in more detail we studied the complete V_{eff} numerically. By fixing $|F/X|$ in eq. (3.6.4) at $100\,\mathrm{T}eV$ one can find t_{min}, t_{max} as functions of r for various values of d and h in scenarios 1 and 2, see fig. 3.2. As expected the instanton term does not have a significant effect on t_{min} but decreases t_{max} from 1 with increasing severity for larger r. This effectively defines a maximum value of r for which there can still be a local minimum of V_{eff}, and r_{max} appears approximately $\propto d$ for fixed Λ, Λ_{UV}.

We can explain this behavior of r_{max} analytically. For fixed other parameters, r_{max} is approximately the value of r for which the scale of the gradient of $V_{\rm CW}$ near the minimum becomes smaller than the scale of the gradient of V_{tree} (eq. (3.7.2)). Therefore, we can roughly estimate r_{max} by equating the gradient of the leading log approximation to $V_{\rm CW}$ (eq. (3.7.5)) to the gradient of V_{tree} for $M_{sing} \sim \sqrt{h/d}f$ and $t \sim 0.5$. This yields

$$r_{max} \sim d^{5/6} \left(\frac{\Lambda}{|F/X|} \right)^{1/3} \tag{3.7.10}$$

and explains the approximate linear dependence of r_{max} on d observed numerically. For Scenarios 1 and 2 this gives $r_{max} \sim 10^2$ and $\sim 10^1$, depending on the exact value of d. This

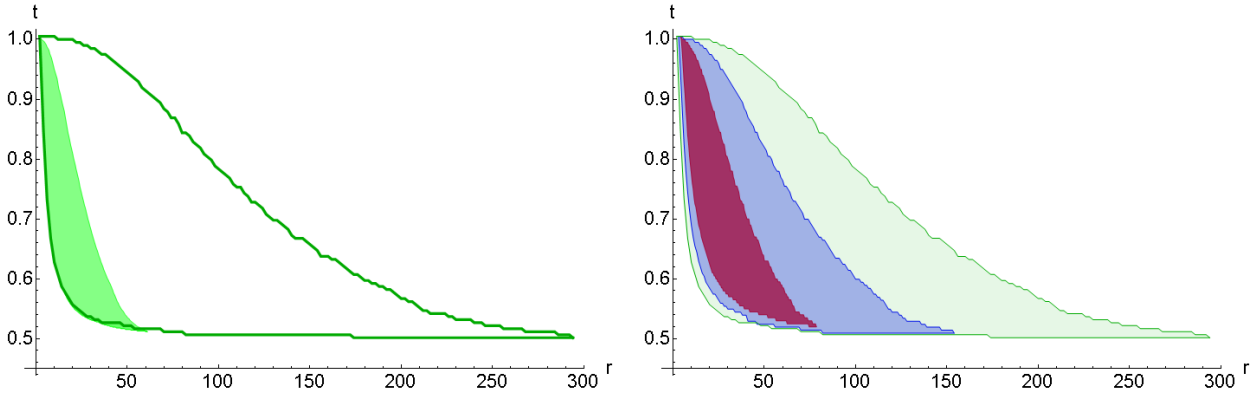

Figure 3.2: (a) For $|F/X| = 100\,\mathrm{TeV}$ and $d = 0.04 = 4 \times \Lambda/\Lambda_{UV}$ in Scenario 1, V_{eff} has a local minimum in area of the r-t plane enclosed by the green curve. For Scenario 2 this area shrinks down to the shaded region due to the increased effect of the instanton term. (b) Areas of the r-t plane where V_{eff} has a local minimum for $d = 0.04, 0.02, 0.01$ (green/light, blue/medium, red/dark) in Scenario 1. $r_{max} \propto d^{5/6}$, so decreasing d from 0.04 to 0.01 decreases the area where there is a minimum. These areas do not depend significantly on h.

agrees with our numerical results to $\sim 30\%$.

In Figure 3.3 we illustrate the range of allowed r-values by plotting the approximate r_{max} from eq. (3.7.10) as a function of Λ and Λ_{UV}. Since $r > 1$ is required for singlet VEVs, the shrinking of r_{max} with decreasing Λ effectively defines a minimum allowed value of Λ/Λ_{UV}, and for $\Lambda \lesssim \Lambda_{UV}/1000$ it becomes very difficult to find a metastable uplifted vacuum because the allowed range of r shrinks to nothing. This means that Λ as large as possible is favored in our model, and justifies considering only our two scenarios with $\Lambda/\Lambda_{UV} \sim 1/100$.

Finally, we can also use these ideas to get a rough estimate of the pseudomodulus mass scale. Simply differentiating eq. (3.7.5) and setting $t \sim 0.5$ yields eq. (3.5.18).

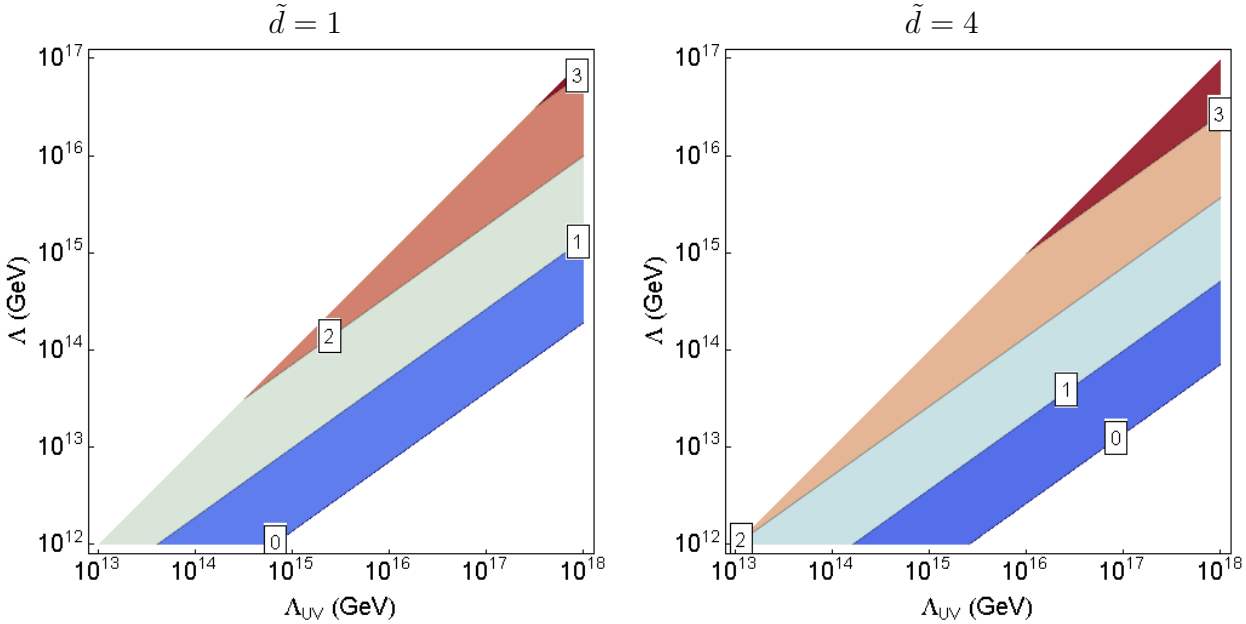

(a) (b)

Figure 3.3: Estimate of $\log_{10} r_{max}$ for two possible values of $\tilde{d} = \frac{d}{\Lambda/\Lambda_{UV}}$. The upper and lower regions are excluded to satisfy $\Lambda < \Lambda_{UV}/100$ and $r > 1$ respectively. This demonstrates that the allowed range for r shrinks to nothing for $\Lambda/\Lambda_{UV} \ll 1/1000$, making large Λ heavily favored in our model.

3.7.3 Validity of 1-loop calculation

The smallness of $d \sim 0.01$ compared to $h \sim 1$ and g (depending on the size of r) might cause us to suspect that all these results would be invalidated by 2-loop corrections. Fortunately, this naive expectation is not realized due to the nature of contributions to the effective potential. The leading-log approximation to the 1-loop potential eq. (3.7.5) is a very good approximation for the *complete* contributions from messengers (loops involving the h-coupling) and singlets with D-term masses (involving the g-coupling), as well as the *logarithmic* contributions from singlets with F-term masses. The only components not included are the small-x contributions from singlets with F-term masses, and those are the

contributions with non-trivial features required to generate the minimum.

The tuning can be understood as canceling the smooth logarithmic contributions to the effective potential to high enough precision so that the minimum created by the contributions from singlets with F-term masses survives. Since d is so small, this local minimum is pushed out to rather large field values $M_{sing} \sim \sqrt{h/d}\ f$ where the leading log approximation for the 'uninteresting' contributions is excellent. This makes the two-loop corrections involving two h and g couplings (messengers and singlets with D-term masses, respectively) very smooth as well, meaning they do not introduce any gross new features to the effective potential. Therefore they just generate a smooth correction to eq. (3.7.5), which can be compensated for by slightly adjusting the gauge coupling g (or the ratio m'/f) and should not significantly affect the existence of local minima or the severity of tuning (though eq. (3.7.8) might have to be slightly adjusted). Therefore the important features of our analysis are valid.

3.7.4 Lifetime Constraints on Uplifted Vacuum Stabilization

We now check that the uplifted vacuum is stable enough to have not decayed in the lifetime of the universe. For each decay path across the potential landscape we estimate the Bounce Action B which exponentially suppresses the decay width [78]. We require $B \gtrsim 10^3$ [79]. For rough estimates of the bounce action we approximate the potential along the decay path as a triangular barrier, which yields very simple analytical expressions for B [80].

There are two decay paths that are only forbidden by loop-sized effects. As illustrated in fig. 3.1, M_{sing} can either tunnel towards the origin, in which case the messengers become tachyonic and the fields roll towards the ISS vacuum, or it can tunnel away from the origin and roll towards the SUSY-minimum.

To estimate the bounce action for decay to the ISS vacuum along the pseudoflat direction we take limit where the height of the potential barrier and the distance from the edge of the barrier to the ISS vacuum goes to zero. This *underestimates* B and gives

$$B_{\rm ISS} > 2\pi^2 \frac{N_f - 1}{N_f} \frac{r^4(2r^2-1)^2}{(d/b^2)^2} \sim \underbrace{\frac{8\pi^2}{5}}_{\sim 15} \underbrace{\left(\frac{\Lambda_{UV}}{\Lambda}\right)^2}_{>10^4} b^4 \underbrace{r^4\left(2r^2-1\right)^2}_{>1} \gg 10^3 \tag{3.7.11}$$

Turning to the bounce action for decay to the SUSY vacuum along the pseudoflat direction we again take the height of the potential barrier to zero and neglect several unknown or parametrically smaller contributions to the length of the decay path. Using ΔV^0 from eq. (3.5.22) as the depth of the potential well on the other side of the barrier we obtain (neglecting $O(1)$ factors)

$$B_{\rm SUSY} > \frac{32\pi^2}{3} \sqrt{\frac{\Lambda}{f}} \frac{1}{d^{3/2}} \gg 10^3 \tag{3.7.12}$$

Both decays are sufficiently suppressed.

3.8 Conclusions

The ISS framework [53] is an extremely appealing model building arena for exploring non-perturbative meta-stable SUSY-breaking. However, previous ISS-based models of Direct Gauge Mediation are plagued by several problems, both aesthetic and phenomenological, which include small gaugino masses (exacerbating the little hierarchy problem), Landau Poles and non-renormalizable operators with somewhat contrived flavor contractions. Since the issue of small gaugino masses has been understood to be related to the vacuum structure of the theory [63], one model-building challenge is the formulation of plausible uplifted ISS models.

We first outlined some simple but general model-building guidelines for stabilizing up-

lifted ISS models, which lead us to conclude that meson-deformations are required (or at least heavily favored) to stabilize the adjoint component of the magnetic meson in the hidden sector. However, the singlet can be stabilized by a variety of mechanisms, which makes it possible that an uplifted hidden sector with minimal flavor group might be viable.

This lead us to propose Singlet Stabilized Minimal Gauge Mediation as a simple ISS-based model of Direct Gauge Mediation which avoids both light gauginos and Landau Poles. The hidden sector has trivial magnetic gauge group and minimal unbroken $SU(5)$ flavor group, while the uplifted vacuum is stabilized by a singlet sector with its own $U(1)$ gauge symmetry, generating a nonzero VEV for the singlet meson via the inverted hierarchy mechanism.

The stabilization mechanism used in our model necessitates adjusting parameters to a precision of $\sim (\Lambda/\Lambda_{UV})^2 \sim 10^{-4}$, a common problem with quantum-stabilized models. While this tuning can be reduced by being less conservative about the separation of scales, one might question the advantage of this tuning compared to the tuning in the MSSM Higgs-sector associated with a split-SUSY spectrum. Apart from the fact that a split-SUSY spectrum might not be experimentally observed, the key is that a split-SUSY spectrum *cannot be avoided* in most models of Direct Gauge Mediation that are in the ground state, in particular standard ISS[1]. This chapter shows that it is possible to stabilize an *uplifted* ISS model with *very small flavor group*, a necessary condition for avoiding Landau Poles of the SM gauge couplings, and while the current stabilization mechanism requires said tuning it seems plausible that an alternative mechanism with generically stabilized uplifted vacua exists. That makes our stabilization-tuning preferable to the 'unavoidable' Higgs-sector tuning from a split-SUSY spectrum.

[1]One might have an independent suppression mechanism for the sfermion masses, see for example [81]

Acknowledgements

We are extremely grateful to Csaba Csaki, Zohar Komargodski, Maxim Perelstein and Liam McAllister for valuable insights and comments on the manuscript for the paper this chapter is based on. We would also like to thank Markus Luty, John Terning, Jesse Thaler, David Shih, Rouvan Essig, Nathan Seiberg, Andrey Katz and Flip Tanedo for helpful discussion. The work of D.C. and Y.T. was supported in part by the National Science Foundation under grant PHY-0355005. D.C. was also supported by the John and David Boochever Prize Fellowship in Fundamental Theoretical Physics 2010-11. Y.T. is also supported by a Fermilab Fellowship in Theoretical Physics. Fermilab is operated by Fermi Research Alliance, LLC, under Contract No. DE-AC02-07CH11359 with the United States Department of Energy.

CHAPTER 4

THE SUSY-YUKAWA SUM RULE AND M_{T2} COMBINATORICS

Based on the 2010 article "SUSY-Yukawa Sum Rule at the LHC", written in collaboration with Monika Blanke and Maxim Perelstein and published in Phys.Rev. D82 (2010) 035020.

4.1 Introduction

Experiments at the Large Hadron Collider (LHC) have begun probing physics at the TeV scale. The primary goal of these experiments is to understand the mechanism of electroweak symmetry breaking (EWSB), and since supersymmetry provides such an elegant solution to the hierarchy problem, searches for SUSY will be one of the main directions pursued by the LHC experiments.

Assuming that some of the signatures predicted by SUSY models are seen at the LHC, the next major task for the experiments will be to determine the nature of the new particles involved, such as their masses and spins. In addition, there is a large number of couplings involving the new particles that one can attempt to measure. Among those, there is a small set of couplings that is, in our opinion, truly special, and deserves special attention. These are the couplings that ensure the cancellation of the quadratically divergent diagrams contributing to the Higgs mass parameter at one loop. Specific relations between these couplings and the SM gauge and Yukawa couplings are required to solve the hierarchy problem, and SUSY guarantees that these relations are satisfied. Testing these relations experimentally would clearly demonstrate the role of SUSY in restoring naturalness to the EWSB sector. The first goal of this chapter is to suggest a simple sum rule, which follows unambiguously from one such coupling relation, and involves only physically measurable quantities. The second goal is to outline the set of measurements that would need to be performed to test this sum rule, and evaluate the prospects for these measurements at the LHC. While a test of the sum rule will have to await a next-generation lepton collider, we find that the LHC may be able to measure several ingredients of the sum rule. Within the framework of SUSY, the sum rule can then be used to infer parameters, such as stop and sbottom mixing angles, which will be difficult or impossible to measure directly. This analysis also includes the first

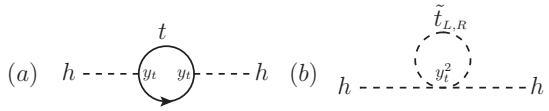

Figure 4.1: Quadratically divergent one-loop contribution to the Higgs mass parameter in the SM (a), cancelled by scalar superpartner contributions in a SUSY model (b).

serious attempt to perform mass measurements using the M_{T2} family of kinematic variables in the presence of large combinatorics background. We show that these variables remain useful in such scenarios, though much extra work must be done to extract their information.

4.2 SUSY-Yukawa Sum Rule

The strongest coupling of the SM Higgs boson is the top Yukawa. At the one-loop level, this coupling introduces a quadratically divergent contribution to the Higgs mass parameter, via the diagram in Fig. fig. 4.1 (a). In SUSY models, this contribution is canceled by the diagrams in fig. 4.1 (b), with the *stops*, scalar superpartners of the top quark, running in the loop. The cancellation relies on the precise relation between the top Yukawa and the stop-Higgs quartic coupling, shown in the figure, which is enforced by SUSY. We would like to test this relation experimentally. The most direct test, measuring the stop-Higgs quartic vertex, appears impossible at the LHC due to extreme smallness of all cross sections involving this vertex. However, once the Higgs gets a vacuum expectation value (vev), the quartic vertex generates a contribution to stop masses, which are in principle measurable. The challenge is to isolate this term from other contributions to the stop mass matrix.

SUSY makes two kinds of predictions: (1) it dictates a particular *particle content* (i.e. superpartners to the SM fields), and (2) it imposes certain *relations between couplings* of the fields, such as the relation in Fig. fig. 4.1. We want to separate the two, fixing the particle

content (which we assume could be tested by independent observations), while attempting to test the coupling relation.

Start with a SUSY-like particle content for the 3rd generation, i.e. a set of scalars with gauge charges

$$\begin{pmatrix} \tilde{t}_L \\ \tilde{b}_L \end{pmatrix} \sim (3,2)_{1/6}, \quad \tilde{t}_R \sim (3,1)_{2/3}, \quad \tilde{b}_R \sim (3,1)_{-1/3}. \tag{4.2.1}$$

Leaving the $SU(2)_L \times U(1)_Y$ gauge symmetry unbroken and working in the $(\tilde{t}_L, \tilde{t}_R)$-basis, the only allowed mass terms are

$$M^2_{\tilde{t}} = \begin{pmatrix} M_L^2 & \\ & M_t^2 \end{pmatrix}, \quad M^2_{\tilde{b}} = \begin{pmatrix} M_L^2 & \\ & M_b^2 \end{pmatrix} \tag{4.2.2}$$

(in the MSSM these are just the soft masses). Within the chosen particle content, we can parameterize EWSB model-independently by inserting spurions $Y^{t,b}$. The $(1,1)$ entries of the top- and bottom-partner mass matrices become

$$(M^2_{\tilde{t}})_{11} = M_L^2 + v^2 Y^t_{11} \quad , \quad (M^2_{\tilde{b}})_{11} = M_L^2 + v^2 Y^b_{11} \tag{4.2.3}$$

where $v = 246$ GeV. Let us define an observable

$$\Upsilon \equiv \frac{1}{v^2}\left(m^2_{t1}c_t^2 + m^2_{t2}s_t^2 - m^2_{b1}c_b^2 - m^2_{b2}s_b^2\right), \tag{4.2.4}$$

where the top-partner eigenmasses $m_{t1} < m_{t2}$, the bottom-partner eigenmasses $m_{b1} < m_{b2}$, and the mixing angles θ_t and θ_b are all, in principle, measurable. (We use the notation $c_{t,b} \equiv \cos\theta_{t,b}$, $s_{t,b} \equiv \sin\theta_{t,b}$.) Writing the top-partner mass matrix in terms of these quantities:

$$M^2_{\tilde{t}} = \begin{pmatrix} m^2_{t1}c_t^2 + m^2_{t2}s_t^2 & c_t s_t (m^2_{t1} - m^2_{t2}) \\ c_t s_t (m^2_{t1} - m^2_{t2}) & m^2_{t1}s_t^2 + m^2_{t2}c_t^2 \end{pmatrix}, \tag{4.2.5}$$

(similarly for $M^2_{\tilde{b}}$) and canceling the soft mass M_L^2 by evaluating $(M^2_{\tilde{t}})_{11} - (M^2_{\tilde{b}})_{11}$, we obtain

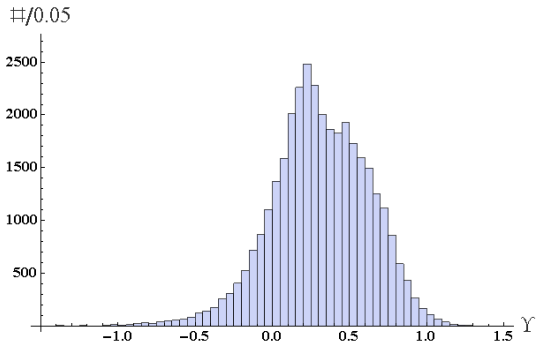

Figure 4.2: Distribution of Υ for a SuSpect random scan of pMSSM parameter space. Scanning range was $\tan\beta \in (5, 40)$; $M_A, M_1 \in (100, 500)$ GeV; $M_2, M_3, |\mu|, M_{QL}, M_{tR}, M_{bR} \in (M_1 + 50 \text{ GeV}, 2 \text{ TeV})$; $|A_t|, |A_b| < 1.5$ TeV; random sign(μ). EWSB, neutralino LSP, and experimental constraints ($m_H, \Delta\rho$, $b \to s\gamma$, a_μ, $m_{\tilde{\chi}_1^\pm}$ bounds) were enforced.

$$\Upsilon = Y_{11}^t - Y_{11}^b \,. \tag{4.2.6}$$

In other words, Υ probes the spurions only. Note, however, that Eq. eq. (4.2.6) will receive non-trivial corrections beyond the tree level, since Υ is defined in terms of physical (pole) masses, while in the above derivation all masses are evaluated at the same scale.

At tree level, SUSY makes a definite prediction for Υ. Using the standard sfermion tree-level mass matrices (see e.g. [82]) and neglecting flavor mixing, we obtain

$$\begin{aligned} \Upsilon_{\text{SUSY}}^{\text{tree}} &= \frac{1}{v^2}\left(\hat{m}_t^2 - \hat{m}_b^2 + m_Z^2 \cos^2\theta_W \cos 2\beta\right) \\ &= \begin{cases} 0.39 & \text{for } \tan\beta = 1 \\ 0.28 & \text{for } \tan\beta \to \infty \end{cases} \end{aligned} \tag{4.2.7}$$

Here the hats denote tree-level (or "bare") masses. The numerical values assume the renormalization scale $Q = 600$ GeV (so that i.e. $\hat{m}_t \approx 153$ GeV), but do not depend strongly on the precise value of Q. This prediction, which we call the *SUSY-Yukawa sum rule*, relies on the same relation between the fermion and scalar Higgs couplings which leads to the cancelation in Fig. fig. 4.1. Measuring Υ would therefore provide a powerful, if somewhat indirect

method of testing whether it is SUSY that solves the hierarchy problem. (This argument is conceptually similar to the tests of the Little Higgs cancellation mechanism, proposed in [83]. Earlier examples of SUSY sum rules, devised within the mSUGRA framework, can be found in [84].)

Radiative corrections to the SUSY prediction for Υ can be important, since the sum rule typically involves a rather delicate cancellation between stop and sbottom mass terms. The full analytical expressions for the radiative corrections to superpartner masses within the MSSM can be found in [82], and a convenient numerical implementation is provided by the SuSpect package [85]. The corrections depend on a large number of MSSM parameters. To estimate their effect on Υ, we conducted several scans of the MSSM parameter space using SuSpect. We did not assume a particular model of SUSY breaking, but allowed the weak-scale soft terms to vary independently. A representative result for the distribution of Υ is shown in Fig. fig. 4.2. (As usual, the reader must exercise caution in interpreting this plot, since it necessarily reflects our sampling bias of parameter space.) It shows that radiative corrections can change the value of Υ significantly from its tree level prediction (eq. (4.2.7)). However, a measurement of $|\Upsilon| > O(1)$ would disfavor TeV-scale SUSY as the solution to the hierarchy problem. It should be noted that in a generic theory with the particle content of Eq. (4.2.1), the scalar-Higgs quartic couplings are only constrained by perturbativity, leading to the possible range of $-16\pi^2 \lesssim \Upsilon \lesssim 16\pi^2$. Moreover, if some of the parameters in the sum rule are misidentified, an even broader range is possible. For example, if the mixing angle measurements were off by $\pi/2$, the right-hand side of Eq. eq. (4.2.4) would contain the *right-right* elements of the squark mass matrices, which are of course independent for stop and sbottom, so any value of Υ is in principle possible. Thus, even with radiative corrections included, the SUSY-Yukawa sum rule presents a useful and non-trivial consistency check on SUSY.

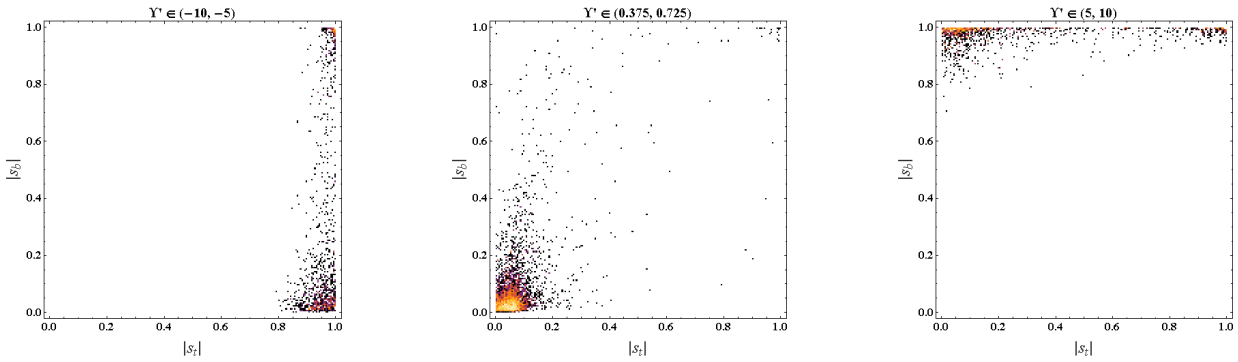

(a) (b) (c)

Figure 4.3: Scatter plot of pMSSM parameter points produced by the `SuSpect` scan from fig. 4.2, showing the correlations between the stop and sbottom mixing angles for different ranges of Υ'. Each 0.005×0.005 bin is colored according to the number of scan points contained in it, with hot (bright) and cold (dark) colors indicating high and low scan point density, and unpopulated bins left uncolored. These correlations are a direct consequence of the SUSY-Yukawa Sum Rule, and any measurement of $\Upsilon' \gtrsim 0$ provides valuable information about the sbottom mixing angle.

It is also interesting to ask if the sum rule can be used as a tool for model discrimination. Recently, several SUSY "look-alikes", *i.e.* models whose LHC signatures are similar to SUSY but arise from completely different underlying physics, have been studied. The most studied examples are universal extra dimensions (UED) [86] and little Higgs with T-parity (LHT) [87] models. These models contain particles with the quantum numbers of Eq. (4.2.1), but instead of scalars, they are spin-1/2 fermions. (The minimal LHT model does not contain a $\tilde{b}_R$ counterpart; however, such a particle can easily be added.) This leads to a different Higgs coupling structure: for example, the 4-point coupling in Fig. 1 (b) does not exist, at renormalizable level, in these theories. As a result, UED and LHT predictions for Υ are generically different from SUSY, at least at the tree level. As an example, the tree-level prediction of the minimal LHT model is

$$\Upsilon_{\rm LHT}^{\rm tree} = -\frac{g'}{2\sqrt{10}}\frac{m_{b_H}}{m_{A_H}} + \mathcal{O}\left(\frac{v^2}{f^2}\right), \tag{4.2.8}$$

where m_{b_H} and m_{A_H} are the masses of the heavy, T-odd partners of the left-handed b quarks and the hypercharge gauge boson, respectively. In contrast to SUSY, Υ is always negative at tree level in the LHT; for typical parameter values $\Upsilon \approx -0.5$. Unfortunately, radiative corrections can shift Υ in SUSY significantly, including changing the sign, as can be seen in Fig. fig. 4.2. Presumably, the LHT prediction will also receive important loop corrections, although they have not yet been calculated. Depending on the resulting ranges and on the measured value of Υ, the measurement may be interpreted as supporting one or the other model, but it seems unlikely that a sharp model-discriminating statement could be made. On the other hand, one should keep in mind that a measurement of parameters *not* directly entering the sum rule (such as the gluino mass) would generally shrink the range of possible Υ values in each model by constraining the possible radiative corrections, improving the model-discriminating power of this observable.

Measuring all the ingredients of Υ is very difficult at a hadron collider, and the determination of the complete 3$^{\text{rd}}$-generation sfermion spectrum and mixing angles will most likely have to be performed at a future lepton machine. However, for favorable MSSM parameters, some progress can be made at the LHC. In particular, if some of the ingredients of the sum rule can be measured, and the sum rule is assumed to be valid, it can be used to put interesting constraints on the remaining ingredients. The easiest terms to measure at the LHC are the masses of the lightest stop and sbottom squarks. To understand the implications of such a measurement, let us rewrite Υ as

$$\Upsilon = \underbrace{\frac{1}{v^2}\left(m_{t1}^2 - m_{b1}^2\right)}_{\Upsilon'} + \underbrace{\frac{s_t^2}{v^2}\left(m_{t2}^2 - m_{t1}^2\right)}_{\Delta\Upsilon_t} - \underbrace{\frac{s_b^2}{v^2}\left(m_{b2}^2 - m_{b1}^2\right)}_{\Delta\Upsilon_b} . \tag{4.2.9}$$

Assuming that the SUSY framework is correct, a measurement of Υ' together with the sum rule can be used to constrain the third-generation mixing angles, even if nothing is known about the masses of the heavier superpartners $\tilde{t}_2$ and $\tilde{b}_2$. This is illustrated by the scatter

plots in Fig. fig. 4.3. If Υ' is small, then either both $\tilde{t}_1$ and $\tilde{b}_1$ must be mostly left-handed so that $\Delta\Upsilon_{t,b}$ is small, or the two $\Delta\Upsilon$'s must precisely cancel each other. (Obviously, the second possibility is less likely, as reflected in the distribution of points in Fig. fig. 4.3 (b).) A large and negative Υ' would require a right-handed $\tilde{t}_1$, whereas a large and positive Υ' requires a right-handed $\tilde{b}_1$. Thus, mass measurements together with the sum rule can provide non-trivial information on the mixing angles, which are difficult or impossible to measure directly at the LHC. (For some proposals for measuring the stop mixing angle, see Refs. [88, 89].)

4.3 Prospects at the LHC: a Case Study

The MSSM parameter point we will consider is defined by the following weak-scale inputs (from here on all masses in GeV unless otherwise noted):

$\tan\beta$	M_1	M_2	M_3	μ	M_A	M_{Q3L}	M_{tR}	A_t
10	100	450	450	400	600	310.6	778.1	392.6

with all other A-terms zero and all other sfermion soft masses set at $1\,\mathrm{T}eV$. The relevant spectrum (calculated with SuSpect) is

m_{t1}	m_{t2}	s_t	m_{b1}	m_{b2}	s_b	$m_{\tilde{g}}$	$m_{\tilde{\chi}_1^0}$
371	800	-0.095	341	1000	-0.011	525	98

At this benchmark point, $\Upsilon = 0.423$, and $\Upsilon' = 0.350$. We will show below that the LHC can measure Υ' rather accurately.

To measure the $\tilde{t}_1$ and $\tilde{b}_1$ masses, we propose to use kinematic edges, the classical M_{T2} variable [90], and recently proposed "subsystem-M_{T2}" variables [91] to analyze the two

processes

(I) $\tilde{g} \to \tilde{b}_1 b \to b b \chi_1^0$ via gluino pair production,

(II) $\tilde{t}_1 \to t \chi_1^0$ via stop pair production

(where we omit antiparticle indices). For our benchmark point each of the above decays has 100% branching fraction, completely eliminating irreducible SUSY backgrounds to the measurements discussed below. The process (I) yields the $\tilde{g}, \tilde{b}_1$, and χ_1^0 masses, and the process (II) provides m_{t1}. Below, we briefly outline these measurements, and estimate their accuracy; the details of this analysis will be presented in [92].

We ignore issues related to hadronization and ISR by performing the analysis at leading order in α_s and at parton level. We use MadGraph/MadEvent (MGME) package [93] to simulate gluino and stop production, and BRIDGE [94] to simulate decays. We use the CTEQ6l1 [95] parton distribution functions throughout, with the MGME default (p_T-dependent) factorization/renormalization scale choice. To roughly model detector response to jets and electrons, we introduce a Gaussian smearing of their energies according to [96]

$$\frac{\Delta E_j}{E_j} = \frac{50\%}{\sqrt{E_{\mathrm{GeV}}}} \oplus 3\% \quad , \quad \frac{\Delta E_e}{E_e} = \frac{10\%}{\sqrt{E_{\mathrm{GeV}}}} \oplus 0.7\% \, . \tag{4.3.10}$$

4.3.1 Measuring the $\tilde{b}_1, \tilde{g}, \tilde{\chi}_1^0$ masses

We study gluino pair production with subsequent decay into $4b + 2\tilde{\chi}_1^0$ at the LHC with $\sqrt{s} = 14\,\mathrm{T}eV$ and 10 fb^{-1} of integrated luminosity. The selection cuts are as follows: (a) $\not{E}_T > 200\mathrm{G}eV$, (b) exactly 4 tagged b-jets, (c) $p_T^{\max} > 100\mathrm{G}eV$, (d) $p_T^{\mathrm{b-jet}} > 40\mathrm{G}eV$, (e) $|\eta| < 2.5, \Delta R > 0.4$. The gluino pair production cross section is $\sigma_{\tilde{g}\tilde{g}} \approx 11.6$ pb. We assumed a b-tag efficiency of 0.6 and b-mistag rates for c-, τ-, and light quark/gluon jets of 0.1, 0.1 and 0.01, respectively, leaving about 1.5 pb of fully b-tagged signal. The other

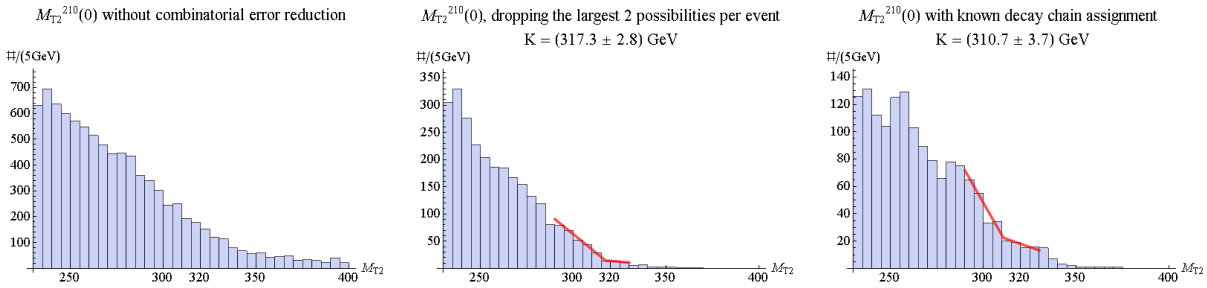

(a) (b) (c)

Figure 4.4: $M_{T2}^{210}(0)$ distributions. The analytical prediction for the edge position is 320.9GeV. We emphasize that even though we show the linear kink fits only over a certain range, K depends very little on the fit domain.

kinematic cuts (a, c-e) have an efficiency of 32%, yielding 480 fb, or about 4800 signal events at 10 fb^{-1}.

We computed the cross sections of the two main SM background processes, $4j + Z$ with $Z \to \nu\bar{\nu}$, and $t\bar{t}$ with one or both tops decaying leptonically. The cross sections, including efficiencies of the cuts (a-e), are $\lesssim$ 10 fb and 25 fb, respectively. Thus, we conclude that the SM backgrounds can be effectively eliminated by cuts, and do not take them into account further in the mass determination analysis.

The main background for mass determination comes from combinatorics. Consider the dijet invariant mass M_{bb}. If both b's come from the same decay chain, the distribution has a *kinematic edge* at

$$M_{bb}^{\max} = \sqrt{\frac{(m_{\tilde{g}}^2 - m_{b1}^2)(m_{b1}^2 - m_{\tilde{\chi}_1^0}^2)}{m_{b1}^2}} = 382.3\text{G}eV. \tag{4.3.11}$$

For each event, there are three possible ways to assign 4 b's to two decay chains, and the M_{bb} distributions of the wrong combinations extend well beyond $M_{bb}^{\max}$. If all combinations are included, the edge is washed out. We find that the combinatoric background can be reduced with simple cuts: very generally, the directions of jets from the same decay chain should be correlated, and the pairings with the largest invariant masses are likely to be incorrect.

Denoting the two b's assigned to each decay chain as (1,2) and (3,4) respectively, we drop the combination with the largest Max$[M_{12}, M_{34}]$ in each event, and require Max$[\Delta R_{12}, \Delta R_{34}] <$ 2.5. The resulting distribution shows a clear edge. We fit to it with a simple trial-PDF, the *linear kink function*, which we will use throughout this analysis:

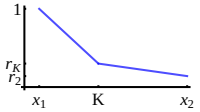

An unbinned maximum-likelihood fit reliably finds the edge position K, yielding a measurement of the kinematic edge position $M_{bb}{}^{\max}_{\rm meas} = (395 \pm 5)\mathrm{G}eV$. This is quite close to the correct value, Eq. (4.3.11), but the use of the simple linear fit function clearly does introduce a systematic error into the edge measurement. To account for this effect, we will simply assume a systematic error of 3 times the statistical error for each edge measurement; this is sufficient to bring across the main points of our analysis. More sophisticated methods for kinematic edge extraction exist in the literature (e.g. [88]), and would be used in practice.

The position of the kinematic edge provides one function of the three unknown masses; two more are required to solve for the spectrum. These can be obtained from the endpoints of distributions of events in M_{T2}-subsystem variables [91] $M_{T2}^{220}(0)$ and $M_{T2}^{210}(0)$, predicted to be at

$$\begin{aligned} M_{T2}^{210}(0)^{\max} &= \frac{[(m_{b1}^2 - m_{\tilde{\chi}_1^0}^2)(m_{\tilde{g}}^2 - m_{\tilde{\chi}_1^0}^2)]^{1/2}}{m_{\tilde{g}}} = 320.9\mathrm{G}eV\,, \\ M_{T2}^{220}(0)^{\max} &= m_{\tilde{g}} - m_{\tilde{\chi}_1^0}^2/m_{\tilde{g}} = 506.7\mathrm{G}eV. \end{aligned} \tag{4.3.12}$$

Of the several possible M_{T2} variables for this system, these two show the clearest edges, allowing precise mass determination; the complete analysis of all M_{T2} variables will be presented in [92].

To calculate M_{T2}^{210} for each event, we must divide the four b's into an upstream and a downstream pair, giving 6 possible combinations. fig. 4.4 (a) shows the complete $M_{T2}^{210}(0)$

distribution; the edge is completely washed out. It turns out that of the 5 possible wrong pairings, the two where b's from the same decay chain are put into up- and down-stream pairs are the most problematic, since their M_{T2}^{210} distributions extend significantly beyond the edge. Based on this observation, we developed two techniques to reduce the combinatorial error. Firstly, for each event we can simply drop the two largest M_{T2}'s. The corresponding distribution is shown in fig. 4.4 (b). Secondly, we can use our measurement of the kinematic edge. For each event there are three possible ways to assign the 4 b's to two decay chains. For some events (about 30% in our sample) we find that for two of these combinations, at least one same-chain invariant mass is larger than $M_{bb}^{\max}$, whereas for the other combination both same-chain invariant masses are smaller – this combination must be the correct one. Using only those events and keeping only the correct decay chain assignments, we obtain the distribution of $M_{T2}^{210}(0)$ shown in fig. 4.4 (c). We performed linear kink fits on the distributions in fig. 4.4 (b) and (c), and found that they are in agreement, indicating the robustness of our approach. Combining the two fits yields $M_{T2}^{210}(0)_{\rm meas}^{\max} = (314.0 \pm 4.6)\mathrm{G}eV$. We used a similar method to extract the M_{T2}^{220} edge, and obtained $M_{T2}^{220}(0)_{\rm meas}^{\max} = (492.1 \pm 4.8)\mathrm{G}eV$. As for the kinematic edge, the linear fit function works rather well, but it does introduce some systematic error into the edge measurements, which we again model by inflating the error bars by a factor of 3. To summarize, the measured edges are:

$$\begin{aligned} M_{bb}{}_{\rm meas}^{\max} &= (395 \pm 15)\mathrm{G}eV\,, \\ M_{T2}^{210}(0)_{\rm meas}^{\max} &= (314 \pm 14)\mathrm{G}eV\,, \\ M_{T2}^{220}(0)_{\rm meas}^{\max} &= (492 \pm 14)\mathrm{G}eV\,. \end{aligned} \tag{4.3.13}$$

Each of these edges defines a subvolume of $(m_{\tilde{g}}, m_{\tilde{\chi}_1^0}, m_{b_1})$-space, which yields the mass measurements given in Table 4.1.

mass	theory	median	mean	68% c.l.	95% c.l.	process
m_{b_1}	341	324	332	(316, 356)	(308, 432)	I
$m_{\tilde{g}}$	525	514	525	(508, 552)	(500, 634)	I
$m_{\tilde{\chi}_1^0}$	98	–	–	(45, 115)	(45, 179)	I + LEP
m_{t_1}	371	354	375	(356, 414)	(352, 516)	I + II

Table 4.1: Mass measurements (all in GeV), assuming Gaussian edge measurement uncertainties. We imposed the lower bound $m_{\tilde{\chi}_1^0} > 45\text{G}eV$, which generically follows from the LEP invisible Z decay width measurement [98].

4.3.2 Measuring the $\tilde{t}_1$-mass

We simulate $pp \to \tilde{t}_1\tilde{t}_1^* \to t\bar{t} + 2\tilde{\chi}_1^0$ for 100 fb^{-1} integrated luminosity. The signal production cross section is 2 pb. The dominant irreducible background is $(Z \to \nu\nu)t\bar{t}$ with $\sigma_{\text{BG}} = 135$ fb. Following [97], we demand two fully reconstructed hadronic tops in each event, in order to use the classical M_{T2} variable [90]. Our signal cuts are (a) exactly 2 tagged b-jets and at least 4 other jets with $p_T > 30\text{G}eV$ and $|\eta| > 2.5$ (b) lepton veto (c) $\Delta R > 0.4$ between all the b- and light jets (d) $\not{E}_T > 100\text{G}eV$ (e) $H_T > 500\text{G}eV$ (e) $p_T^{\max} > 100\text{G}eV$ (f) require $4j$ to reconstruct to two W's with a mass window of $(60, 100)\text{G}eV$ and the two W's to reconstruct with the two b's to two tops with a mass window of $(140, 200)\text{G}eV$. After cuts we are left with 1481 signal and 105 background events. Plotting the classical M_{T2} distribution we see a clear edge, and using the linear kink fit trial PDF with error scaling yields

$$M_{T2}(0)^{\max}_{\text{meas}} = (340 \pm 4)\text{G}eV. \tag{4.3.14}$$

Compare this to the analytical prediction [99] $M_{T2}(0)^{\max} = 336.7\text{G}eV$. Combined with the $m_{\tilde{\chi}_1^0}$ measurement from (I), this yields the stop mass m_{t1}, see Table 4.1. Taking into account all correlations, we find:

$$\Upsilon'_{\text{meas}} = \frac{1}{v^2}\left(m_{t1}^2 - m_{b1}^2\right) = 0.525^{+0.20}_{-0.15}\,, \tag{4.3.15}$$

in good agreement with the theoretical value $\Upsilon' = 0.350$. As explained above, a measurement of Υ' does not by itself provide a consistency check of SUSY, or help in discriminating it from other models. However, if the SUSY-Yukawa sum rule is assumed to be valid, this measurement can be used to place a constraint on the 3rd generation squark mixing. The measurement in Eq. (**??**) corresponds to the range of Υ' assumed in Fig. fig. 4.3 (b). Thus, even without using information from any other measurements, one could conclude that, most likely, the stop and sbottom mixing angles are rather small and the observed light stop and sbottom states are mostly left-handed (although right-handed light states, with an accidental cancellation of $\Delta\Upsilon_b$ and $\Delta\Upsilon_t$, would remain as a logical possibility at this point).

4.4 Discussion and Conclusions

We proposed the SUSY Yukawa sum rule with direct connection to the cancelation of quadratic Higgs mass divergence, and introduce an observable Υ that can be used to test it. This constitutes a significant check on TeV-scale SUSY as the solution to the hierarchy problem. While full measurement of Υ will have to be left to a future lepton machine, we have demonstrated that progress could already be made at the LHC. In particular, we showed that, for the MSSM benchmark point we chose, two masses entering the sum rule, m_{t1} m_{b1}, can be measured. Given these measurements, one could then use the sum rule (within the SUSY framework) to put interesting constraints on other parameters, such as third-generation squark mixing angles, whose direct measurement would be difficult or impossible.

In the course of the analysis we developed new techniques for reducing combinatorial background for M_{T2}-measurements, allowing for complete mass determination of $\tilde{t}_1, \tilde{b}_1, \tilde{g}$ and $\tilde{\chi}_1^0$. At this point, we performed the analysis at the parton level, with only a crude Gaussian

smearing to account for detector effects. It is important to confirm the proposed techniques with more detailed simulations including initial and final state radiation, showering and fragmentation, and better detector modeling. Results of a study including some of these effects will be presented in Ref. [92]. In the future, it will also be interesting to assess the abilities of the LHC to test the sum rule (fully or partially) in the MSSM parameter regions with spectra different from our benchmark point, as well as to study in detail how the sum rule tests can be completed at a future lepton collider.

Acknowledgments — We are grateful to James Alexander and Konstantin Matchev for useful discussions. This work is supported by the U.S. National Science Foundation through grant PHY-0757868 and CAREER award PHY-0844667. MB thanks the Galileo Galilei Institute for Theoretical Physics for the hospitality and the INFN for partial support during the completion of this work.

CHAPTER 5

CONCLUSION

The dawn of the LHC era is an exciting time to be a theoretical particle physicist. After four decades of relative experimental deprivation we will finally receive new clues about the physics that must lie beyond the Standard Model. Much theoretical effort has been invested in preparing for the influx of experimental data, and many models for potential BSM physics have been proposed. The research in this thesis represents the author's effort to contribute to this preparation, by furthering the development of RS and SUSY models and developing new ways to extract information from experimental data.

Of course, a major motivation for our current ideas for physics beyond the Standard Model was always the few existing experimental inconsistencies that we already know about. But we are also guided by purely theoretical considerations, which are ultimately rooted in our belief in a beautiful universe. There is historical justification for this belief. Whenever a supposedly fundamental theory requires finely tuned parameters or initial conditions we often found it to be some approximation to a more complete theory where the tuning is explained by some deep principle. This precedent gives us reason to hope for truly fundamental discoveries at the Large Hadron Collider.

The task facing us is fundamentally different to the work of the previous generation of theorists. With a constant stream of new data coming in we might be able to assemble the 'next' Standard Model in almost real-time, on historical time scales. We might find evidence for one of the scenarios proposed decades ago, or we might get lucky and find that nature begs for an entirely new explanation. Either way, I am thrilled and humbled to be a part of it. It is a privilege to be contributing to this monumental effort, the attempt of furthering humanity's understanding of the fundamental laws governing the universe.

BIBLIOGRAPHY

[1] Richard Feynman, "Chapter 1". QED: The Strange Theory of Light and Matter. Princeton University Press. p. 6. (1985), ISBN 978-0691125756.

[2] M. E. Peskin, D. V. Schroeder, Reading, USA: Addison-Wesley (1995) 842 p.

[3] K. Nakamura et al. (Particle Data Group), J. Phys. G 37, 075021 (2010).

[4] J. Terning, Oxford, UK: Clarendon (2006) 324 p.

[5] J. Wess, J. Bagger, Princeton, USA: Univ. Pr. (1992) 259 p.

[6] S. R. Coleman, J. Mandula, Phys. Rev. **159**, 1251-1256 (1967).

[7] Y. .A. Golfand, E. P. Likhtman, JETP Lett. **13**, 323-326 (1971).

[8] R. Haag, J. T. Lopuszanski, M. Sohnius, Nucl. Phys. **B88**, 257 (1975).

[9] S. Dimopoulos, H. Georgi, Nucl. Phys. **B193**, 150 (1981).

[10] H. Georgi, S. L. Glashow, Phys. Rev. Lett. **32**, 438-441 (1974).

[11] N. Arkani-Hamed, S. Dimopoulos, G. R. Dvali, Phys. Lett. **B429**, 263-272 (1998). [hep-ph/9803315].

[12] V. Khachatryan *et al.* [CMS Collaboration], Phys. Lett. **B697**, 434-453 (2011). [arXiv:1012.3375 [hep-ex]].

[13] L. Randall and R. Sundrum, Phys. Rev. Lett. **83**, 3370 (1999) [arXiv:hep-ph/9905221].

[14] C. Csaki,
[hep-ph/0404096].

[15] C. Csaki, C. Grojean, H. Murayama, L. Pilo and J. Terning, Phys. Rev. D **69**, 055006 (2004) [arXiv:hep-ph/0305237].

[16] C. Csaki, C. Grojean, L. Pilo and J. Terning, Phys. Rev. Lett. **92**, 101802 (2004) [arXiv:hep-ph/0308038].

[17] R. S. Chivukula, D. A. Dicus, H. J. He and S. Nandi, Phys. Lett. B **562**, 109 (2003) [arXiv:hep-ph/0302263]; R. S. Chivukula, E. H. Simmons, H. J. He, M. Kurachi and M. Tanabashi, Phys. Rev. D **71**, 115001 (2005) [arXiv:hep-ph/0502162].

[18] R. Casalbuoni, S. De Curtis and D. Dominici, Phys. Rev. D **70** (2004) 055010 `hep-ph/0405188`; R. S. Chivukula, E. H. Simmons, H. J. He, M. Kurachi and M. Tanabashi, Phys. Rev. D **70** (2004) 075008 `hep-ph/0406077`; H. Georgi, Phys. Rev. D **71**, 015016 (2005) `hep-ph/0408067`; R. Sekhar Chivukula, E. H. Simmons, H. J. He, M. Kurachi and M. Tanabashi, Phys. Rev. D **71** (2005) 035007 `hep-ph/0410154`; R. S. Chivukula, B. Coleppa, S. Di Chiara, E. H. Simmons, H. J. He, M. Kurachi and M. Tanabashi, Phys. Rev. D **74**, 075011 (2006) [arXiv:hep-ph/0607124].

[19] Y. Nomura, JHEP **0311**, 050 (2003) [arXiv:hep-ph/0309189]; G. Burdman and Y. Nomura, Phys. Rev. D **69**, 115013 (2004) [arXiv:hep-ph/0312247]; R. Barbieri, A. Pomarol and R. Rattazzi, Phys. Lett. B **591**, 141 (2004) [arXiv:hep-ph/0310285] H. Davoudiasl, J. L. Hewett, B. Lillie and T. G. Rizzo, Phys. Rev. D **70**, 015006 (2004) [arXiv:hep-ph/0312193]; H. Davoudiasl, J. L. Hewett, B. Lillie and T. G. Rizzo, JHEP **0405**, 015 (2004) [arXiv:hep-ph/0403300]; J. L. Hewett, B. Lillie and T. G. Rizzo, JHEP **0410**, 014 (2004) [arXiv:hep-ph/0407059].

[20] G. Cacciapaglia, C. Csaki, C. Grojean and J. Terning, Phys. Rev. D **71**, 035015 (2005) [arXiv:hep-ph/0409126]; R. Foadi, S. Gopalakrishna and C. Schmidt, Phys. Lett. B **606**, 157 (2005) [arXiv:hep-ph/0409266]; R. S. Chivukula, E. H. Simmons, H. J. He, M. Kurachi and M. Tanabashi, Phys. Rev. D **72**, 015008 (2005) [arXiv:hep-ph/0504114]; R. Casalbuoni, S. De Curtis, D. Dolce and D. Dominici, Phys. Rev. D **71**, 075015 (2005) [arXiv:hep-ph/0502209].

[21] K. Agashe, R. Contino, L. Da Rold and A. Pomarol, Phys. Lett. B **641**, 62 (2006) [arXiv:hep-ph/0605341].

[22] G. Cacciapaglia, C. Csaki, G. Marandella and J. Terning, Phys. Rev. D **75**, 015003 (2007) [arXiv:hep-ph/0607146].

[23] Y. Grossman and M. Neubert, Phys. Lett. B **474**, 361 (2000) [arXiv:hep-ph/9912408]; T. Gherghetta and A. Pomarol, Nucl. Phys. B **586**, 141 (2000) [arXiv:hep-ph/0003129].

[24] G. Burdman, Phys. Rev. D **66**, 076003 (2002) [arXiv:hep-ph/0205329]; Phys. Lett. B **590**, 86 (2004) [arXiv:hep-ph/0310144]. S. J. Huber, Nucl. Phys. B **666**, 269 (2003) [arXiv:hep-ph/0303183]; S. J. Huber and Q. Shafi, Phys. Lett. B **498**, 256 (2001) [arXiv:hep-ph/0010195].

[25] K. Agashe, G. Perez and A. Soni, Phys. Rev. D **71**, 016002 (2005) [arXiv:hep-ph/0408134]; Phys. Rev. Lett. **93**, 201804 (2004) [arXiv:hep-ph/0406101].

[26] K. Agashe, M. Papucci, G. Perez and D. Pirjol, arXiv:hep-ph/0509117; Z. Ligeti, M. Papucci and G. Perez, Phys. Rev. Lett. **97**, 101801 (2006) [arXiv:hep-ph/0604112].

[27] S. Davidson, G. Isidori and S. Uhlig, Phys. Lett. B **663**, 73 (2008) [arXiv:0711.3376 [hep-ph]].

[28] G. Cacciapaglia, C. Csaki, J. Galloway, G. Marandella, J. Terning and A. Weiler, JHEP **0804**, 006 (2008) [arXiv:0709.1714 [hep-ph]].

[29] C. Csaki, A. Falkowski and A. Weiler, JHEP **0809**, 008 (2008) [arXiv:0804.1954 [hep-ph]].

[30] S. Casagrande, F. Goertz, U. Haisch, M. Neubert and T. Pfoh, JHEP **0810**, 094 (2008) [arXiv:0807.4937 [hep-ph]]; M. Blanke, A. J. Buras, B. Duling, S. Gori and A. Weiler, JHEP **0903**, 001 (2009) [arXiv:0809.1073 [hep-ph]]; M. Blanke, A. J. Buras, B. Duling, K. Gemmler and S. Gori, JHEP **0903**, 108 (2009) [arXiv:0812.3803 [hep-ph]]; M. E. Albrecht, M. Blanke, A. J. Buras, B. Duling and K. Gemmler, arXiv:0903.2415 [hep-ph].

[31] A. L. Fitzpatrick, G. Perez and L. Randall, arXiv:0710.1869 [hep-ph]; J. Santiago, JHEP **0812**, 046 (2008) [arXiv:0806.1230 [hep-ph]]; C. Csaki, A. Falkowski and A. Weiler, arXiv:0806.3757 [hep-ph]; K. Agashe, A. Azatov and L. Zhu, arXiv:0810.1016 [hep-ph].

[32] K. Agashe, A. E. Blechman and F. Petriello, Phys. Rev. D **74**, 053011 (2006) [arXiv:hep-ph/0606021]; M. C. Chen and H. B. Yu, Phys. Lett. B **672**, 253 (2009) [arXiv:0804.2503 [hep-ph]]; G. Perez and L. Randall, JHEP **0901**, 077 (2009) [arXiv:0805.4652 [hep-ph]]; C. Csaki, C. Delaunay, C. Grojean and Y. Grossman, JHEP **0810**, 055 (2008) [arXiv:0806.0356 [hep-ph]]; K. Agashe, T. Okui and R. Sundrum, Phys. Rev. Lett. **102**, 101801 (2009) [arXiv:0810.1277 [hep-ph]].

[33] K. Agashe, A. Delgado, M. J. May and R. Sundrum, JHEP **0308**, 050 (2003) [arXiv:hep-ph/0308036].

[34] G. Cacciapaglia, C. Csaki, C. Grojean and J. Terning, Phys. Rev. D **70**, 075014 (2004) [arXiv:hep-ph/0401160].

[35] L. Randall and M. D. Schwartz, JHEP **0111**, 003 (2001) [arXiv:hep-th/0108114];

W. D. Goldberger and I. Z. Rothstein, Phys. Rev. Lett. **89**, 131601 (2002) [arXiv:hep-th/0204160]; Phys. Rev. D **68**, 125011 (2003) [arXiv:hep-th/0208060]; Phys. Rev. D **68**, 125012 (2003) [arXiv:hep-ph/0303158]; K. w. Choi and I. W. Kim, Phys. Rev. D **67**, 045005 (2003) [arXiv:hep-th/0208071]; K. Agashe, A. Delgado and R. Sundrum, Nucl. Phys. B **643**, 172 (2002) [arXiv:hep-ph/0206099]; Annals Phys. **304**, 145 (2003) [arXiv:hep-ph/0212028]; R. Contino, P. Creminelli and E. Trincherini, JHEP **0210**, 029 (2002) [arXiv:hep-th/0208002].

[36] C. Csaki, C. Grojean, J. Hubisz, Y. Shirman and J. Terning, Phys. Rev. D **70**, 015012 (2004) [arXiv:hep-ph/0310355].

[37] R. Contino and G. Servant, JHEP **0806**, 026 (2008) [arXiv:0801.1679 [hep-ph]].

[38] T. Aaltonen *et al.* [CDF Collaboration], arXiv:0811.0053 [hep-ex]; T. Aaltonen *et al.* [CDF Collaboration], arXiv:0902.3276 [hep-ex]; A. Abulencia *et al.* [CDF Collaboration], Phys. Rev. Lett. **95**, 252001 (2005) [arXiv:hep-ex/0507104]; A. Abulencia *et al.* [CDF Collaboration], Phys. Rev. Lett. **96**, 211801 (2006) [arXiv:hep-ex/0602045]; T. Aaltonen *et al.* [CDF Collaboration], Phys. Rev. Lett. **99**, 171802 (2007) [arXiv:0707.2524 [hep-ex]].

[39] T. Aaltonen *et al.* [CDF Collaboration], Phys. Rev. D **77**, 051102 (2008) [arXiv:0710.5335 [hep-ex]].

[40] CDF Collaboration, "A Search for Massive Gluon Decaying to Top Pair in Lepton+Jet Channel" [www-cdf.fnal.gov/physics/exotic/exotic.html].

[41] B. Lillie, L. Randall and L. T. Wang, JHEP **0709**, 074 (2007) [arXiv:hep-ph/0701166].

[42] M. Bona *et al.* [UTfit Collaboration], JHEP **0803**, 049 (2008) [arXiv:0707.0636 [hep-ph]].

[43] J. A. Bagger, K. T. Matchev and R. J. Zhang, Phys. Lett. B **412**, 77 (1997) [arXiv:hep-ph/9707225]; M. Ciuchini, E. Franco, V. Lubicz, G. Martinelli, I. Scimemi and L. Silvestrini, Nucl. Phys. B **523** (1998) 501 [arXiv:hep-ph/9711402]; A. J. Buras, S. Jager and J. Urban, Nucl. Phys. B **605** (2001) 600 [arXiv:hep-ph/0102316].

[44] A. Birkedal, K. Matchev and M. Perelstein, Phys. Rev. Lett. **94**, 191803 (2005) [arXiv:hep-ph/0412278]; C. Englert, B. Jager and D. Zeppenfeld, JHEP **0903**, 060 (2009) [arXiv:0812.2564 [hep-ph]]; A. Martin and V. Sanz, to appear.

[45] M. Dine, W. Fischler and M. Srednicki, Nucl. Phys. B **189**, 575 (1981); S. Dimopoulos and S. Raby, Nucl. Phys. B **192**, 353 (1981); M. Dine and W. Fischler, Phys. Lett. B

110, 227 (1982); M. Dine and M. Srednicki, Nucl. Phys. B **202**, 238 (1982); L. Alvarez-Gaume, M. Claudson and M. B. Wise, Nucl. Phys. B **207**, 96 (1982); C. R. Nappi and B. A. Ovrut, Phys. Lett. B **113**, 175 (1982).

[46] M. Dine and A. E. Nelson, Phys. Rev. D **48**, 1277 (1993) [arXiv:hep-ph/9303230]; M. Dine, A. E. Nelson and Y. Shirman, Phys. Rev. D **51**, 1362 (1995) [arXiv:hep-ph/9408384]; M. Dine, A. E. Nelson, Y. Nir and Y. Shirman, Phys. Rev. D **53**, 2658 (1996) [arXiv:hep-ph/9507378].

[47] G. F. Giudice and R. Rattazzi, Phys. Rept. **322**, 419 (1999) [arXiv:hep-ph/9801271].

[48] I. Affleck, M. Dine and N. Seiberg, Nucl. Phys. B **256**, 557 (1985); E. Poppitz and S. P. Trivedi, Phys. Rev. D **55**, 5508 (1997) [arXiv:hep-ph/9609529]; N. Arkani-Hamed, J. March-Russell and H. Murayama, Nucl. Phys. B **509**, 3 (1998) [arXiv:hep-ph/9701286]; H. Murayama, Phys. Rev. Lett. **79**, 18 (1997) [arXiv:hep-ph/9705271]; M. A. Luty, Phys. Lett. B **414**, 71 (1997) [arXiv:hep-ph/9706554]; S. Dimopoulos, G. R. Dvali and R. Rattazzi, Phys. Lett. B **413**, 336 (1997) [arXiv:hep-ph/9707537]; Y. Shirman, Phys. Lett. B **417**, 281 (1998) [arXiv:hep-ph/9709383]; K. Agashe, Phys. Lett. B **435**, 83 (1998) [arXiv:hep-ph/9804450].

[49] K. I. Izawa, Y. Nomura, K. Tobe and T. Yanagida, Phys. Rev. D **56**, 2886 (1997) [arXiv:hep-ph/9705228].

[50] M. Dine and J. D. Mason, Phys. Rev. D **78**, 055013 (2008) [arXiv:0712.1355 [hep-ph]].

[51] M. Ibe, Y. Nakayama and T. T. Yanagida, Phys. Lett. B **649**, 292 (2007) [arXiv:hep-ph/0703110].

[52] N. Seiberg, T. Volansky and B. Wecht, JHEP **0811**, 004 (2008) [arXiv:0809.4437 [hep-ph]]; H. Elvang and B. Wecht, JHEP **0906**, 026 (2009) [arXiv:0904.4431 [hep-ph]]; R. Argurio, M. Bertolini, G. Ferretti and A. Mariotti, arXiv:0912.0743 [hep-ph].

[53] K. Intriligator, N. Seiberg and D. Shih, JHEP **0604** (2006) 021 [arXiv:hep-th/0602239].

[54] P. Meade, N. Seiberg and D. Shih, Prog. Theor. Phys. Suppl. **177**, 143 (2009) [arXiv:0801.3278 [hep-ph]].

[55] C. Cheung, A. L. Fitzpatrick and D. Shih, JHEP **0807**, 054 (2008) [arXiv:0710.3585 [hep-ph]].

[56] E. Witten, Nucl. Phys. B **202**, 253 (1982).

[57] N. Seiberg, Nucl. Phys. B **435**, 129 (1995) [arXiv:hep-th/9411149].

[58] R. Kitano, H. Ooguri and Y. Ookouchi, Phys. Rev. D **75**, 045022 (2007) [arXiv:hep-ph/0612139];

[59] N. Haba and N. Maru, Phys. Rev. D **76**, 115019 (2007) [arXiv:0709.2945 [hep-ph]]; A. Giveon and D. Kutasov, JHEP **0802**, 038 (2008) [arXiv:0710.1833 [hep-th]]; R. Essig, J. F. Fortin, K. Sinha, G. Torroba and M. J. Strassler, JHEP **0903**, 043 (2009) [arXiv:0812.3213 [hep-th]].

[60] S. Abel, C. Durnford, J. Jaeckel and V. V. Khoze, Phys. Lett. B **661**, 201 (2008) [arXiv:0707.2958 [hep-ph]].

[61] C. Csaki, Y. Shirman and J. Terning, JHEP **0705**, 099 (2007) [arXiv:hep-ph/0612241].

[62] Z. Komargodski and D. Shih, JHEP **0904**, 093 (2009) [arXiv:0902.0030 [hep-th]].

[63] A. Giveon, A. Katz and Z. Komargodski, JHEP **0907**, 099 (2009) [arXiv:0905.3387 [hep-th]].

[64] N. Maru, arXiv:1008.1440 [hep-ph].

[65] D. Koschade, M. McGarrie and S. Thomas, JHEP **1002**, 100 (2010) [arXiv:0909.0233 [hep-ph]].

[66] R. Auzzi, S. Elitzur and A. Giveon, JHEP **1003**, 094 (2010) [arXiv:1001.1234 [hep-th]].

[67] J. Barnard, JHEP **1002**, 035 (2010) [arXiv:0910.4047 [hep-ph]].

[68] M. Dine and J. Mason, arXiv:hep-ph/0611312.

[69] N. Seiberg, Phys. Rev. D **49**, 6857 (1994) [arXiv:hep-th/9402044]; K. A. Intriligator and N. Seiberg, Nucl. Phys. Proc. Suppl. **45BC**, 1 (1996) [arXiv:hep-th/9509066].

[70] E. Witten, Phys. Lett. B **105**, 267 (1981).

[71] K. A. Intriligator and N. Seiberg, Class. Quant. Grav. **24**, S741 (2007) [arXiv:hep-ph/0702069].

[72] A. E. Nelson and N. Seiberg, Nucl. Phys. B **416**, 46 (1994) [arXiv:hep-ph/9309299].

[73] J. Bagger, E. Poppitz and L. Randall, Nucl. Phys. B **426**, 3 (1994) [arXiv:hep-ph/9405345].

[74] S. Shirai, M. Yamazaki and K. Yonekura, JHEP **1006**, 056 (2010) [arXiv:1003.3155 [hep-ph]].

[75] Y. Nakai and Y. Ookouchi, arXiv:1010.5540 [hep-th].

[76] D. Malyshev, Ph.D. Thesis (2008)

[77] S. Abel and V. V. Khoze, JHEP **0811**, 024 (2008) [arXiv:0809.5262 [hep-ph]].

[78] S. R. Coleman, Phys. Rev. D **15**, 2929 (1977) [Erratum-ibid. D **16**, 1248 (1977)].

[79] A. H. Guth and E. J. Weinberg, Phys. Rev. D **23**, 876 (1981); K. Blum, C. Delaunay and Y. Hochberg, Phys. Rev. D **80**, 075004 (2009) [arXiv:0905.1701 [hep-ph]].

[80] M. J. Duncan and L. G. Jensen, Phys. Lett. B **291**, 109 (1992).

[81] D. Green, A. Katz and Z. Komargodski, arXiv:1008.2215 [hep-th].

[82] D. M. Pierce *et. al.*, Nucl. Phys. B **491**, 3 (1997) [arXiv:hep-ph/9606211].

[83] G. Burdman, M. Perelstein and A. Pierce, Phys. Rev. Lett. **90**, 241802 (2003) [arXiv:hep-ph/0212228]; M. Perelstein, M. E. Peskin and A. Pierce, Phys. Rev. D **69**, 075002 (2004) [arXiv:hep-ph/0310039].

[84] S. P. Martin and P. Ramond, Phys. Rev. D **48**, 5365 (1993) [arXiv:hep-ph/9306314].

[85] A. Djouadi, J. L. Kneur and G. Moultaka, Comput. Phys. Commun. **176**, 426 (2007) [arXiv:hep-ph/0211331].

[86] T. Appelquist, H. C. Cheng and B. A. Dobrescu, Phys. Rev. D **64**, 035002 (2001) [arXiv:hep-ph/0012100]; H. C. Cheng, K. T. Matchev and M. Schmaltz, Phys. Rev. D **66**, 056006 (2002) [arXiv:hep-ph/0205314].

[87] N. Arkani-Hamed, A. G. Cohen, E. Katz and A. E. Nelson, JHEP **0207**, 034 (2002) [arXiv:hep-ph/0206021]; H. C. Cheng and I. Low, JHEP **0309**, 051 (2003) [arXiv:hep-ph/0308199]. For a review and further references, see M. Perelstein, Prog. Part. Nucl. Phys. **58**, 247 (2007) [arXiv:hep-ph/0512128].

[88] J. Hisano, K. Kawagoe and M. M. Nojiri, Phys. Rev. D **68**, 035007 (2003) [arXiv:hep-ph/0304214].

[89] M. Perelstein and A. Weiler, JHEP **0903**, 141 (2009) [arXiv:0811.1024 [hep-ph]]; K. Rolbiecki, J. Tattersall and G. Moortgat-Pick, arXiv:0909.3196 [hep-ph].

[90] A. Barr, C. Lester and P. Stephens, J. Phys. G **29**, 2343 (2003) [arXiv:hep-ph/0304226].

[91] M. Burns, K. Kong, K. T. Matchev and M. Park, JHEP **0903**, 143 (2009) [arXiv:0810.5576 [hep-ph]].

[92] M. Blanke, D. Curtin, M. Perelstein, in preparation.

[93] J. Alwall *et al.*, JHEP **0709**, 028 (2007) [arXiv:0706.2334 [hep-ph]].

[94] P. Meade and M. Reece, arXiv:hep-ph/0703031.

[95] J. Pumplin et. al., JHEP **0207**, 012 (2002) [arXiv:hep-ph/0201195].

[96] ATLAS Collaboration TDR Vol. 1. CERN-LHCC-99-14, ATLAS Collaboration TDR Vol. 2. CERN-LHCC-99-15; G. L. Bayatian *et al.* [CMS Collaboration], CERN-LHCC-2006-001; G. L. Bayatian *et al.* [CMS Collaboration], J. Phys. G **34**, 995 (2007).

[97] P. Meade and M. Reece, Phys. Rev. D **74**, 015010 (2006) [arXiv:hep-ph/0601124].

[98] M. Acciarri *et al.* [L3 Collaboration], Phys. Lett. B **431**, 199 (1998); R. Akers *et al.* [OPAL Collaboration], Z. Phys. C **65**, 47 (1995); D. Buskulic *et al.* [ALEPH Collaboration], Phys. Lett. B **313**, 520 (1993).

[99] W. S. Cho, K. Choi, Y. G. Kim and C. B. Park, JHEP **0802**, 035 (2008) [arXiv:0711.4526 [hep-ph]].